

EFFECT OF EVAPOTRANSPIRATION ON RAINFALL-GENERATED RUNOFF

A DISSERTATION

*Submitted in partial fulfillment of the
requirements for the award of the degree*

of

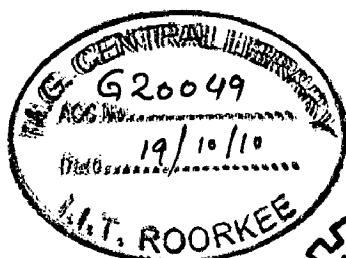
MASTER OF TECHNOLOGY

in

WATER RESOURCES DEVELOPMENT

By

ALAMGIR ALAM



DEPARTMENT OF WATER RESOURCES DEVELOPMENT & MANAGEMENT
INDIAN INSTITUTE OF TECHNOLOGY ROORKEE
ROORKEE-247 667 (INDIA)

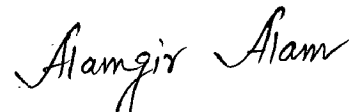
JUNE, 2010

CANDIDATE'S DECLARATION

I hereby certify that the work, which is being presented in this Dissertation entitled "**EFFECT OF EVAPOTRANSPIRATION ON RAINFALL-GENERATED RUNOFF**" in partial fulfillment of the requirements for the award of the degree of MASTER OF TECHNOLOGY in Water Resources Development(Civil) and submitted to the Department of Water Resources Development and Management, Indian Institute of Technology Roorkee, Roorkee, is an authentic record of my own work carried out during the period from July 2009 to June 2010 under the supervision and guidance of Dr. S.K. Mishra, Associate Professor, Department of Water Resources Development and Management, Indian Institute of Technology Roorkee, India.

I have not submitted the matter embodied in this dissertation for the award of any other degree.

Dated: 30th June, 2010
Place: Roorkee.



(ALAMGIR ALAM)
Enrollment No: 08548001

This is to certify that the above mentioned statement made by the candidate is correct to the best of my knowledge.



(Dr. S.K. Mishra)
Associate Professor
WRD&M, IIT Roorkee
Roorkee-247667
INDIA

ACKNOWLEDGEMENT

First of all I would like to thank ALLAH, the Almighty for giving me the opportunity to be part of this prestigious Institute and guiding me and helping me to complete this work.

It is a privilege to express my sincere and profound gratitude to Dr. S.K.Mishra, Associate Professor, Department of Water Resources Development and Management for his guidance, encouragement and suggestions at every stage of this study, in spite of his busy schedule, without which it would have been very difficult to complete this work in time.

I would also like to express my sincere gratitude to Dr. Nayan Sharma, Professor and Head of WRD&M Department, IIT-Roorkee and also to Prof. G. C Mishra, Prof. Rampal Singh, Prof. G. Chauhan, Prof. U.C. Chaube, Prof. D. D. Das, Dr. M. L. Kansal, Dr. Deepak Khare, Dr. Ashish Pandey, Faculty members of WRD&M, IIT for their valuable suggestion and support.

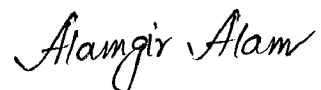
I wish to express my sincere gratitude to the Chairman, West Bengal State Electricity Distribution Company Ltd. (WBSEDCL) for giving me this opportunity to study at this premiere institute for M.Tech. Degree. I also wish to express wholehearted gratitude to Mr. R.K.Mishra, Director, WBSEDCL for his support and encouragement.

I also want to share my happiness with all my fellow trainee officers, and extend my deep gratitude for creating a warm and homely atmosphere throughout the course.

Last but not the least; I want to extend my sincere gratitude to my mother for her support and prayer, and my brother and sister for their support and encouragement.

Date: 30th June, 2010

Place: Roorkee



(ALAMGIR ALAM)

M. Tech (WRD&M)

IIT Roorkee

ABSTRACT

The considerable variation of rainfall and runoff from year to year is part of the natural variability in the climatic system. The management of water resources involves designing and operating to cope with this variability. Estimation of potential evapotranspiration (PET) which is an integrated outcome of the variables describing climate, on hydrology essentially involves projections of climatic changes (e.g. temperature, humidity, mean sea level pressure etc.) is required for water availability computations; estimation of daily, weekly, and monthly flows for multipurpose reservoir operation; scheduling of irrigation projects; preparation of long-term flow forecasts; and many other aspects of water resources planning and management. A general change in surface air temperature might be expected to cause changes in both evaporation and transpiration (or evapotranspiration, ET), hence change in PET. In general, ET is the second largest component of the catchment water balance and PET data. This study presents a Soil Conservation Service Curve Number (SCS-CN) based concept for the assessment of mean PET using long term daily rainfall-runoff data. To this end, the curve numbers (CN) were derived from rainfall-runoff data of three different agro-climatic river basins in India and Nepal for different rain durations and these were correlated with PET derived for respective watersheds using Hargreaves's method. The study reveals quantitatively that as PET increases, CN decreases or S increases and, in turn, the rainfall-generated runoff decreases, and vice versa. Such a relationship invokes determination of PET from the available CN values, and therefore, it may be quite useful in field application.

CONTENTS

	<u>Page No</u>
Candidate's declaration	i
Acknowledgement	ii
Abstract	iii
List of Tables	vii
List of Figures	viii
List of symbols	xi
List of abbreviations	xiii
1. INTRODUCTION	01
1.1 Objective of the study	02
1.2 Organization of Work	02
2. LITERATURE REVIEW	03
2.1 Evapotranspiration as a Climatic Variable	04
2.2 Role of Evapotranspiration in Climate	05
2.3 Observed Changes in Climatic variables	05
2.3.1 Precipitation	05
2.3.2 Evapotranspiration	07
2.3.3 Runoff and river discharge	08
2.4 Projected Changes in Climatic variables	11
2.4.1 Precipitation	11
2.4.2 Evapotranspiration	11

2.4.3	Runoff and river discharge	12
2.5	SCS- CN Method	16
2.5.1	Estimation of Potential Maximum Retention	17
2.5.2	Determination of Curve Number (CN)	18
2.6	Evapotranspiration	19
2.7	Remarks	21
3.	METHODOLOGY	23
3.1	Existing SCS-CN Method	23
3.2	Proposed PET-CN relationship	25
3.3	Justification of ET-CN relationship	26
3.3.1	Mathematical	26
3.3.2	Factors governing CN	28
3.4	Derivation of Curve Numbers and PET	32
3.4.1	Derivation of CN	32
3.4.2	Computation of Potential Evapotranspiration (PET)	33
3.4.3	Derivation of PET-CN Relationship	34
4.	STUDY AREA AND DATA AVAILABILITY	35
4.1	Maithon Catchment	35
4.2	Ramganga Catchment	37
4.3	Rapti Catchment	40
4.4	Data Acquisition	42
4.4.1	Maithon Catchment	42

4.4.2 Ramganga Catchment	42
4.4.3 Rapti Catchment	43
4.5 Data Processing	44
5. RESULTS AND DISCUSSION	45
5.1 Determination of Curve Number, CN	45
5.2 Determination of PET_{av}	46
5.3 Determination of PET_{av} and S relation	46
5.4 Analysis and Discussion of Results	46
5.4.1 Effect of Rain Duration on Curve Number	49
5.4.2 Effect of Rain Duration on PET	51
5.5 Relation between S and PET	52
5.6 Advantages and limitations of the proposed study	54
6. CONCLUSION	55
APPENDIX-I	56
APPENDIX-II	63
APPENDIX-III	65
References	86

LIST OF TABLES

Table No.	Title	Page No.
4.1	Rainfall data availability at different raingauge stations.	39
4.2	Rainfall data availability at different raingauge stations.	39
4.3	Rainfall data availability at different raingauge stations.	40
5.1	Statistics of the fitted curve numbers to daily data of different watersheds.	45
I.1	Greenhouse gases influenced by human activities.	57
II.1	Extraterrestrial Radiation in mm of evaporable water per day.	60

LIST OF FIGURES

Fig. No.	Title	Page No.
2.1	Simplified water balance showing potential evapotranspiration (PET) as climate variables and actual evapotranspiration (E_v) dependent on soil moisture, plant canopy, and PET). $E_v = f$ (available moisture, PET) and $PET_v = f(\text{Climate})$	19
3.1	Proportionality concept of the existing SCS-CN method.	22
4.1	Index map of Maithon Catchment (India).	33
4.2	Index map of Ramganga Catchment.	36
4.3	Index map of Rapti Catchment (Nepal).	38
5.1a	Ordered daily runoff data of Maithon catchment for determination of CN for three AMCs. Upper and lower bound curve numbers refer to AMC-II and AMC-I respectively and best-fit to AMC-II.	44
5.1b	Ordered daily runoff data of Ramganga catchment for determination of CN for three AMCs. Upper and lower bound curve numbers refer to AMC-II and AMC-I respectively and best-fit to AMC-II.	44

Fig. No.	Title	Page No.
5.1c	Ordered daily runoff data of Rapti catchment for determination of CN for three AMCs. Upper and lower bound curve numbers refer to AMC-II and AMC-I respectively and best-fit to AMC-II.	45
5.2a	CN Variation with rainfall duration (greater than or equal to 1 day) for Barakar river at Maithon.	46
5.2b	CN Variation with rainfall duration (greater than or equal to 1 day) for Ramganga.	46
5.2c	CN Variation with rainfall duration (greater than or equal to 1 day) for Rapti.	47
5.3a	PET _{av} variation with rainfall duration (greater than or equal to 1 day) for Maithon catchment.	47
5.3b	PET _{av} variation with rainfall duration (greater than or equal to 1 day) for Ramganga catchment.	48
5.3c	PET _{av} variation with rainfall duration (greater than or equal to 1 day) for Rapti catchment.	48
5.4a	Potential maximum retention for AMC I (S ₁) and PET relationship for Maithon watershed.	49
5.4b	PET and potential maximum retention for AMC I (S ₁) relationship for Ramganga catchment.	50

Fig. No.	Title	Page No.
5.4c	PET and potential maximum retention for AMC I (S _i) relationship for Rapti catchment.	50
I.1	The components of the global climate system.	54
III.1	Ordered different daily runoff data of Maithon catchment for determination of CN for three AMCs. Upper and lower bound curve numbers refer to AMC-II and AMC-I respectively and best-fit to AMC-II.	67
III.2	Ordered different daily runoff data of Ramganga catchment for determination of CN for three AMCs. Upper and lower bound curve numbers refer to AMC-II and AMC-I respectively and best-fit to AMC-II.	74
III.3	Ordered different daily runoff data of Rapti catchment for determination of CN for three AMCs. Upper and lower bound curve numbers refer to AMC-II and AMC-I respectively and best-fit to AMC-II.	81

LIST OF SYMBOLS

Nomenclature

$\beta_{T,S}$	=	Coefficient of transpiration plus soil evaporation
α	=	Coefficient
β	=	Exponent
$^{\circ}\text{N}$	=	Degree North
$^{\circ}\text{S}$	=	Degree South
$^{\circ}\text{C}$	=	Degree Celsius
B	=	Coefficients
B	=	Coefficients
C	=	runoff factor
CN	=	Curve Number
CO ₂	=	Carbon dioxide
E*	=	Daily Potential Evapotranspiration
e.g.	=	exempli gratia (=for example)
E _I	=	daily interception loss
E _S	=	daily soil evaporation
et al.	=	et alia (=and others)
E _T	=	daily transpiration
ET	=	Evapotranspiration
E _v	=	Actual Evapotranspiration

Ev	=	Actual Evapotranspiration
F	=	Actual Infiltration
Fig.	=	Figure
ha	=	hector
I_a	=	Initial Abstraction
LAI_{active}	=	Active Leaf Area Index
m	=	metre
mm	=	Millimetre
MM^3	=	Million Cubic Metre
P	=	Precipitation
PET_{av}	=	Average Potential evapotranspiration
Q	=	Runoff
R_a	=	Extraterrestrial radiation
S	=	Potential Maximum Retention
T_{max}	=	Daily maximum temperature
T_{mean}	=	Daily mean temperature
T_{min}	=	Daily minimum temperature
W	=	Root-Zone Moisture at the End of the Day
W^*	=	Root-Zone Storage Capacity
λ	=	Initial Abstraction Coefficient

LIST OF ABBREVIATIONS

AMC	=	Antecedent Moisture Condition
CRU	=	Climatic Research Unit
EDS	=	Expanded Downscaling Method
GCM	=	Global Climate Model
GHCN	=	Global Historical Climatology Network
GPCC	=	Global Precipitation Climatology Centre
GPCP	=	Global Precipitation Climatology Project
IPCC	=	Intergovernmental Panel on Climate Change
MODIS	=	Moderate Resolution Imaging Spectroradiometer
NEH-4	=	National Engineering Handbook, Section-4
PDSI	=	Palmer Drought Severity Index
PREC/L	=	Precipitation Reconstruction over Land
SMD	=	Soil-Moisture Deficit
SVL	=	Soil-Vegetation-Land use
US\$	=	United States Dollar
WMO	=	World Meteorological Organisation
USDA	=	United State Department of Agriculture
USA	=	United States of America
MCM	=	Million Cubic Metre
PET	=	potential evapotranspiration
SCS	=	Soil Conservation Service

CHAPTER I

INTRODUCTION

Rainfall-generated runoff is very important in various activities of water resources development and management such as flood control and its management, irrigation scheduling, design of irrigation and drainage works, design of hydraulic structures, and hydro-power generation etc. Determining a robust relationship between rainfall and runoff for a watershed has been one of the most important problems for hydrologists, engineers, and agriculturists since its first documentation by P. Perrault (In: Mishra and Singh 2003) about 330 years ago. The process of transformation of rainfall to runoff is highly complex, dynamic, non-linear, and exhibits temporal and spatial variability, further affected by many and often interrelated physical factors. Rain (precipitation) is the major object of hydrologic cycle and this is the primary cause of runoff. The rainfall is subjected to the physical processes which depend on climatological factors like temperature, humidity, wind velocity, cloud cover, evaporation and evapotranspiration, topographical features like depressions, slope of the catchments, vegetation and land use pattern, the soil characteristics like permeability, antecedent moisture content and irrigability characteristics; and the hydrological condition like rock formation, elevation of water table and sub-surface channels too affect this process considerably. The considerable variation of rainfall and hence runoff from year to year is part of the natural variability in the climate system. Climate, whether of the earth as a whole or of a single country or location, is often described as the synthesis of weather recorded over a long period of time. It is defined in terms of long-term averages and other statistics of weather conditions, including the frequencies of extreme events.

Water is one of several current and future critical issues facing the universe. Water supplies from rivers, lakes and rainfall are characterised by their unequal natural geographical distribution and accessibility, and unsustainable water use. Only 2.5% of 1386 million cubic kilolitres of water available on earth is freshwater and only one-third of this smaller quantity is available for human use. Total water drawn globally for human use has almost tripled in the last 50 years and is projected to increase even further by 2025. Climate change has the potential to impose additional pressures on water availability and accessibility. There is increasing concern on the

impact of climate change on rainfall generated runoff. Likely impacts range from more extreme floods to longer droughts; however the scales of these are somewhat unclear. The quantities used to describe the climate are most often surface variables such as temperature, precipitation, humidity, wind, evapotranspiration etc.

Assessing the impact of evapotranspiration, which an integrated outcome of the variables describing climate, on hydrology essentially involves projections of climatic changes (e.g. temperature, humidity, mean sea level pressure etc.) at a global scale, downscaling of global scale climatic variables into local scale hydrologic variables and computations of risk of hydrologic extremes in future for water resources planning and management. For estimation of potential evapotranspiration (PET) which is related with temperature and several other climatic factors is required for water availability computations; estimation of daily, weekly, and monthly flows for multipurpose reservoir operation; hydro power projects; scheduling of irrigation projects; preparation of long-term flow forecasts; and many other aspects of water resources planning and management.

The evapotranspiration is usually estimated using water balance or water budgeting, mass transfer, and their combination methods. Water balance method has wide acceptability in estimation of long term mean evaporation from large river basin, due to its most accurate results. It is worth notable that SCS-CN method is also based on water balance equation and two proportionality hypotheses. Therefore, a common characteristic, i.e. evapotranspiration, is estimated from water balance method. Since the SCS-CN method is based on water balance equation, it suggests the coupling of Curve number (or potential maximum retention, S) with evapotranspiration (or potential evapotranspiration, PET).

1.1 Objective of the study

The objective of this study is to investigate the existence of a relationship between PET and the parameter Curve Number (CN) of the SCS-CN concept for two watersheds in India and one from Nepal.

1.2 Organization of Work

The present thesis has been divided into six chapters including the present one. CHAPTER II presents a review of the literature. CHAPTER III contains methodology. CHAPTER IV presents the study area, the data and data preparation. CHAPTER V presents results and discussion. Finally, CHAPTER VI concludes the study.

CHAPTER II

LITERATURE REVIEW

Climate, whether of the earth as a whole or of a single country or location, is often described as the synthesis of weather recorded over a long period of time. It is defined in terms of long-term averages and other statistics of weather conditions, including the frequencies of extreme events. Climate is far from static. Just as weather patterns change from day to day, the climate changes too, over a range of time frames from years, decades and centuries to millennia, and on the longer time-scales corresponding to the geological history of the earth. Recently, there is a growth in scientific evidence that global climate has changed, is changing and will continue to change. Three distinct signals of climate change witnessed in recent decades are: (a) Rise in global average temperatures (b) Change in regional precipitation patterns and (c) rise in sea levels. Observations that delineate how global temperature has increased in the past reveal that the global average surface temperature has increased by 0.740 C per Century (IPCC, 2007).

It is observed that in the 20th century, 1990s was the warmest decade and 1998 was the warmest year (IPCC, 2001). One of the major causes of global warming is the emission of greenhouse gases due to anthropogenic activities (IPCC, 2001). Observed warming over several decades has been linked to changes in the large-scale hydrological cycle such as increasing atmospheric water vapour content; changing precipitation patterns, intensity and extremes; reduced snow cover and widespread melting of ice; and changes in soil moisture and runoff. Precipitation changes show substantial spatial and inter-decadal variability. Over the 20th century, precipitation has mostly increased over land in high northern latitudes, while decreases have dominated from 10°S to 30°N since the 1970s. The frequency of heavy precipitation events (or proportion of total rainfall from heavy falls) has increased over most areas. Globally, the area of land classified as very dry has more than doubled since the 1970s. There have been significant decreases in water storage in mountain glaciers and Northern Hemisphere snow cover. Shifts in the amplitude and timing of runoff in glacier and snowmelt-fed rivers, and in ice-related phenomena in rivers and lakes, have been observed. By the middle of the 21st century, annual average river runoff and water availability are projected to increase as a result of climate change at high

latitudes and in some wet tropical areas, and decrease over some dry regions at mid-latitudes and in the dry tropics. Many semi-arid and arid areas (e.g., the Mediterranean Basin, western USA, southern Africa and north-eastern Brazil) are particularly exposed to the impacts of climate change and are projected to suffer a decrease of water resources due to climate change.

2.1 Evapotranspiration as a Climatic Variable

Climate change refers to any systematic change in the long-term statistics of climatic elements (such as temperature, pressure, winds, humidity, evapotranspiration etc) sustained over several decades or longer time periods. Recently, there is a growth in scientific evidence that global climate has changed, is changing and will continue to change. Its anthropogenic causes are briefly described in Appendix-I.

Evaporation is the process whereby liquid water is converted to water vapour (vaporization) and removed from the evaporating surface (vapour removal). Water evaporates from a variety of surfaces, such as lakes, rivers, pavements, soils and wet vegetation. Energy is required to change the state of the molecules of water from liquid to vapour. Direct solar radiation and, to a lesser extent, the ambient temperature of the air provide this energy.

Where the evaporating surface is the soil surface, the degree of shading of the crop canopy and the amount of water available at the evaporating surface are other factors that affect the evaporation process. Frequent rains, irrigation and water transported upwards in a soil from a shallow water table wet the soil surface. Where the soil is able to supply water fast enough to satisfy the evaporation demand, the evaporation from the soil is determined only by the meteorological conditions. However, where the interval between rains and irrigation becomes large and the ability of the soil to conduct moisture to near the surface is small, the water content in the topsoil drops and the soil surface dries out. Under these circumstances the limited availability of water exerts a controlling influence on soil evaporation. In the absence of any supply of water to the soil surface, evaporation decreases rapidly and may cease almost completely within a few days.

Transpiration consists of the vaporization of liquid water contained in plant tissues and the vapour removal to the atmosphere. Crops predominately lose their water through stomata. Transpiration, like direct evaporation, depends on the energy supply, vapour pressure gradient and wind. Hence, radiation, air temperature, air humidity and wind terms should be considered when assessing transpiration.

The combination of two separate processes whereby water is lost on the one hand from the soil surface by evaporation and on the other hand from the crop by transpiration, is called the Evapotranspiration.

2.2 Role of Evapotranspiration in Climate

Knowledge of the moisture balance at the earth's surface is essential to an understanding of climate. Precipitation and its areal distribution have been investigated in much detail. Evapotranspiration, which is the reverse of precipitation and represents the combined evaporation from the soil surface and transpiration from plants, is little understood and seldom measured. Actual evapotranspiration depends on climatic factors but is limited by the amount of available moisture in the soil. On the other hand, potential evapotranspiration which may be defined as the amount of water which would be lost from a surface completely covered with vegetation if there is sufficient water in the soil at all times for the use of the vegetation depends on climate alone. In order to evaluate the moisture factor in climate, the moisture supply or the precipitation must be compared with the water need or the potential evapotranspiration. The distribution of precipitation through the year never coincides with, and seldom parallels, the distribution of potential evapotranspiration. When the precipitation is in excess of need, the surplus goes to recharge ground water and produce runoff. When the precipitation does not equal the need, there is a deficiency which results in drought.

2.3 Observed Changes in Climatic variables

2.3.1 Precipitation

Trends in land precipitation have been analysed using a number of data sets; notably the Global Historical Climatology Network (GHCN: Peterson and Vose, 1997), but also the Precipitation Reconstruction over Land (PREC/L: Chen et al., 2002), the Global Precipitation Climatology Project (GPCP: Adler et al., 2003), the Global

Precipitation Climatology Centre (GPCC: Beck et al., 2005) and the Climatic Research Unit (CRU: Mitchell and Jones, 2005). Precipitation over land generally increased over the 20th century between 30°N and 85°N, but notable decreases have occurred in the past 30–40 years from 10°S to 30°N. Salinity decreases in the North Atlantic and south of 25°S suggest similar precipitation changes over the ocean. From 10°N to 30°N, precipitation increased markedly from 1900 to the 1950s, but declined after about 1970. There are no strong hemispheric-scale trends over Southern Hemisphere extra-tropical land masses. At the time of writing, the attribution of changes in global precipitation is uncertain, since precipitation is strongly influenced by large-scale patterns of natural variability. The largest negative trends since 1901 in annual precipitation are observed over western Africa and the Sahel, although there were downward trends in many other parts of Africa, and in south Asia. Since 1979, precipitation has increased in the Sahel region and in other parts of tropical Africa, related in part to variations associated with teleconnection patterns. Over much of north-western India the 1901–2005 period shows increases of more than 20% per century, but the same area shows a strong decrease in annual precipitation since 1979. North-western Australia shows areas with moderate to strong increases in annual precipitation over both periods. Conditions have become wetter over northwest Australia, but there has been a marked downward trend in the far south-west, characterised by a downward shift around 1975. Widespread increases in heavy precipitation events (e.g., above the 95th percentile) have been observed, even in places where total amounts have decreased. These increases are associated with increased atmospheric water vapour and are consistent with observed warming. However, rainfall statistics are dominated by interannual to decadal-scale variations, and trend estimates are spatially incoherent (e.g., Peterson et al., 2002; Griffiths et al., 2003; Herath and Ratnayake, 2004). Moreover, only a few regions have data series of sufficient quality and length to assess trends in extremes reliably. Statistically significant increases in the occurrence of heavy precipitation have been observed across Europe and North America (Klein Tank and Können, 2003; Kunkel et al., 2003; Groisman et al., 2004; Haylock and Goodess, 2004). Seasonality of changes varies with location: increases are strongest in the warm season in the USA, while in Europe changes were most notable in the cool season (Groisman et al., 2004; Haylock and Goodess, 2004).

2.3.2 Evapotranspiration

There are very limited direct measurements of actual evapotranspiration over global land areas, while global analysis products¹⁰ are sensitive to the type of analysis and can contain large errors, and thus are not suitable for trend analysis. Therefore, there is little literature on observed trends in evapotranspiration, whether actual or potential.

a. Evaporation

The hydrological cycle is intimately linked with changes in atmospheric temperature and radiation balance. Warming of the climate system in recent decades is unequivocal, as is now evident from observations of increases in global average air and ocean temperatures, widespread melting of snow and ice, and rising global sea level. Understanding and attribution of observed changes also presents a challenge. For hydrological variables such as runoff, non-climate-related factors may play an important role locally (e.g., changes in extraction). The climate response to forcing agents is also complex. For example, one effect of absorbing aerosols (e.g., black carbon) is to intercept heat in the aerosol layer which would otherwise reach the surface, driving evaporation and subsequent latent heat release above the surface. Hence, absorbing aerosols may locally reduce evaporation and precipitation. Many aerosol processes are omitted or included in somewhat simple ways in climate models, and the local magnitude of their effects on precipitation is in some cases poorly known. Despite the above uncertainties, a number of statements can be made on the attribution of observed hydrological changes.

b. Pan evaporation

Decreasing trends during recent decades are found in sparse records of pan evaporation (measured evaporation from an open water surface in a pan, a proxy for potential evapotranspiration) over the USA (Peterson et al., 1995; Golubev et al., 2001; Hobbins et al., 2004), India (Chattopadhyay and Hulme, 1997), Australia (Roderick and Farquhar, 2004), New Zealand (Roderick and Farquhar, 2005), China (Liu et al., 2004; Qian et al., 2006b) and Thailand (Tebakari et al., 2005). Pan measurements do not represent actual evaporation (Brutsaert and Parlange, 1998), and trends may be caused by decreasing surface solar radiation (over the USA and parts of Europe and Russia) and decreased sunshine duration over China that may be related to increases in air pollution and atmospheric aerosols and increases in cloud cover.

c. Actual evapotranspiration

Actual evapotranspiration increased during the second half of the 20th century over most dry regions of the USA and Russia (Golubev et al., 2001), resulting from greater availability of surface moisture due to increased precipitation and larger atmospheric moisture demand due to higher temperature. Using observations of precipitation, temperature, cloudiness-based surface solar radiation and a comprehensive land surface model, Qian et al. (2006a) found that global land evapotranspiration closely follows variations in land precipitation. Global precipitation values peaked in the early 1970s and then decreased somewhat, but reflect mainly tropical values, and precipitation has increased more generally over land at higher latitudes. Changes in evapotranspiration depend not only on moisture supply but also on energy availability and surface wind. Other factors affecting actual evapotranspiration include the direct effects of atmospheric CO₂ enrichment on plant physiology. The literature on these direct effects, with respect to observed evapotranspiration trends, is non-existent, although effects on runoff have been seen. Annual amounts of evapotranspiration depend, in part, on the length of the growing season.

2.3.3 Runoff and river discharge

A large number of studies have examined potential trends in measures of river discharge during the 20th century, at scales ranging from catchment to global. Some have detected significant trends in some indicators of flow, and some have demonstrated statistically significant links with trends in temperature or precipitation. Many studies, however, have found no trends or have been unable to separate out the effects of variations in temperature and precipitation from the effects of human interventions in the catchment. The methodology used to search for trends can also influence results. For example, different statistical tests can give different indications of significance; different periods of record (particularly start and end dates) can suggest different rates of change; failing to allow for cross-correlation between catchments can lead to an overestimation of the numbers of catchments showing significant change. Another limitation of trend analysis is the availability of consistent, quality-controlled data. Available streamflow gauge records cover only about two-thirds of the global actively drained land area and often contain gaps and vary in record length (Dai and Trenberth, 2002). Finally, human interventions have affected flow regimes in many catchments. At the global scale, there is evidence of a broadly coherent pattern of change in annual runoff, with some regions experiencing

an increase in runoff (e.g., high latitudes and large parts of the USA) and others (such as parts of West Africa, southern Europe and southernmost South America) experiencing a decrease in runoff (Milly et al., 2005, and many catchment-scale studies). Variations in flow from year to year are also influenced in many parts of the world by large-scale climatic patterns associated. One study (Labat et al., 2004) claimed a 4% increase in global total runoff per 1°C rise in temperature during the 20th century, with regional variations around this trend, but debate around this conclusion (Labat et al., 2004; Legates et al., 2005) has focused on the effects of non-climatic drivers on runoff and the influence of a small number of data points on the results. Gedney et al. (2006) attributed widespread increases in runoff during the 20th century largely to the suppression of evapotranspiration by increasing CO₂ concentrations (which affect stomatal conductance), although other evidence for such a relationship is difficult to find. Trends in runoff are not always consistent with changes in precipitation. This may be due to data limitations (in particular the coverage of precipitation data), the effect of human interventions such as reservoir impoundment (as is the case with the major Eurasian rivers), or the competing effects of changes in precipitation and temperature (as in Sweden, Lindstrom and Bergstrom, 2004).

There is, however, far more robust and widespread evidence that the timing of river flows in many regions where winter precipitation falls as snow has been significantly altered. Higher temperatures mean that a greater proportion of the winter precipitation falls as rain rather than snow, and the snowmelt season begins earlier. Snowmelt in parts of New England shifted forward by 1 to 2 weeks between 1936 and 2000 (Hodgkins et al., 2003), although this has had little discernible effect on summer flows (Hodgkins et al., 2005).

Beside the above numerous studies have been conducted at scales ranging from small watersheds to the entire globe to assess the impacts of climate change on hydrologic systems. Arnell et al. (2001) list nearly 80 studies published in the late 1990s in which climate change impacts for one or more watersheds were analyzed using an approach that coupled climate models with hydrologic models. These studies represented various subregions of the six inhabited continents; over half of the studies were performed for watersheds in Europe. U.S. studies have been performed at both a national scale (48-state conterminous region) and for specific watersheds. Many of the

studies have been performed for watersheds in the western section of the United States, including all or portions of the Colorado River Basin (Christensen et al. 2003; Rosenberg et al. 2003), the Columbia River Basin (Hamlett and Lettenmaier 2003; Miles et al. 2000; Payne et al. 2004; Mote et al. 2003; Rosenberg et al. 2003), and the Missouri River Basin (Rosenberg et al. 2003). In addition, the effects of climate change on the hydrological cycle and on the runoff behaviour of river catchments have been discussed extensively in recent years. However, it is at present rather uncertain how, how much and at which spatial scale these environmental changes are likely to affect the generation of storm runoff, and consequently the flood discharges of rivers. The impact of a climate change scenario on regional climate conditions and runoff characteristics has been investigated for the Mulde catchment (L. Menzel, G. Bürger, 2002) a meso-scale sub-basin of the Elbe in Germany. First, the semi-distributed, conceptual model HBV-D has been successfully applied to simulate discharge for present climate conditions. Further, the expanded downscaling method (EDS) was calibrated and applied to observed global circulation fields in order to produce local climate input data for HBV-D. Finally, the coupled atmosphere-ocean model ECHAM4/OPYC3, driven by a climate change scenario, provided simulated global circulation patterns for application with EDS. The regionalised scenario conditions then served as input to HBV-D in order to investigate the impact of global climate change on regional hydrology. The results indicate that an obvious increase in temperature is accompanied by a clear tendency to reduced precipitation over the investigated area for the next 100 years. These conditions lead to a decrease in simulated mean discharges of the Mulde. The study is considered to be a contribution for regional impact studies on global climate change. At the same time, it demonstrates existing shortcomings and limitations of current climate impact research. In 2005, M.A. Mimikou et al. have tried to assess the impacts of climate change on water resources (surface runoff) and on water quality. Two GCM-based climate change scenarios are considered: transient (HadCM2) and equilibrium (UKHI). A conceptual, physically based hydrological model (WBUDG) is applied on a catchment in central Greece, simulating the effect of the two climate scenarios on average monthly runoff. Both scenarios suggest increase of temperature and decrease of precipitation in the study region. Those changes result in a significant decrease of mean monthly runoff for almost all months with a considerable negative impact on

summer drought. Moreover, quality simulations under future climatic conditions entail significant water quality impairments because of decreased stream flows.

2.4 Projected Changes in Climatic variables

In projected changes in the hydrological system so many uncertainties arise due to uncertainty in future greenhouse gas, aerosol emissions etc. Despite these uncertainties, some robust results are available in the following section.

2.4.1 Precipitation

Climate projections using multi-model ensembles show increases in globally averaged mean water vapour, evaporation and precipitation over the 21st century. The models suggest that precipitation generally increases in the areas of regional tropical precipitation maxima (such as the monsoon regimes, and the tropical Pacific in particular) and at high latitudes, with general decreases in the sub-tropics. Increases in precipitation at high latitudes in both the winter and summer seasons are highly consistent. Precipitation increases over the tropical oceans and in some of the monsoon regimes, e.g., the south Asian monsoon in summer (June to August) and the Australian monsoon in summer (December to February), is notable and, while not as consistent locally, considerable agreement is found at the broader scale in the tropics. There are widespread decreases in mid-latitude summer precipitation, except for increases in eastern Asia. Decreases in precipitation over many sub-tropical areas are evident in the multi-model ensemble mean, and consistency in the sign of change among the models is often high – particularly in some regions such as the tropical Central American—Caribbean and the Mediterranean. It is *very likely* that heavy precipitation events will become more frequent. Intensity of precipitation events is projected to increase, particularly in tropical and high-latitude areas that experience increases in mean precipitation. There is a tendency for drying in mid-continental areas during summer, indicating a greater risk of droughts in these regions. In most tropical and mid- and high-latitude areas, extreme precipitation increases more than mean precipitation.

2.4.2 Evapotranspiration

Evaporative demand, or ‘potential evaporation’, is projected to increase almost everywhere. This is because the water-holding capacity of the atmosphere increases with higher temperatures, but relative humidity is not projected to change markedly. Water vapour deficit in the atmosphere increases as a result, as does the evaporation

rate (Trenberth et al., 2003). Actual evaporation over open water is projected to increase, e.g., over much of the ocean and lakes, with the spatial variations tending to relate to spatial variations in surface warming. Changes in evapotranspiration over land are controlled by changes in precipitation and radiative forcing, and the changes would, in turn, impact on the water balance of runoff, soil moisture, and water in reservoirs, the groundwater table and the salinisation of shallow aquifers. Carbon dioxide enrichment of the atmosphere has two potential competing implications for evapotranspiration from vegetation. On the one hand, higher CO₂ concentrations can reduce transpiration because the stomata of leaves, through which transpiration from plants takes place, need to open less in order to take up the same amount of CO₂ for photosynthesis (Gedney et al., 2006, although other evidence for such a relationship is difficult to find). Conversely, higher CO₂ concentrations can increase plant growth, resulting in increased leaf area, and thus increased transpiration. The relative magnitudes of these two effects vary between plant types and in response to other influences, such as the availability of nutrients and the effects of changes in temperature and water availability. Accounting for the effects of CO₂ enrichment on evapotranspiration requires the incorporation of a dynamic vegetation model. A small number of models now do this (Rosenberg et al., 2003; Gerten et al., 2004; Gordon and Famiglietti, 2004; Betts et al., 2007), but usually at the global, rather than catchment, scale. Although studies with equilibrium vegetation models suggested that increased leaf area may offset stomatal closure (Betts et al., 1997; Kergoat et al., 2002), studies with dynamic global vegetation models indicate that the effects of stomatal closure exceed those of increasing leaf area. Taking into account CO₂-induced changes in vegetation, global mean runoff under a 2×CO₂ climate has been simulated to increase by approximately 5% as a result of reduced evapotranspiration due to CO₂ enrichment alone (Leipprand and Gerten, 2006; Betts et al., 2007).

2.4.3 Runoff and river discharge

Changes in river flows, as well as lake and wetland levels, due to climate change depend primarily on changes in the volume and timing of precipitation and, crucially, whether precipitation falls as snow or rain. Changes in evaporation also affect river flows. Several hundred studies of the potential effects of climate change on river flows have been published in scientific journals, and many more studies have been presented in internal reports. Studies are heavily focused towards Europe, North

America and Australasia, with a small number of studies from Asia. Virtually all studies use a catchment hydrological model driven by scenarios based on climate model simulations, and almost all are at the catchment scale. The few global-scale studies that have been conducted using both runoff simulated directly by climate models and hydrological models run off-line show that runoff increases in high latitudes and the wet tropics, and decreases in mid-latitudes and some parts of the dry tropics.

Runoff is notably reduced in southern Europe and increased in south-east Asia and in high latitudes, where there is consistency among models in the sign of change (although less in the magnitude of change). The larger changes reach 20% or more of the simulated 1980–1999 values, which range from 1 to 5 mm/day in wetter regions to below 0.2 mm/day in deserts. Flows in high-latitude rivers increase, while those from major rivers in the Middle East, Europe and Central America tend to decrease. The magnitude of change, however, varies between climate models and, in some regions such as southern Asia; runoff could either increase or decrease. As the effects of CO₂ enrichment may lead to reduced evaporation, and hence either greater increases or smaller decreases in the volume of runoff. In areas where rainfall and runoff are very low (e.g., desert areas), small changes in runoff can lead to large percentage changes. In some regions, the sign of projected changes in runoff differs from recently observed trends. In some areas with projected increases in runoff, different seasonal effects are expected, such as increased wet-season runoff and decreased dry-season runoff.

Hence, hydrological changes may have impacts that are positive in some aspects and negative in others. For example, increased annual runoff may produce benefits for a variety of both instream and out-of-stream water users by increasing renewable water resources, but may simultaneously generate harm by increasing flood risk. In recent decades, a trend to wetter conditions in parts of southern South America has increased the area inundated by floods, but has also improved crop yields in the Pampas region of Argentina, and has provided new commercial fishing opportunities (Magrin et al., 2005). Increased runoff could also damage areas with a shallow water table. In such areas, a water-table rise disturbs agricultural use and damages buildings in urban areas. In Russia, for example, the current annual damage caused by shallow water tables is estimated to be US\$ 5–6 billion (Kharkina, 2004) and is *likely* to increase in the future. In addition, an increase in annual runoff may not

lead to a beneficial increase in readily available water resources, if that additional runoff is concentrated during the high-flow season.

In the context of estimation of Potential Evapotranspiration (PET) and hence its effect in rainfall generated runoff is required to measure for many aspects of water resources planning and management. Thornthwaite (1948) first used the concept of PET and described it as the maximum rate of evapotranspiration (ET) from the large area covered completely and uniformly by vegetation growing with unlimited water supply. In general, ET is the second largest component of the catchment water balance and PET data, therefore, form a key input to rainfall-runoff modeling studies. On an average, 70% of the mean annual rainfall is returned to the atmosphere as ET (Brutsaert, 1982, 1986; Kustas, 1990; Philip, 2002). Assessment of ET is a very complex problem involving spatial and temporal heterogeneity in meteorological and climatic parameters, soil moisture status, plant water availability, surface cover type, soil classes etc. (Makkeasorn et al., 2006). Lysimeter, a popular instrument for measuring ET, is often expensive in terms of its construction, and its operation requires skill. It is, however, most accurate if surface cover condition of the catchment perfectly matches the inside cover conditions of the lysimeter, but not appropriate for routine measurements. Therefore, several empirical and semi-empirical approaches have been developed for different regions based on available meteorological data. However, a few or sometimes only one meteorological station represents the climate of the entire watershed. All empirical methods however work in a certain range of conditions and, therefore, care should be taken not to use them outside the prescribed range (Beven, 2001). PET can be estimated using energy balance, mass transfer, combination of energy balance and mass transfer based empirical and semi-empirical approaches (Brutsaert, 1982; Allen et al. 1989; Jenson et al., 1990; Morton 1994; Xu and Singh, 2002). The combination approach (Penman, 1948) is however considered as the most physically satisfying approach (Jenson et al., 1990; Smith et al., 1991; Shuttleworth, 1993; Beven, 2001). Though the Penman-Monteith method has been recommended as the sole standard method by Food and Agricultural Organization (Allen et al., 1998), the Penman equation yields the most accurate estimates of evaporation from saturated surfaces, if model assumptions are met and adequate input data are available. The Calder (1983) study showed that a simple evaporation formula requiring no direct meteorological measurements other than rainfall performed better

than the more data demanding PET equations, such as those of Priestley-Taylor (1972), Penman (1948), and Thom-Oliver (1977), widely used for predicting soil-moisture deficit (SMD). SMD prediction improves with use of mean climatological PET (Andersson and Harding, 1991); perhaps due to a negative feedback mechanism between stomatal resistance and evaporative demand, not accounted for by the more sophisticated PET equations. The validity of mean monthly PET was investigated and supported by Fowler (2002) in long-term daily water balance studies. The substitution of mean PET estimates into the daily water balance produced a soil water regime very similar to that derived using actual PET, particularly in relatively extreme periods. Using a large sample of 308 catchments of France, Australia, and the United States, Qudin et al. (2005) investigated the validity of 27 PET formulae in stream flow simulation, and found the observed daily PET data not necessary as input to a rainfall-runoff model, rather a long-term regime (for example, annual) curve is sufficient. Therefore, many studies did not find any difference in the use of PET and mean PET (Burnash, 1995), even in extreme situations (Fowler, 2002). The water balance method yields the best estimates of mean long-term evaporation from large (plain) river basin (Gidrometeoizdat, 1967). The estimation of ET using soil water balance method is however often limited due to inconvenience and inaccuracy in measurement of ground water inflow and outflow. Nevertheless, for the reasons of computational simplicity, stability, ease in understanding and grasping, the soil-water balance method is still frequently used in rainfall-runoff modeling. However, in PET estimation using remote sensing, an uncertainty of 20-30% in western riparian corridors of cottonwood has been reported (Nagler et al., 2005). According to Cleugh et al. (2007), the most sophisticated Penman-Monteith method using MODIS remote sensing data and surface meteorology as input also yielded an error between 20 and 25%, attributed to inaccuracy in measurement of input parameters. It is worth noting here that the methods like Penman-Monteith are high data demanding and are also sensitive to data. Furthermore, the simple methods like Blaney-Criddle (1950) and Thornthwaite (1948) and Hargreeves (1982), employing only temperature data, are not very accurate especially under extreme climatic conditions. These methods underestimated (up to 60%) PET in windy, dry, and sunny areas, while in calm, humid, and cloudy areas, PET is overestimated (up to 40%). Brutsaert (1982) points out that "...in the case of evaporation besides sampling, there is also the problem of simply determining it at a point location." However, in many situations, a single

meteorological station data represents the climate of a large catchment, a poor spatial representation. This problem is frequently encountered in PET calculation using formulae requiring large data input.

Thus, the usefulness of more data demanding complex methods in PET estimation appears to be questionable and it, in turn, invokes a need for development of simpler methods to derive mean PET, representing the whole catchment and compatible with the available complex methods. In this paper, the proportionality concept of the popular SCS-CN method (SCS, 1971) is employed in the simple water balance equation to derive mean PET from the usually available long-term daily rainfall-runoff data and it forms the major objective of this paper.

2.5 SCS- CN Method

The United State Department of Agriculture (USDA) Soil Conservation Service Curve Number (SCS-CN) method has its origin in the unit hydrograph approach to rainfall-runoff modelling. The unit hydrograph approach always requires a method of predicting how much of the rainfall contributes to the “storm runoff”. The SCS-CN method arose out of the empirical analysis of runoff from small catchments and hill slope plot monitored by the USDA. Mockus (1949) related storm runoff to rainfalls and showed that the ratio of cumulative discharge to cumulative storm rainfall shows a characteristics form. Mockus (1949) proposed that such data could be represented by an equation of the following form

$$\frac{Q}{P-I_a} = [1 - (10)^{-b(P-I_a)}] \quad (2.1)$$

or

$$\frac{Q}{P-I_a} = [1 - \exp\{-B(P - I_a)\}] \quad (2.2)$$

where Q is the volume of storm runoff; P is the volume of precipitation, I_a is an initial retention of rainfall in the soil; and b and B are coefficients. Mockus (1949) suggested the coefficient b was related to antecedent rainfall, a soil and cover management index, a seasonal index, and storm duration.

Mishra and Singh (1999b) show how this equation can be derived from water balance equation with the assumption that the rate of change of retention with

effective precipitation is a linear function of retention and with the constraint that $B(P-I_a) < 1$. Approximately the right hand side of equation (2.2) as a series expansion results into an equation equivalent to standard SCS-CN formulation

$$\frac{Q}{P-I_a} = \frac{P-I_a}{S+P-I_a} \quad (2.3)$$

where $S (=1/B)$ is the maximum volume of retention. Mishra and Singh (1999b) proposed a further generalisation resulting from a more accurate series representation of equation (2.3) (and giving better fits to data from five catchments) as:

$$\frac{Q}{P-I_a} = \frac{P-I_a}{S+a(P-I_a)} \quad (2.4)$$

This is equivalent to assuming that the cumulative volume of retention F can be predicted as:

$$\frac{F}{S} = \frac{Q}{P-I_a} \quad (2.5)$$

F is often interpreted as a cumulative volume of infiltration, but it is not necessary to assume that the predicted storm flow is all overland flow, since it may not have been in original small catchment data on which the method is based (application of the method to one of the permeable, forested, Coweeta catchments in Hjelmfelt et. al. (1982) is such an example).

A further assumption is usually made in the SCS-CN method that $I_a = \lambda S$ with λ commonly assumed to be ≈ 0.2 . Thus, with this assumption, the volume of storm runoff may be predicted from a general form of the SCS-CN equation:

$$Q = \frac{(P-\lambda S)^2}{P+(1-\lambda)S} \quad (2.6)$$

2.5.1 Estimation of Potential Maximum Retention

The parameter S is called potential maximum retention or maximum potential infiltration. This is also called watershed/catchment storage factor. Its value depends on characteristics of the soil-vegetation-land use (SVL) complex and antecedent soil-moisture conditions in a watershed. For each SVL complex, there is a lower limit and upper limit of S . The parameter S can vary in the range of $0 \leq S \leq \infty$. It is mapped

onto a dimensionless curve number CN, varying in a more appealing range $0 \leq CN \leq 100$, as:

$$S = \frac{25400}{CN} - 254 \quad (2.7)$$

where S is in mm. When S is in inches the equation is:

$$S = \frac{1000}{CN} - 10 \quad (2.8)$$

The difference between S and CN is that the former is a dimensional quantity (L) whereas the later is non-dimensional. CN = 100 represents a condition of zero potential maximum retention ($S = 0$), that is, an impermeable watershed. Conversely, CN = 0 represents a theoretical upper bound to potential maximum retention ($S = \infty$), that is an infinitely abstracting watershed. However, the practical design values validated by experience lie in the range (40, 98) (Van and Mullem, 1998). It is to explicitly mention here that CN has no intrinsic meaning; it is only a convenient transformation of S to establish a 0-100 scale (Hawkins,1978). Obviously, higher is the S, lower will be the CN and vice-versa. It infers that the runoff potential increases with increase in CN and decreases with decrease in CN.

Thus, the SCS-CN method relies on only one parameter, the curve number CN, which is a function of the runoff producing watershed characteristics. The method of selecting a curve number (CN) value for a watershed under various hydrologic conditions is available in the National Engineering Handbook, Section 4 as well as in subsequent publications (McCuen, 1982, 1989; Ponce, 1989; Singh, 1992; Mishra and Singh, 2003a).

2.5.2 Determination of Curve Number (CN)

The curve number is determined from either field data of rainfall and runoff or using (NEH-4) Tables (Mishra and Singh, 2003a). In this Table, soils have been classified into four groups of USA have been classified so. A complete listing of all soils in the United States (more than 4000 soils) along with their group classification can be obtained from the Soil Conservation Service (1969). Depending on other factors a suitable value of CN can be chosen from the table. This is mostly used for ungauged watersheds.

In most cases, the curve numbers were determined using observed rainfall-runoff data of gauged watersheds. The CN is worked out for each Rainfall (P)-runoff (Q) pair. The average is later extended to imply the average soil moisture condition (Miller and Cronshey, 1989). It is worth mentioning that not all soils cover types, and hydrological conditions were represented by rainfall-runoff data; rather these were interpolated to complete the information contained in NEH-4 (SCS, 1971). For the given soil type, hydrologic condition, various types of land use/ treatment and antecedent moisture conditions, CN-values are derived from the National Engineering Handbook, Section-4; as suggested by SCS (1971) (McCuen, 1982, 1989; Ponce, 1989; Singh, 1992; Mishra and Singh, 2003a).

To derive the average CN-values for AMC II mathematically from the rainfall-runoff data of a gauged watershed, Hawkins (1993) suggested the following equation, for $\lambda = 0.2$, for computation of S (or CN), which can be derived from equation (2.11)

$$S=5\{P + 2Q - \sqrt{Q(4Q + 5P)}\} \quad (2.9)$$

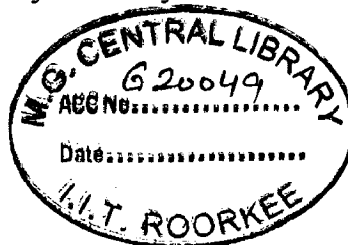
A detailed description of the application procedure is available elsewhere (McCuen, 1982; Ponce, 1989; Mishra and Singh, 2003a; Michel et al., 2005).

2.6 Evapotranspiration

A key component in the hydrologic cycle (Figure 2.1) is evapotranspiration: the (ET) conversion of liquid water at the earth-atmosphere boundary to vapour and the subsequent mixing of this vapour with the atmosphere (Hagan, et. al; 1967). The evaluation of evapotranspiration is important in the study of the impact of climate change on water resources, as evapotranspiration can be considered a key "link" between the atmosphere and the soil matrix within the hydrologic cycle (Figure 2. 1). The importance of this link has been observed by Dooge (1992) who states that any estimate of climate change impacts on water resources depends on the ability to relate changes in actual evapotranspiration to predicted changes in precipitation and potential evapotranspiration (PET). To predict proper *changes* in evapotranspiration it is obviously important to begin with good *estimates* of the driving mechanisms of that change. A number of approaches have been used to assess

evapotranspiration and runoff changes within the context of an altered climate. Gleick (1987) used the Thornthwaite method for estimating PET and a monthly water balance model in the Sacramento-San Joaquin Basin as did McCabe and Ayers (1989) in the Delaware River Basin. Nemeć and Schaaké (1982) performed an impact assessment on two basins in the U.S. (one humid and one arid). They used the Budyko radiation method for the computation of PET combined with a daily hydrologic model to estimate evapotranspiration changes and basin discharge. Reibsame et al. (1994) used a mass balance approach to estimate evapotranspiration (eliminating the need for PET estimates) for the Zambezi River Basin, while in the same work the Penman method was used to calculate PET for the Uruguay basin. Mimikou et. al (1991) used the Blaney-Criddle method for estimating potential evapotranspiration in combination with a monthly water balance for three basins in the central mountainous regions in Greece. Schaake (1990) applied uniform changes in potential evapotranspiration of $\pm 10\%$ to river basins in the Eastern US, suggesting that this change was primarily caused by increased temperatures. Rind et al. (1990) report the use of the Thornthwaite method for computing PET within the Palmer Drought Severity Index (PDSI) model of the U.S., which was then used to create drought scenarios under climate change.

There are a large number of models and equations that compute evaporation and transpiration as a function of climatological and hydrological data. In Evapotranspiration studies, the concept of Potential Evapotranspiration (PET) attributed to Thornthwaite (Thornthwaite et al. 1944) is widely used. PET is the amount of Evapotranspiration that occurs under the ample availability of moisture at all times. PET is taken as an indicator of crop water requirement. Several equations have been developed for its consumption is available elsewhere (Mishra and Singh); the formula which is used in this study is briefly described in Appendix-II.



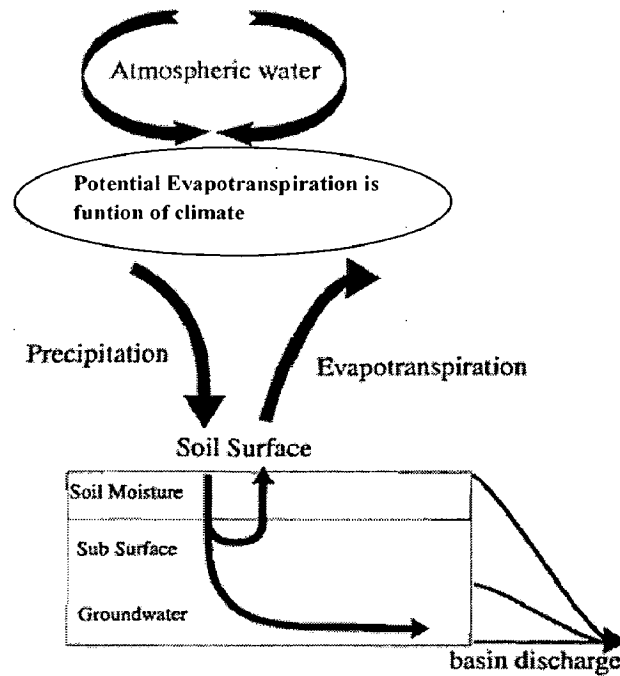


Figure 2.1 Simplified water balance showing potential evapotranspiration (PET) as climate variables and actual evapotranspiration (E_v) dependent on soil moisture, plant canopy, and PET). $E_v = f(\text{available moisture, PET})$ and $PET, = f(\text{Climate})$

2.7 Remarks

The literature reviewed indicates the existence of abundant evidence from observational records and climate projections that freshwater resources are vulnerable and have the potential to be strongly impacted by climate change. However, the ability to quantify future changes in hydrological variables, and their impacts on systems and sectors, is limited by uncertainty at all stages of the assessment process. Uncertainty comes from the range of socio-economic development scenarios, the range of climate model projections for a given scenario, the downscaling of climate effects to local/regional scales, impacts assessments, and feedbacks from adaptation and mitigation activities. Limitations in observations and understanding restrict our current ability to reduce these uncertainties. Because of the uncertainties involved, probabilistic approaches are required to enable water managers to undertake analyses of risk under climate change. A review of SCS-CN method indicated that the method is used for estimating surface runoff from storm rainfall and is simple and easy to apply. Beside that several empirical and semi-empirical methods have been developed

over the last 50 years in different parts of the world but none can be recommended as the best one for any area or any season in terms of its accuracy and profitability. The literature reviewed also encourages to study the existence of a complex relationship between PET and rainfall generated runoff and it can be conveniently accomplished by the popular SCS-CN-based concept, especially in developing countries where establishment of new meteorological stations are not ever possible due to their high installation and operational costs. The existence of a link between PET and CN does not appear to have been explored, which forms to be the prime objective of this study.

The SCS-CN method is frequently used in hydrology and environmental engineering because of its simplicity, its easiness in understanding and application, stability and capability of incorporating several watershed characteristics. During last three decades, the methodology has gone through the rigors of peer review and discussions about its capabilities, limitations, uses, and for sounder hydrologic perception on mathematical footing.

3.1 Existing SCS-CN Method

The existing SCS-CN equation can be derived from water balance equation and two fundamental hypotheses. The first hypothesis equates the ratio of actual amount of direct surface runoff Q to the total rainfall P to the ratio of actual infiltration (F) to the amount of the potential maximum retention S . The second hypothesis relates the initial abstraction (I_a) to the potential maximum retention (McCuen, 2002). Expressed mathematically,

(a) Water balance equation

$$P = I_a + F + Q \quad (3.1)$$

(b) Proportional equality (First hypothesis)

$$\frac{Q}{P - I_a} = \frac{F}{S} \quad (3.2)$$

(c) I_a - S relationship (Second hypothesis)

$$I_a = \lambda S \quad (3.3)$$

The values of P , Q , and S are given in depth dimensions, while the initial abstraction coefficient λ is dimensionless. Though the original method was developed in U. S. Customary units (in.), an appropriate conversion to SI units (cm) is possible (Ponce, 1989). In a typical case, a certain amount of rainfall is initially as interception, infiltration and surface storage before runoff begins, and a sum of these is termed as “initial abstraction”.

The first (or fundamental) hypothesis, Eq. (3.1), is primarily a proportionality concept (Mishra and Singh, 2003a). Fig. 3.1 graphically represents this proportionality concept. Apparently, as $Q \rightarrow (P-I_a)$, $F \rightarrow S$. This proportionality enables dividing $(P-I_a)$ into two components: surface water Q and sub-surface water F for given watershed characteristics.

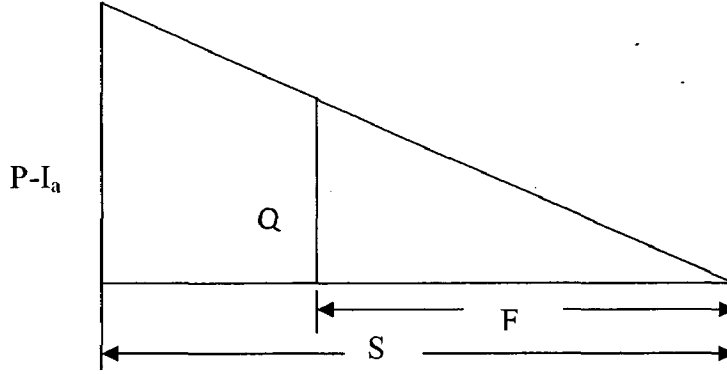


Figure 3.1 Proportionality concept of the existing SCS-CN method.

The parameter S of the SCS-CN method depends on soil type, land use, hydrologic condition, and antecedent moisture condition (AMC). The initial abstraction coefficient λ is frequently viewed as a regional parameter depending on geologic and climatic factors (McCuen, 1982, 1989; Boszanyi, 1989; Mishra and Singh, 2003a). The existing SCS-CN method assumes λ to be equal to 0.2 for practical applications. Many other studies carried out in the United States and other countries (SCD, 1972; Springer et al. 1980; Cazier and Hawkins, 1984; Ramasastri and Seth, 1985; Bosznay, 1989) report λ to vary in the range of (0, 0.3). However, as the initial abstraction component accounts for the short-term losses such as interception, surface storage, and infiltration before runoff begins, λ can take any value ranging from 0 to ∞ (Mishra and Singh, 1999a, b). A study of Hawkins et al. (2001) suggested that value of $\lambda = 0.05$ gives a better fit to data and would be more appropriate for use in runoff calculations.

The second hypothesis, Eq. (3.3), is a linear relationship between initial abstraction I_a and potential maximum retention S . Coupling Eq. (3.1) and (3.2), the expression for Q can be given as:

$$Q = \frac{(P-I_a)^2}{P-I_a+S} = \frac{(P-\lambda S)^2}{P-\lambda S+S} \quad (3.4)$$

Eq. (3.4) is the general form of the popular SCS-CN method and is valid for $P \geq I_a$; $Q=0$ otherwise. For $\lambda = 0.2$, the coupling of Eq. (3.3) and (3.4) results:

$$Q = \frac{(P - 0.2S)^2}{P + 0.8S} \quad (3.5)$$

Eq. (3.5) is the popular form of existing SCS-CN method. Thus, the existing SCS-CN method with $\lambda = 0.2$ is a one-parameter model for computing surface runoff from a storm rainfall event.

Evapotranspiration is the second largest component of the catchment water balance, and an average 70% of the mean annual rainfall is returned to the atmosphere as evapotranspiration. Water balance method has been popularly used for estimation of long term mean evaporation from large river basins. It is worth notable that SCS-CN method is also based on water balance equation and two proportionality hypotheses. Therefore, a common characteristic, i.e. evapotranspiration, is estimated from water balance method. Since the SCS-CN method is also based on water balance equation, it suggests the coupling of Curve number (or potential maximum retention, S) with evapotranspiration (or potential evapotranspiration, PET). Furthermore, the bases of integration are (1) the existence of a mathematical PET-CN relationship; and (2) the parameters affecting the potential evapotranspiration are included in the SCS-CN methodology in terms of initial abstraction. Proposed PET-CN relationship is now discussed in what follows:

3.2 Proposed PET-CN relationship

The estimation of PET utilizes the water balance equation (Eq. 3.1) and the proportionality hypothesis (Eq. 3.2) of the SCS-CN methodology. From the former, the maximum amount of moisture available in the form of (source) rainfall (P) can be lost only when the direct surface runoff (Q) is equal to zero. In other words, $P = I_a + S$. Here, the maximum infiltration losses F will equal S (in magnitude) which includes the initial moisture (Mishra and Singh, 2002). From Eq. 3.1, as $Q \rightarrow (P - I_a)$, $F \rightarrow S$. Since $I_a = 0.2S$, the maximum water loss = $1.2S$. In terms of AMC, it is equal to $1.2S_I$, where the subscript I refers to AMC I (fully dry condition); or S_I corresponds to the capacity of the fully saturated store. Since, by definition, PET corresponds to

unlimited amount of moisture supply to vegetation, as described above, the assumption in the proposed PET computation is that the rainfall (P) is always greater than or equal to $1.2S_1$ during the storm duration. Here, it is worth emphasizing that I_a accounts for all those initial water losses, such as interception, evaporation, surface detention, and infiltration, describable in terms of evaporation and not available for either plant use or runoff generation (Mishra and Singh, 2003a). The water that can transpire through vegetation during the storm duration can be equal to S_1 , if the moisture is fully available. Thus, the sum of I_a and S for AMC I describes the potential amount of evapotranspiration that can occur in a watershed during the storm period. Thus, there appears to be a relation existing between PET and S_1 , which can be described in power form as follows:

$$PET = \alpha S_1^\beta \quad (3.6a)$$

Eq. 3.6a can be more generalized as

$$ET = \alpha S^\beta \quad (3.6b)$$

where α and β are the coefficient and exponent, respectively. Since S and CN are inversely related (Eq. 2.7), Eq. 3.6 suggests ET to be high for the watersheds of low CN , and vice versa. The following text endeavours to support this logic.

3.3 Justification of ET-CN relationship

3.3.1 Mathematical

The governing equations for the root-zone soil moisture W and evapotranspiration E (Mintz and Walker, 1993) are given as follows:

$$E_T + E_S = \beta_{T,S} (E^* - E_1) \quad (3.7a)$$

$$\beta_{T,S} = \frac{W}{W^*} \quad (3.7b)$$

$$E = E_1 + E_T + E_S \quad (3.7c)$$

where E_T is the daily transpiration (moisture transferred from the soil to the atmosphere through the root-stem-leaf system of vegetation); E_S is the daily soil evaporation (moisture transferred from the soil to the atmosphere by hydraulic

diffusion through the pores of the soil); E_i is the daily interception loss (water evaporated from the wet surface of the vegetation and wet surface of the soil) during rain storm; $\beta_{T,S}$ is the coefficient of transpiration plus soil evaporation, taken as a function of soil wetness; E^* is the daily potential evapotranspiration; W is the root-zone moisture at the end of the day; and W^* is the root-zone storage capacity.

From Eq. 3.7a & 3.7c,

$$\beta_{T,S} = \frac{E - E_i}{E^* - E_i} \quad (3.8)$$

Coupling of Eq. 3.7b and 3.8 leads to

$$\frac{E - E_i}{E^* - E_i} = \frac{W}{W^*} \quad (3.9)$$

The right hand term of Eq. 3.9 equates, by above definition, to the ratio of F (= W) to S (= W^*). Thus, Eq. 3.9 states that, similar to the SCS-CN proportionality hypothesis (Eq. 3.2), the ratio of actual evapotranspiration to the potential evapotranspiration is equal to the ratio of actual infiltration (or moisture retention) to the potential maximum retention. A substitution of Eq. 3.2 into Eq. 3.9 yields

$$\frac{E - E_i}{E^* - E_i} = \frac{F}{S} = \frac{Q}{P - I_a} \quad (3.10)$$

Eq. (3.10) when further coupled with Eq. 3.4 yields the following

$$E = E_i + \frac{(P - I_a)(E^* - E_i)}{P - I_a + S} \quad (3.11)$$

Here, E_i , by definition, represents the daily interception loss (water evaporated from the wet surface of the vegetation and wet surface of the soil) during the rain storm. It is however a representation of the above described SCS-CN initial abstraction (I_a) that includes not only interception losses but also surface detention, initial infiltration, and evaporation. This is the water loss abstracted initially and not contributing to either direct runoff or infiltration. On the other hand, E_T and E_S are the water losses occurring during the whole period of rain storm. Thus, within the frame-

work of SCS-CN terminology, E_1 can be taken as to represent I_a . Therefore, Eq. 3.11 can be recast as:

$$E = I_a + \frac{(P - I_a)(E^* - I_a)}{P - I_a + S} \quad (3.12)$$

Taking $I_a = 0.2S$, it is thus possible to derive from Eq. 3.12 the actual evapotranspiration using known values of P , E^* , and S (or CN). Eq. 3.12 also exhibits an implicit relationship between E and I_a and, in turn, CN via Eq. 3.3 & 2.7. The proposed Eq. 3.6 is a versatile form of a non-linear relationship. Further, when $E = P$, an analogy between the above described $P = I_a + S$ relation and Eq. 3.7c (with $E_1 = I_a$) yields S to be analogous to $E_T + E_S$, frequently used in long-term simulation, suggesting a link between S (or CN) and ET .

3.3.2 Factors governing CN

To show the existence of a relationship between CN and ET , it is in order to consider all the factors governing CN and evaluate the impact of their variation on ET . Here, it is worth emphasizing that, since PET represents the maximum rate at which water is transferred to atmosphere, all the factors responsible to ET also affect PET of a watershed.

a. Initial abstraction

The term initial abstraction I_a in SCS-CN methodology consists of interception, surface detention, evaporation and infiltration (before the time to ponding after which runoff begins). The water that contributes to interception and surface detention and storage is evaporated back to the atmosphere and contributes neither to runoff nor to infiltration. The infiltrated water before the time to ponding may be interpreted as to have satisfied the atmospheric demand of water absorption (molecular adsorption in particular) of the soil air column, similar to evaporation. Therefore, the water held by interception, surface detention, and infiltration at the beginning of a storm finally goes back to atmosphere through evapotranspiration. Thus, I_a depends on ET . As I_a increases, direct runoff Q decreases or, in turn, S increases or CN decreases. Thus, ET and CN are inversely related.

b. Landuse

Landuse characterizes the uppermost surface of the soil system and has a definite bearing on infiltration and ET. It describes the watershed cover and includes every kind of vegetation, litter and mulch, and fallow as well as nonagricultural uses, such as water surfaces, roads, roofs, etc. SCS (1956) broadly classified the land use into three categories, urban, agricultural, and woods & forest.

i). Urban Lands

Urban lands are relatively imperviousness in nature. These include residential, paved parking lots, streets, roads, commercial and industrial areas etc. Larger the impervious area, lesser will be transpiration and opportunity time for evaporation, and hence, lesser will be evapotranspiration and, in turn, larger will be the direct runoff or CN. Therefore, curve number increases and ET decreases with increasing relative imperviousness of the area.

ii). Agricultural land

Agricultural lands can be classified as cultivated and uncultivated lands. Cultivated land comprises fallow, row crops, small grain crops, close seeded legumes or rotation meadow, whereas uncultivated refers to pasture or range, and meadow. Cultivated lands are employed by different tillage and intercropping operations in different times of the year. Tillage generally destroys soil structure and breaks down the capillaries. Consequently, tilled layer dries out quickly, and retards liquid movement of water from the underlying untilled layer (Hillel, 1982), and in turn, significant reduction in ET. However, in uncultivated land like pastures and meadows, capillaries are well developed and water continuously transfers from root zone to atmosphere. NEH-4 table (SCS, 1956) also describes cultivated lands to exhibit higher CN values than uncultivated lands do, supporting ET to be high in low CN watersheds.

However, a significant variation in ET and CN values can be seen among species, growth stage, canopy cover, and plant height of the crops/vegetation. Evapotranspiration from any crop/vegetation surface depends on the surface and aerodynamic resistance of specific crop/vegetation. Surface resistance depends on active leaf area index (LAI_{active}) and stomatal resistance of the leaf. LAI_{active} is an index of leaf area that actively contributes to transfer of surface heat and vapor. Since

Biological processes are carried out by the leaves, LAI is fully responsible for energy, water, and gas exchange between the soil/plant to the atmosphere. Normally LAI increases with growing period and it reaches maximum before harvesting or at flowering (Allen et al, 1998). LAI varies greatly among species and within species due to differences in site, age, stand composition, density, and season (Chang, 2005). Species growing in cool and arid climates usually have small LAI and reach maximum LAI at later stage than those growing in warm and wet environments. Since surface resistance and LAI are inversely related, all the factors governing LAI affect surface resistance, and hence, ET.

Auerswald and Haider (1996) determined CN-values for different ground covers, stages of crop growth and seasons by conducting experiments in 70 small plots at 8 sites for different small grain crops in Germany. The measured CN values ranged from 45 to 99 for AMC II. Between seedbed preparation and harvest, CN values decreased with increasing percentage of ground cover and this was described by relationship $CN = 87 - 0.49 \times \text{Cover}$. The existing SCS-CN methodology expressed ground cover by only three different CN values corresponding to three hydrologic conditions, poor, fair, and good. CN, however, changed gradually with ground cover. Seasonal values of CN varied from 44 (July) to 86 (October) for wheat, from 44 (July) to 86 (September) for Barley, from 41 (July) to 86 (October) for Rye, and 39 (July) to 81 (September) for average cover development. It is worth noting here that July is considered as the driest month of the year in Germany. The study reveals that like ET, CN also gets affected by ground cover, crop growth stage, plant height, and type of crop. Furthermore, SCS (1972) reported a CN of 83 and 84 for small grain at AMC II and the hydrologic soil group C for good and poor hydrologic conditions, respectively. Thus, there exists a need to derive CN values for different crops, species, growth stage, and seasons.

Normally, aerodynamic resistance depends on plant height; it decreases with increasing plant height, and therefore, the aerodynamic resistance for short crops, such as grass is larger than that for taller vegetation like forest (Shuttleworth, 1993). It means that taller vegetation (generally woods and forests) are accomplished with higher evapotranspiration values than low growing grasses or brush. According to NEH-4 table, CN values for woods and forest lands are less than those for pasture, grassland or range, and herbaceous (mixture of grass, weeds and low growing brush).

iii) Wood and Forest

Similar to cultivated land, the evapotranspiration from forest is more pronounced by transpiration from the vegetative surface. Since forest comprises greater LAI, taller plant and soils are rich in organic matters, ET from forest is more than the cultivated/agricultural field. LAI for forest stand can be 5 – 50 times greater than the ground area covered by the forest canopies. Chang et al. (1983) studied the depletion rate of soil water (or evapotranspiration) for six forest conditions based on forest coverage on the wood-tell soil by season and depths. The values indicated that depletion rate of soil water (or evapotranspiration) increases with increasing forest coverage. It takes about 35 days for the undisturbed forest, but 62 days for the cultivated plot to deplete initial soil moisture content of 0.45 g cm^{-3} in the 30-cm surface profile to 0.20 g cm^{-3} during growing season. Furthermore, SCS (1985) has briefly described the forest hydrologic condition on the scale of 1 to 6; the forest coverage decreases from 6 to 1 and runoff potential (or CN) increases from 6 to 1. It shows that ET decreases with decreasing forest coverage (6 to 1), and vice versa.

c. Soil Type

Evaporation from soil depends on atmospheric evaporative power and supply of water to the evaporating surface (Hillel, 1971). Supply of water depends on the water retention and transmission properties namely porosity and hydraulic conductivity of the soil, respectively. The finely structured clay soil has a higher water retention capacity owing to higher porosity, but sandy soil will release more water from its large pores due to small or moderate soil water tension (Shaw, 1988). Clay soil pores exhibits higher suction in comparison to most contrasting sandy soil for same water content (Hillel, 1980). Therefore, it would be easier to extract water (for evaporation) from sandy soil compared to clay. SCS (1956) classifies soils as hydrologic soil groups A, B, C, and D based on minimum infiltration and transmission capacity. Group A refers to sandy soils (lowest CN), D to clayey soils (highest CN), and the others lie in between (Mishra and Singh, 2003). Consequently, the CN value increases from sandy (soil group A) to clayey (soil group D) while evaporation (or evapotranspiration) decrease from sandy (soil group A) to clayey (soil group D).

d. Salt concentration

Use of contaminated water to irrigation or other purposes forms the salt crust at the surface of soil which alters the evaporation and infiltration characteristics of the soil. Fujimaki et al. (2006) found considerable reduction of evaporation with time from a bare saline soil under constant meteorological conditions. The decrease in osmotic potential was not the only one factor responsible for reduction in evaporation since the soil surface was kept wet during the experiment, and therefore, suggested to include in bulk transfer equation one more resistance to water vapor diffusion caused by salt crust. The salt however affects soil structure and clogs the soil pores resulting in reduction of hydraulic conductivity and, in turn, infiltration. Alternatively, CN increases and ET reduces with increase in salt content.

e. Antecedent Moisture Conditions (AMC)

ET is more pronounced in growing season than it is in dormant season (SCS, 1956). According to AMC criteria, CN is less in growing season than dormant season for the same antecedent moisture, supporting the existence of an inverse ET-CN relationship. It is worth emphasizing here that the concept of soil-moisture-index (SMI) is generally used to identify the AMC condition in long-term hydrologic simulation. This concept incorporates climatic factors such as daily temperature, solar radiation etc., and thus, the SCS-CN method also accounts for the climatic factors.

f. Size of Watershed

As the size of watershed increases, CN decreases, and vice versa (Mishra and Singh, 2003a), because of increase in infiltration with increase in size of watershed. However, in large watersheds, water takes more time to reach the outlet, rendering more time for water to evaporate than in small catchments. Thus, the larger the area, the larger will be the ET, and lesser the CN.

3.4 Derivation of Curve Numbers and PET

3.4.1 Derivation of CN

In the present study, following Mishra et al. (2008) procedure, curve numbers were derived from Eqs. (3.6) and (3.8) utilizing the available long-term daily rainfall-runoff data, covering a wide range of variation in rainfall/runoff and catchment

characteristics, geography, and climatic change with time. Thus, the three levels of antecedent moisture condition (AMC) are not limited by the seasonal rainfall and, due to use of observed field data, the derived curve number values represent the actual watershed conditions not covered in the NEH-4 table. Here, it is assumed that the available daily rainfall-runoff data of all seven catchments meet the requirements of Eq. 3.4, implying that the rainfall of duration greater than or equal to the time of concentration (T_c) of the respective watershed contributes fully to the surface runoff at its outlet. Since the SCS-CN method ignores the base flow contribution, making the runoff factor $C (= Q/P)$ even greater than 1, only those daily (or any other duration) rainfall-runoff events were considered for the derivation of curve numbers which yielded runoff coefficient less than or equal to 1 ($C \leq 1$). Fig.5.1 depicts the curve numbers for three AMCs for the Ramganga watershed. The data point can be bounded by two upper and lower envelope curves, which are taken to correspond to wet (AMC III) and dry (AMC I) conditions, respectively. In Fig. 5.1, the upper and lower envelopes correspond to $CN = 98$ and $CN = 55$, respectively. The best fit, which falls in the middle of the two upper and lower envelopes, represents the average antecedent moisture condition of the watershed, taken as to correspond to AMC II, for which $CN = 88$. Employing this procedure, curve numbers were derived for different time periods using the rainfall-runoff data summed/averaged for the desired duration (1d (one day), 2d (two days), 3d.....30d (thirty days)). Fig. 5.2 represents the variation of curve number with rain duration for the different watersheds.

3.4.2 Computation of Potential Evapotranspiration (PET)

The daily potential Evapotranspiration has been computed by using Hargreaves method as:

$$PET_o = 0.0023(T_{max}-T_{min})^{0.5}(T_{mean}+17.8) R_a \quad (3.13)$$

where T_{max} is the daily maximum temperature ($^{\circ}C$), T_{min} is the daily minimum temperature ($^{\circ}C$) and R_a is the extraterrestrial radiation (cm/day). Details of the method are provided in Appendix-II.

Since daily temperature data were available, daily PET_o values were computed. For a given duration, similar to the above derived representative CN-value, the average of all daily PET_o values, i.e. PET_{av} corresponding to a rainfall-runoff

series was taken to be representative of the whole watershed for the selected duration. Since AMC I is taken to be representative, CN corresponding to AMC III are related with the PET_{av} as follows.

3.4.3 Derivation of PET-CN Relationship

In steps the procedure is as below:

1. Derive the CN-values for different durations, but for AMC I, which represents the fully dry condition of the watershed.
2. Estimate daily PET_o from Hargreaves method as above and average these PET_o values (PET_{av}) that correspond to the processed (for baseflow) daily rainfall-runoff series used for CN-derivation.
3. Similarly derive CN and PET_{av} values for different rain duration such as 1d, 2d, 3d and so on.
4. Plot S (abscissa) Vs. PET_{av} of step 3 on a graph sheet and fit a power relationship.

CHAPTER IV

STUDY AREA AND DATA AVAILABILITY

This chapter describes the study area and availability of data. The study areas chosen for the present work are Ramganga and Maithon catchments of India and a sub-watershed of Rapti catchment located in Nepal, describing significantly different geo-climatic settings for application and testing of the proposed methodology. A brief of these catchments is given as follows.

4.1 Maithon Catchment

The Barakar River is the main tributary of Damodar River in eastern India. Originating near Padma in Hazaribagh district of Jharkhand it flows for 225 km across the northern part of the Chota Nagpur plateau, mostly in a west to east direction, before joining the Damodar near Dishergarh in Bardhaman district of West Bengal. The study area falls within latitude $23^{\circ}44'N$ to $24^{\circ}0'N$ and longitude $86^{\circ}44'E$ to $86^{\circ}52'E$. It has a catchment area of 6159 km² and has an average altitude of approx. 110.0 metre. The main tributaries, Barsoti and Usri, flow in from the south and north respectively. Apart from the two main tributaries some fifteen medium/small streams join it. Six sub-types of soils have been identified under the main alluvium, either the Ganga alluvium or the Damodar alluvium in the delta area. Open Sal forests (*Shorea robusta*) thrive mainly on laterite and dense Sal forest on red and yellow loams in the upper valley. The climate of the area is characterised by moderate winters and hot & humid summers. Like the rest of India, the region experiences two principal rainy seasons. In the winters from December to March there is little rain. In the summer months, June to September, the flow of air is from sea to land and the season is characterised by high humidity, clouds and rain. The direction of winds being south-westerly, the season is named South-West Monsoon which is the main season producing rains. Between these two principal seasons are the transition seasons of the hot weather months of April & May and the retreating monsoon months of October & November. The annual rainfall over the valley ranges between 1,000 mm and 1,800 mm. Distribution of rainfall varies widely owing to differences of terrain and atmospheric conditions in the different parts of the valley. Within the command area, the upper and the middle parts of the Damodar basin receive 1,209 mm rainfall

annually and the lower valley 1,329 mm above the main plateau escarpment rainfall increases to over 1,500 mm a year. Mean annual rainfall in the basin is of the order of 1,300 mm and about 80% of rain precipitates during the

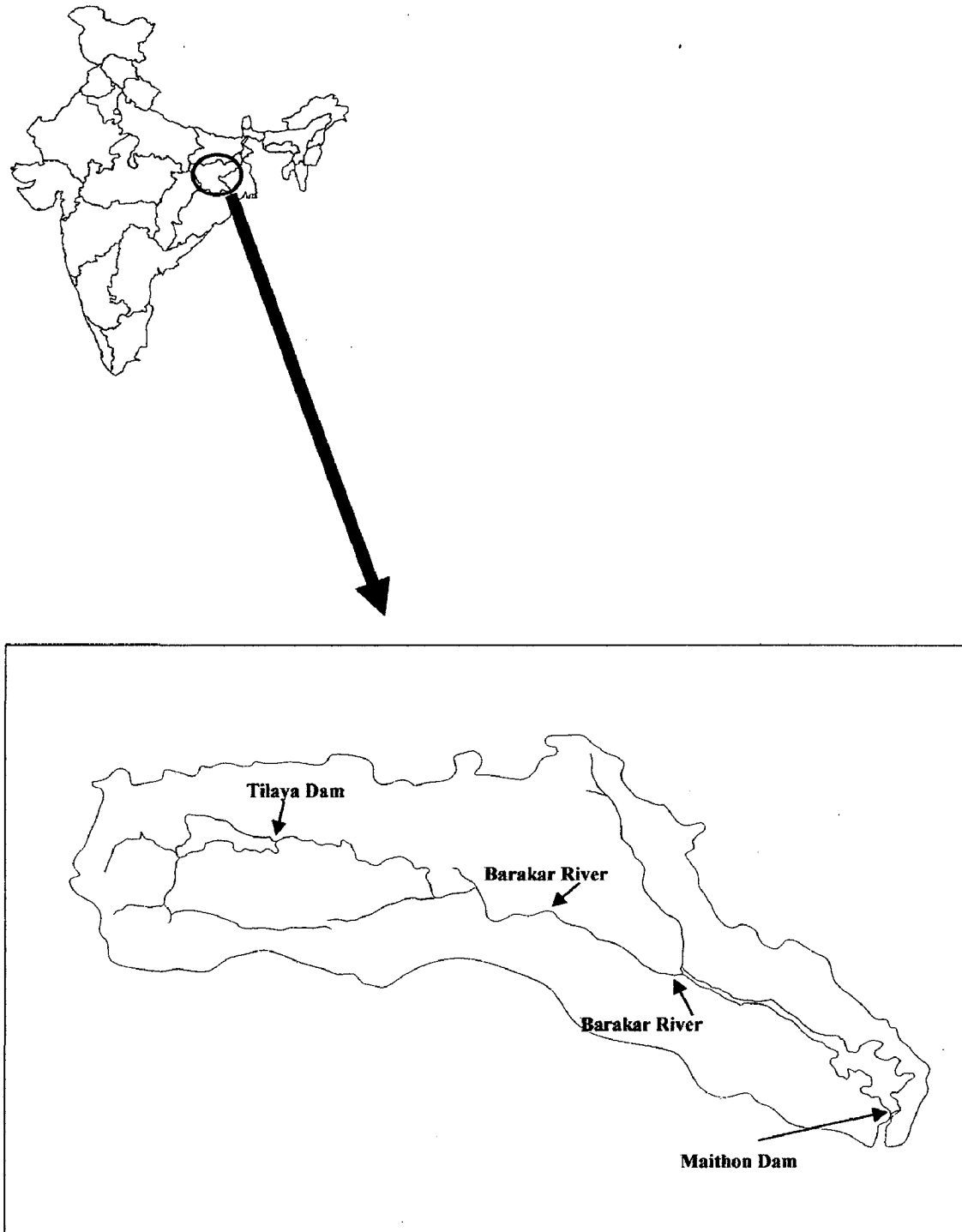


Figure 4.1 Index map of Maithon Catchment (India).

summer monsoon (June to September). The highest maximum temperature exceeding 46 °C was recorded over a larger part of the valley. Normal temperature swings between 40 to 42 degrees Celsius in the summers (May & June) to 23 to 26 degrees Celsius in the cold months (December & January). Mean relative humidity varies from 80% during July to September to 40% in March., April & May. Fig. 4.1 shows the index map of Maithon catchment.

4.2 Ramganga Catchment

The Ramganga river is a major tributary of Ganga and drains a catchment area of 3,134 km² (Fig. 4.2). Its catchment lies in the Sivalik ranges of Himalayas and the valley is known as Patlel Dun. River Ramganga originating at Diwali Khel. It emerges out of the hills at Kalagarh (District Almora) where a major multipurpose Ramganga dam is situated. Its catchments lies between elevation 262 and 2,926 m above mean sea level, and it is considerably below the perpetual snow line of the Himalayas. The river traverses approximately 158 km before it meets the reservoir and then continues its journey in the downstream plains for 370 km before joining River Ganga at Farrukhabad.

During its travel up to Ramganga dam, the river is joined by main tributaries: Ganges, Binoo, Khatraun, Nair, Badangad, Mandal, Helgad, and Sona Nadi. About 50% of the drainage basin is covered with forest, 30% is under cultivation on terraced fields, and the remaining 20% is urban/barren land. Specific features of the area are as follows:

- Located in the foothills of Himalayas in the Uttarakhand.
- River Ramganga originates at Diwali Khel.
- A major tributary of River Ganga.
- It emerges out of the hills at Kalagarh (District Almora)
- At Kalagarh, a major multi-purpose Ramganga dam.

- River traverses approx. 158 km before it joins the reservoir and finally joins Ganga at Farrukhabad, 370 km d/s.
- Main tributaries: Ganges, Binoo, Khatraun, Nair, Badangad, Mandal, Helgad, and Sona Nadi.
- Its catchment area = 3134 sq. km.
- Elevation difference: 262 to 2926 m above msl
- Snow contribution: Almost nil.
- Land use: About 50% forest, 30% cultivated on terraced fields, and 20% is urban/barren land.
- Annual rainfall = 1550 mm.
- Rain gauges: Ranikhet, Chaukhatia, Naula, Marchulla, Lansdowne and Kalagarh.
- Streamflow measurement: records of river stages, instantaneous as well as monthly, are available at Kalagarh since 1958.

At the outlet of the Upper Ramganga catchment, i.e. Kalagarh, there exists a multi-purpose Ramganga dam, the salient features of which are:

- Sanctioned in 1973-74
- Dam: 127.5 m high earth and rock-fill dam
 - Storage capacity = 2448 MCM at FRL
 - Purposes:
 - Irrigation = 0.575 million ha in 11 districts of UP,
 - Drinking water = 5.5 cumec to Delhi
 - Hydro-power = 198 Mega Watt (MW)
 - Flood protection
 - Tourism.
- Estimated life = 100 years
 - based on the estimated sediment rate = 4.25 ha-m/100 sq. km per year

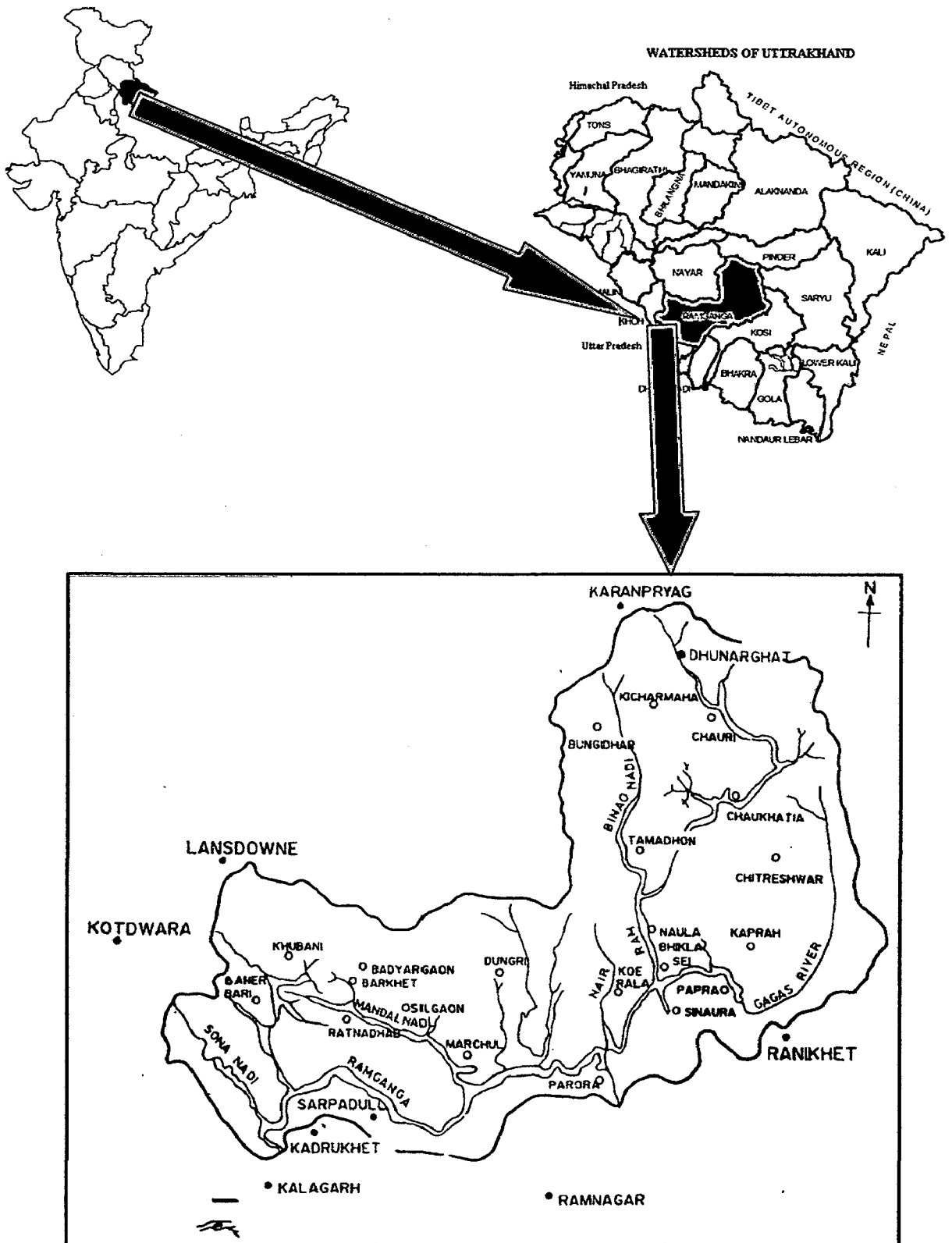


Figure 4.2 Index map of Ramganga Catchment.

4.3 Rapti Catchment

Nepal is a land-locked Himalayan Kingdom located between People's Republic of China and India. Its elevation varies from 60m (msl) at the lowest point to 8848m (msl) (Mt. Everest). The country is divided into three more or less parallel ecological regions namely the Mountains, the Hills and the Terai. The study area i. e. the Rapti sub-watershed geographically lies between 27°51' N & 82°26' E and 28°32' N & 82°64' E. Its area is 3380 km². The climate prevailing in this catchment area is characterised by the monsoon regime with rainfall occurring mainly between July and September (85 % of annual rainfall). Winds are strong and maximum temperatures averages above 32 °C during the remaining months leading to intense average Evapotranspiration 5.6 mm/day. Analysis of the last 30 years of climatic records, established the annual average rainfall at 1401mm. Winds are usually mild. The average minimum temperature for the coldest month is 5.2 °C during December-January. Average maximum during that month reaches 21.8 °C. Air moisture is high during the monsoon months (July to September) with an average of 85 %. It drops sharply during April and May to reach 60%.. Extreme monthly averages, as low as 27%, have been recorded. The major landscape of the catchment area comprise of the foothills of the Churia Muria (Siwalik) ranges and the main Terai plain in the Mid Western Region. Its elevation ranges from 300m (msl) to 1250m (msl). Most of this area is covered by forest and it can be categorised as a Terai Mixed Hardwood forest type.

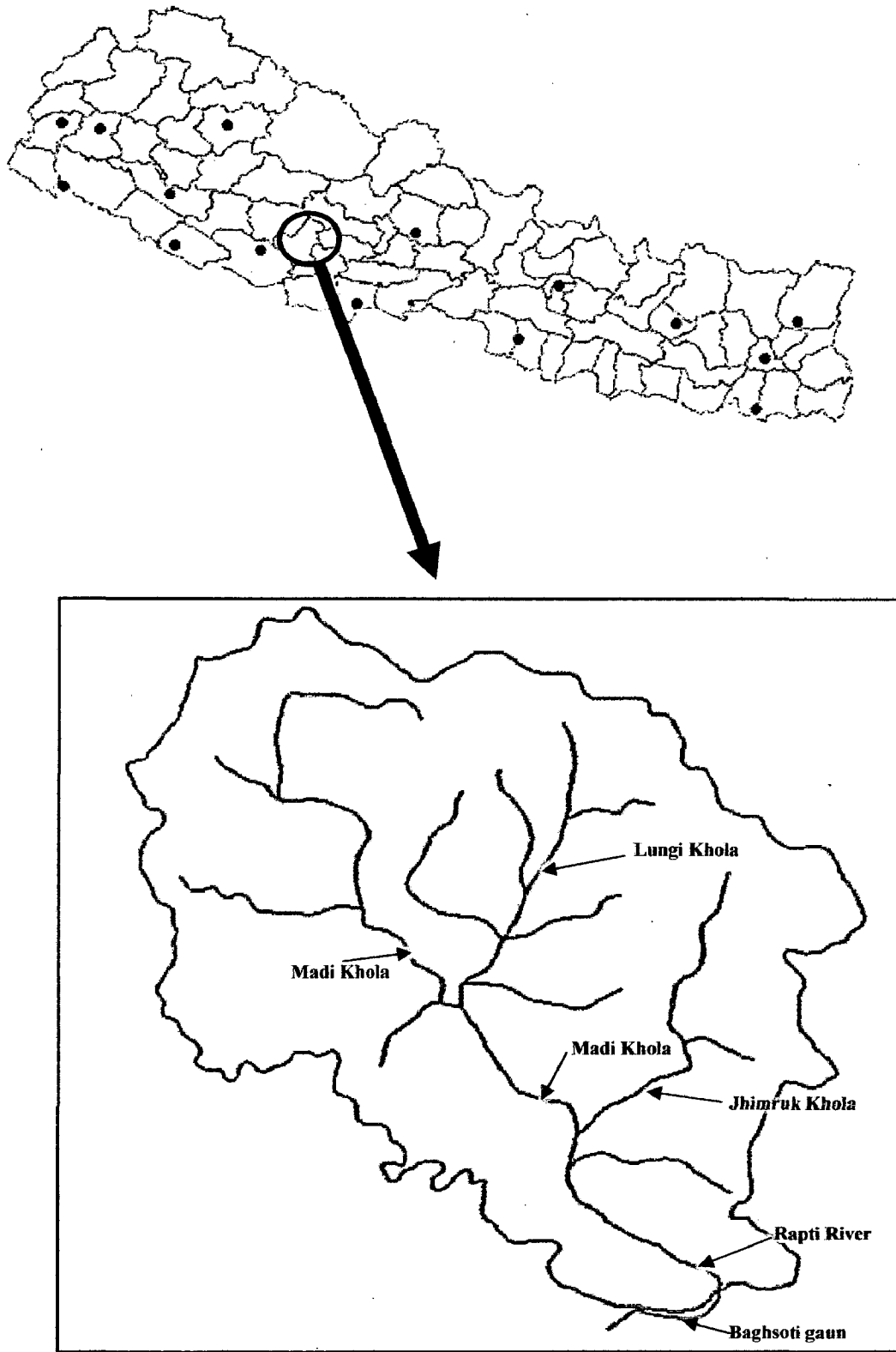


Figure 4.3 Index map of Rapti Catchment (Nepal).

4.4 Data Acquisition

The details of collection of daily rainfall, daily runoff and daily temperature (maximum and minimum) data and other information used in this study are summarised below.

4.4.1 Maithon Catchment

Rainfall Data

Available rainfall data in mm at different raingauge stations along with their Theissen Weight are summarised in Table 4.1.

Table 4.1 Rainfall data availability at different raingauge stations

	Raingauge Stations			
	Maithon Dam Site	Nandadih	Barkisurya	Tilaiya
Data availability	01.06.2000-02.03.2010	01.06.2000-02.03.2010	01.06.2000-02.03.2010	01.06.2000-02.03.2010
Theissen Weight	0.0563	0.3662	0.2817	0.2958

Runoff Data

Runoff data at Maithon were available from 01.06.2000 to 02.03.2010 in ha-m units and these are used in the present study.

Temperature Data

Temperature ($^{\circ}\text{C}$) data at Maithon were available from 01.06.2000 to 02.03.2010 and these are used in the present study to calculate PET.

4.4.2 Ramganga Catchment

Rainfall Data

Available rainfall data in mm at different raingauge stations along with their Theissen Weight are summarised in Table 4.2.

Table 4.2 Rainfall data availability at different raingauge stations

	Rain gauge Stations					
	Chaukhutia	Marchula	Naula	Kalagarh	Ranikhet	Lansdown
Data availability	01.06.78-25.11.09	01.06.78-25.11.09	01.06.78-25.11.09	01.06.78-25.11.09	01.06.78-25.11.09	01.06.78-25.11.09
Theissen Weight	0.298	0.251	0.19	0.081	0.088	0.092

Runoff Data

Runoff data in MM^3 at Kalagarh were available from 01.06.78-25.11.09 and these are used in the present study.

Temperature Data

Temperature data ($^{\circ}\text{C}$) at Kalagarh were available from 01.06.78 to 25.11.09 and these are used in the present study to calculate the PET.

4.4.3 Rapti Catchment

Rainfall Data

Available rainfall data in mm at different raingauge stations along with their Thiessen Weight are summarised in tabular form -

Table 4.3 Rainfall data availability at different raingauge stations

	Rain gauge Stations		
	Shera Gaun	Libang Gaun	Bijuwar Tar
Data availability	01.01.1966- 01.01.2008	01.01.1966- 01.01.2008	01.01.1966- 01.01.2008
Theissen Weight	0.0933	0.4901	0.4165

Runoff Data (m^3/s)

Runoff data in m^3/s at Baghsutigau (27 $^{\circ}$ 51'12"N; 82 $^{\circ}$ 47'34"E) were available from 01.01.1977 to 01.01.2008 and these are used in the present study.

Temperature Data

Due to non availability of climate data of sub-watershed of Rapti catchment, neighbouring station (Surkhet, geographically located at 28 $^{\circ}$ 36'N; 81 $^{\circ}$ 37'E, at an elevation of 720m above msl) data ($^{\circ}\text{C}$) were used for PET estimation. Temperature data at this station were available from 01.01.1973 to 01.01.2008.

To show the adequacy of rainfall data stations, it is in order to present here the World Meteorological Organisation (WMO) recommendations for densities of raingauge stations depending on several feasibilities:

1. In flat regions of temperate, Mediterranean and tropical zones:

Ideal—one station for 600-900 km^2 ,

Acceptable---one station for 900-3000 km^2 ;

2. In mountainous regions of temperate, Mediterranean and tropical zones:

Ideal—one station for 100-250 km²,

Acceptable---one station for 250-1500 km²;

3. In arid and polar zones: one station for 1500-10000 km².

The above indicates the density of rainfall stations in the above catchments was sufficient to describe the data.

4.5 Data Processing

The available data was processed for different catchments as follows:

- a. The daily data (i.e. the Rainfall, Runoff, and Temperature) available from various sources were computerized. These were checked missing data, if any, and wherever found to be missing, it was replaced by the average value for that day of a particular month.
- b. Date-wise weighted average Rainfall (mm) values were computed for each catchment.
- c. The daily runoff data available in either MM³, ha-m or in m³/s units were converted to mm unit.
- d. Daily PET data (in mm) were computed form Hargreaves formula using temperature (max, min) and Extraterrestrial radiation (in mm/day).

This chapter presents the results of application of the methodology (Chapter 3) to the data of Maithon, Ramganga, Rapti catchments. To this end, curve numbers were derived for different durations and different AMCs, then PET values were calculated for the same durations as of curve numbers, and finally the derived curve numbers (or S) for different durations, but for AMC I, were correlated with the PET values of corresponding duration.

5.1 Determination of Curve Number, CN

The daily rainfall (mm), runoff (mm) and PET (mm) were arranged in chronological order and these were sorted in descending order of rainfall. Only those daily rainfall and corresponding runoff and PET values were retained for analysis which showed runoff factor C to be less than or equal to 1. Only these daily (or any other duration) rainfall-runoff events were considered for CN-derivation, as shown in Figs. 5.1a-c. In these figures, the probability of rainfall exceedence [= $m / (N+1)$, where m is the order or rank and N is the total number of events] is computed using the Weibull's plotting position formula applied to the observed rainfall data. Then, trial CN value was considered such that the daily runoff values computed using the daily rainfall (at abscissa of Fig. 5.1a-c) and when plotted on the same figure represented the upper bound of the whole data. This CN-value was taken to correspond to AMC-III. Similarly, CN corresponding to AMC-II fitted the mid of the whole data, and CN corresponding to AMC-I represented the lower bound of the whole data. Here, it is noted that since these CN-values were derived from daily rainfall-runoff data series, these are taken to correspond to 1-d rain duration. Employing this procedure, curve numbers were derived for different rainfall durations using the rainfall-runoff data summed for the desired duration (2d, 3d and so on). The variation of CN with rain duration of 1 day, as an example, is shown in Figs 5.2a-c. For other durations and for all three watersheds, these are shown in Appendix-III.

5.2 Determination of PET_{av}

For each data series of different rainfall duration(s), PET-values were computed for each duration in the series and these were averaged to compute PET_{av} . Figs. 5.3a-c shows the relation between rain duration and corresponding PET_{av} .

5.3 Determination of PET_{av} and S relation

Considering AMC-I to correspond to fully dry condition, which corresponds to the maximum possible or potential water loss in the watershed, the S-values were computed for this condition and for different rainfall durations, viz, 1d, 2d, 3d and so on. Fig. 5.4a-c shows the relation between S and PET_{av} , which is similar to that proposed by Eq. (3.6b).

5.4 Analysis and Discussion of Results

In Figs. 5.1a-c, the ordering of data forces the rainfall to exhibit a definite trend in the resulting runoff. The joining of scattered data points (not shown) revealed in the observed runoff values a cyclic trend of high and diminishing amplitude at low and increasing probability of exceedence, respectively. Thus, the whole runoff spectrum appears to be reasonably bounded within two upper and lower envelopes, which can be distinguished by the curve numbers as shown, for example, in Fig. 5.1a for Maithon watershed. In this figure, the upper and lower fitted bounds correspond to $CN=98$ and $CN=58$, respectively. These limits can be reasonably treated to correspond to wet (AMC III) and dry (AMC I) conditions. The visually fitted mid runoff (Q)-curve can be taken to represent the normal (or AMC II) state, for which, $CN=90$ for the Maithon catchment. Similarly, Figs. 5.1b & c can be explained, for they exhibit similar trends. The derived CN statistic for all the three watersheds is given in Table 5.1.

From Fig. 5.1a, the limiting values of probability of rainfall exceedence for $CN=58$ is equal to 2.85 % which corresponds to rainfall magnitude of $P > 36.8$ mm to start runoff occurring in one day; for $CN=98$, the limiting value is equal to 51.53 %, which corresponds to $P > 1.0$ mm to start runoff generation; and for the normal state ($CN=90$), the limiting value is 4.89 %, which is equal to $P > 28.2$ mm of rainfall to start runoff generation. The limiting rainfall amount of 36.8 mm for the lower bound actually represents the maximum amount of initial abstraction occurring in the Maithon catchment in one day. Table 5.1 also provides the details of 1-d minimum rainfall to produce direct surface runoff and maximum S-values for all the watersheds. Since these curve numbers

are calculated from the observed rainfall-runoff data and, therefore, account for all the watershed and precipitation characteristics, these are better representative of watersheds than those estimated by any other means, such as tabulated values derived using a few runoff producing physical characteristics.

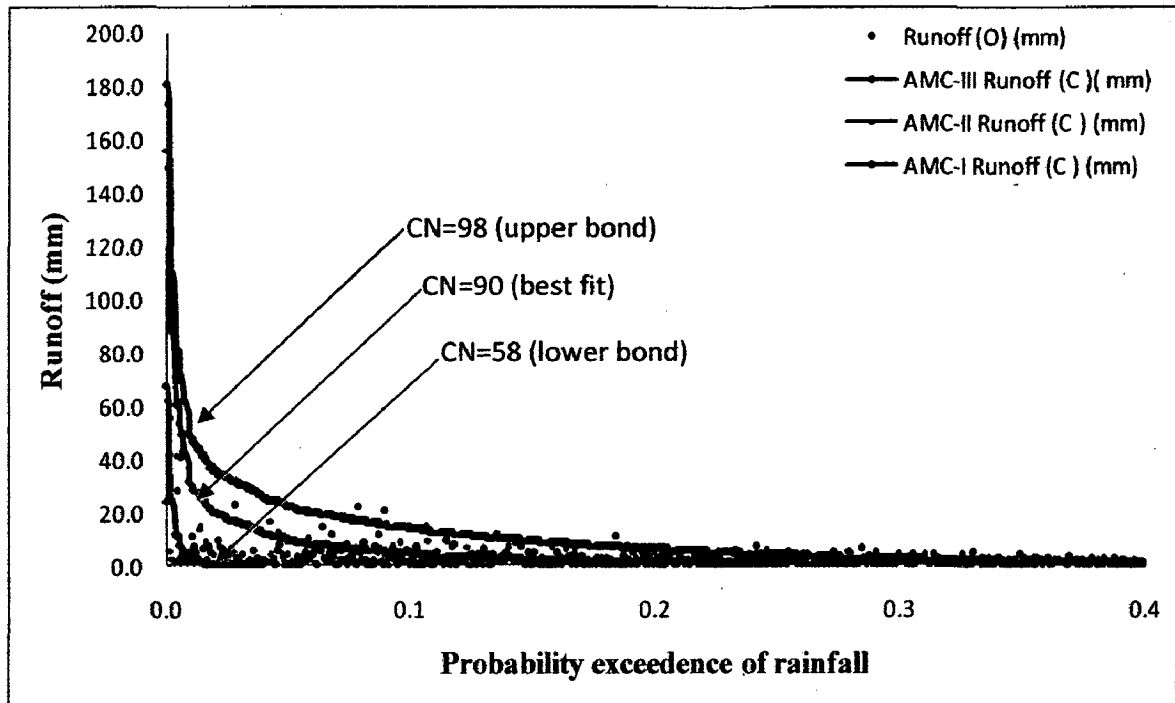


Fig. 5.1a Ordered daily runoff data of Maithon catchment for determination of CN for three AMCs. Upper and lower bound curve numbers refer to AMC-II and AMC-I respectively and best-fit to AMC-II.

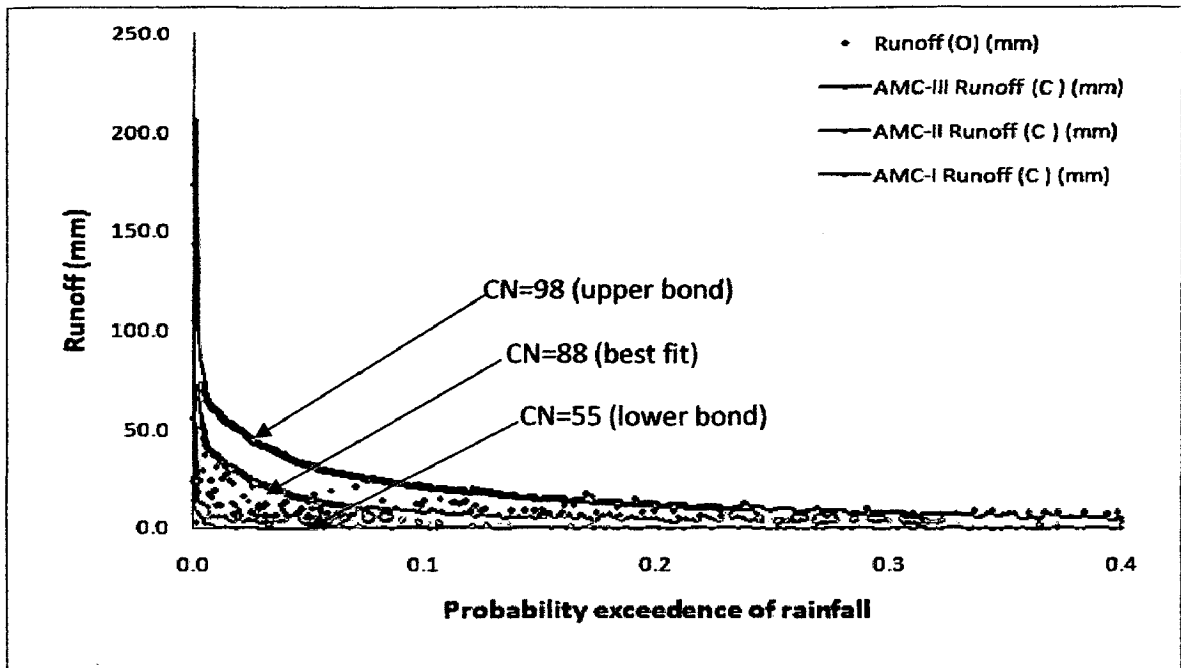


Figure 5.1b Ordered daily runoff data of Ramganga catchment for determination of CN for three AMCs. Upper and lower bound curve numbers refer to AMC-II and AMC-I respectively and best-fit to AMC-II.

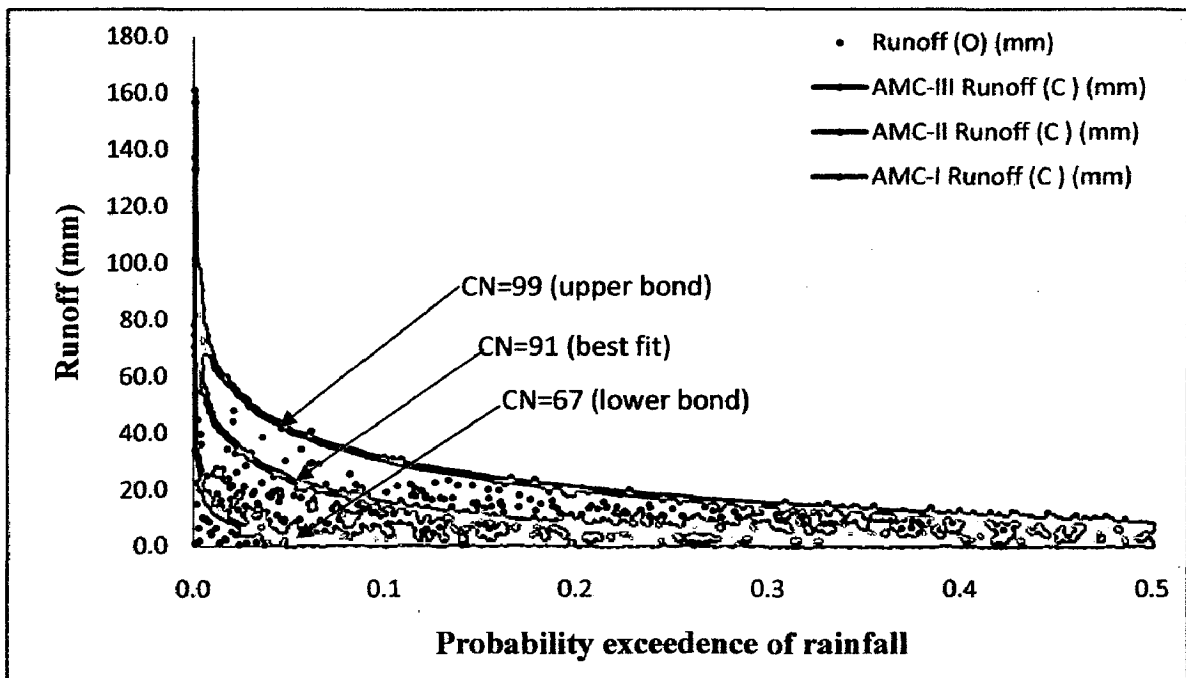


Figure 5.1c Ordered daily runoff data of Rapti catchment for determination of CN for three AMCs. Upper and lower bound curve numbers refer to AMC-II and AMC-I respectively and best-fit to AMC-II.

Table 5.1 Statistics of the fitted curve numbers to daily data of different watersheds

Watershed	No. of P-Q data points (% of total)*	1-d curve numbers (CN)			1-d minimum rainfall (mm)			Max. S (mm)
		AMC I	AMC II	AMC III	AMC I	AMC II	AMC III	
Maithon	1860(50)	58	90	98	36.8	28.2	1.0	183.93
Ramganga	3534(30.7)	55	88	98	41.6	6.9	1.0	207.80
Rapti	2942(25.2)	67	91	99	25.0	5.0	0.5	114.12

*values in () indicate P-Q datasets with $C < 1$.

The following text investigates the effect of rain duration on curve number and PET_{av} , in what follows.

5.4.1 Effect of Rain Duration on Curve Number

The sample plot of the curve numbers varying with storm duration for Maithon watershed is shown in Fig. 5.2a, as other figs. b & c are similar. From Fig. 5.2a, it is clear that CN inversely varies with rainfall duration for all the three AMCs. It is consistent with the expectation that CN would increase with reduction in rain duration, and vice versa, for the reason of less opportunity time available for water loss in the watershed. It is an easy tool to calculate directly CN value for any duration of rainfall of the said catchment.

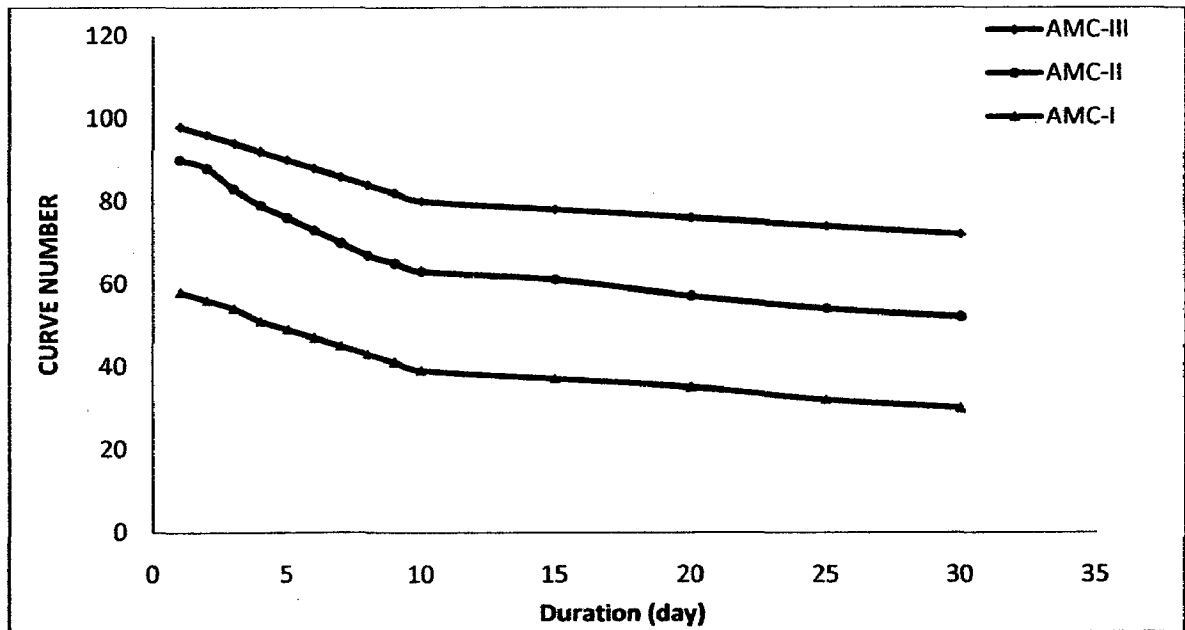


Figure 5.2a CN Variation with rainfall duration (greater than or equal to 1 day) for Maithon.

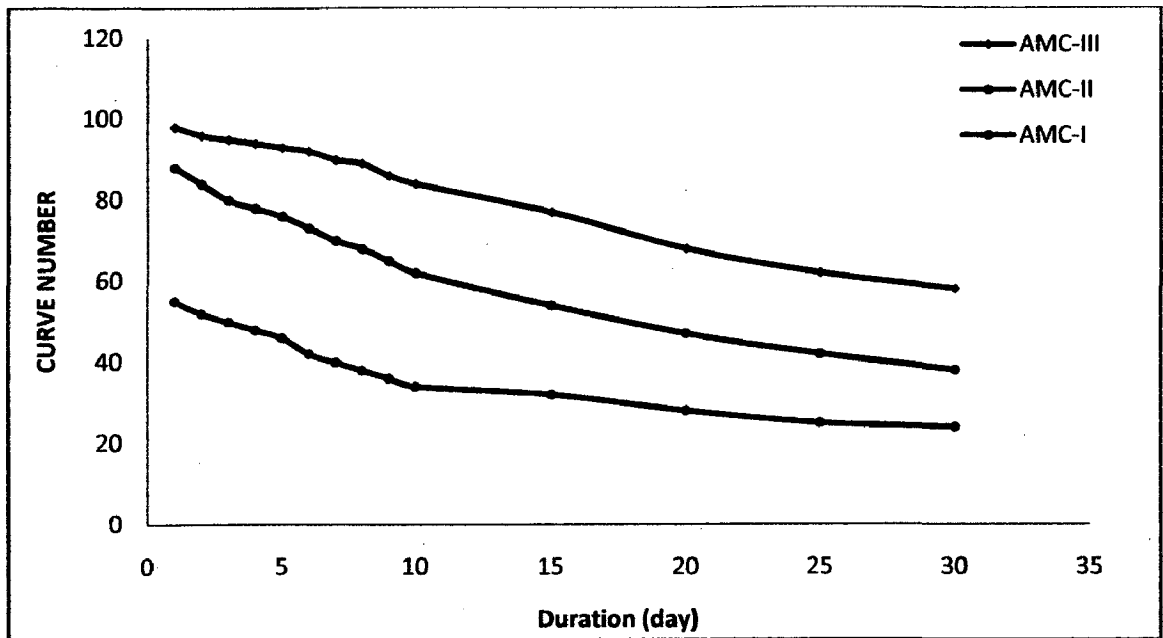


Fig. 5.2b CN Variation with rainfall duration (greater than or equal to 1 day) for Ramganga.

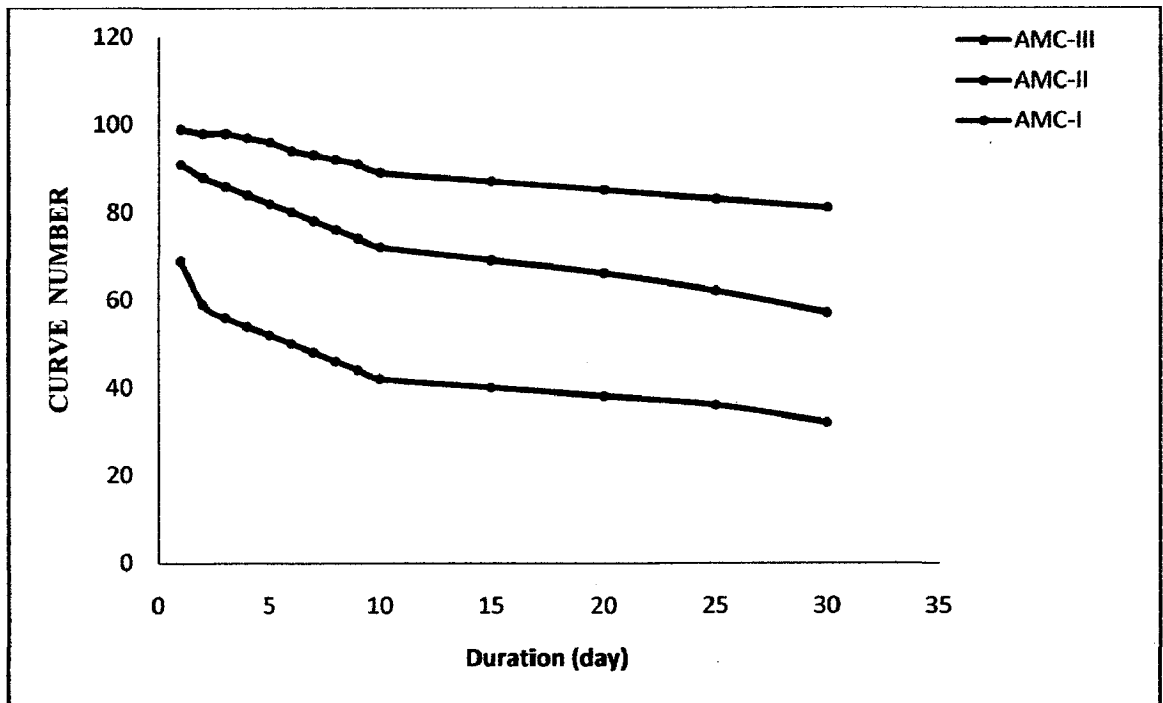


Figure 5.2c CN Variation with rainfall duration (greater than or equal to 1 day) for Rapti.

5.4.2 Effect of Rain Duration on PET

The sample plot of PET_{av} varying with rain duration for Maithon watershed is shown in Fig. 5.3a. From the figure it is clear PET_{av} linearly varies with the rainfall duration. It is consistent with the expectation that as duration increases, PET would increase, and vice versa.

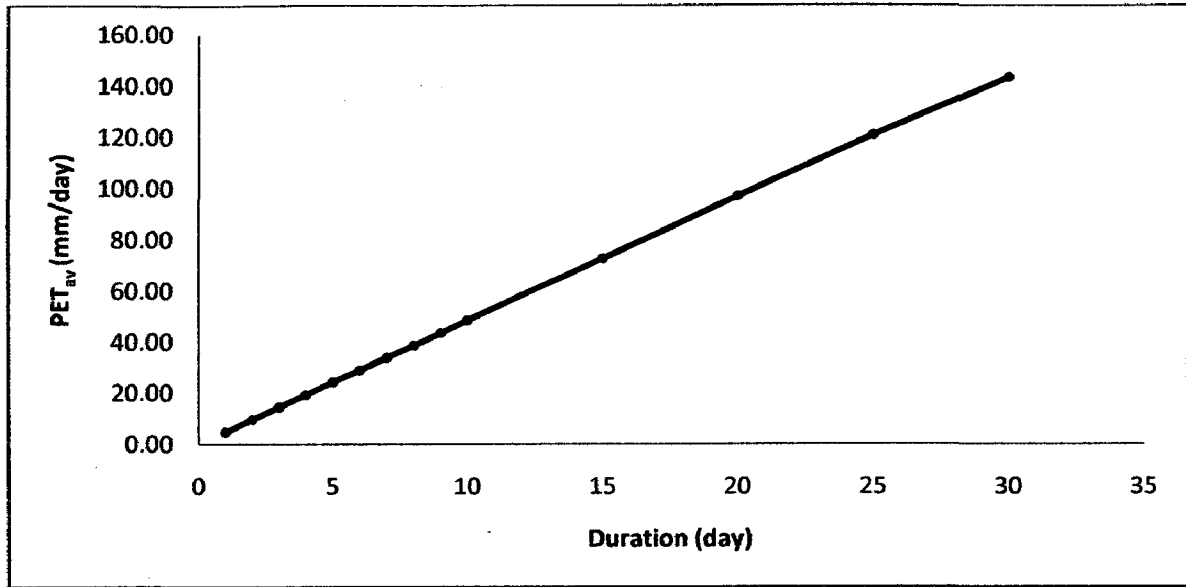


Figure 5.3a PET_{av} variation with rainfall duration (greater than or equal to 1 day) for Maithon catchment.

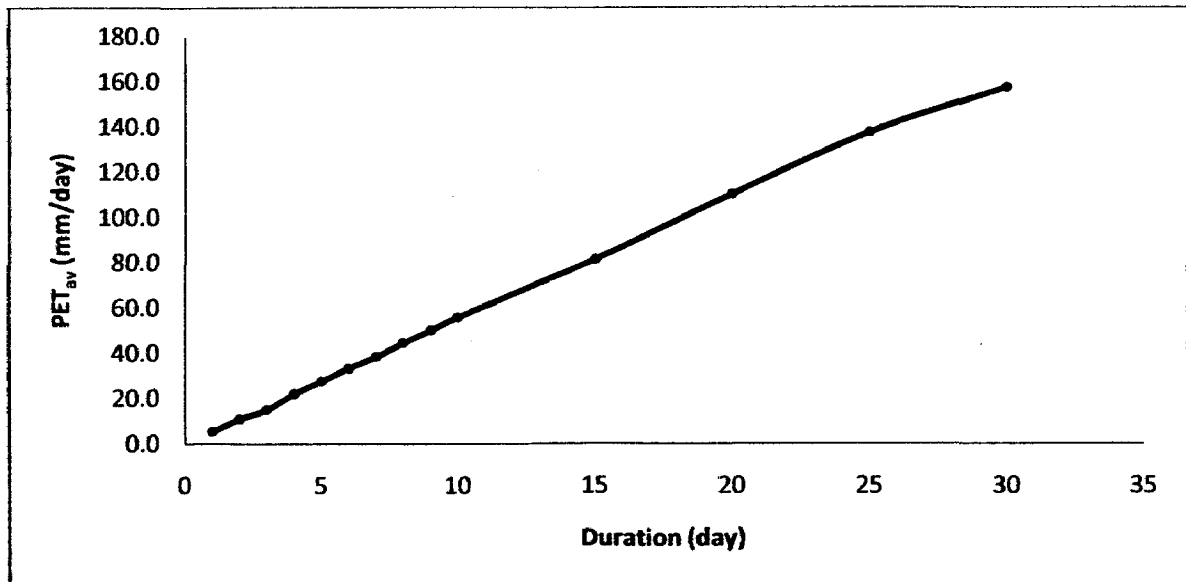


Figure 5.3b PET_{av} variation with rainfall duration (greater than or equal to 1 day) for Ramganga catchment.

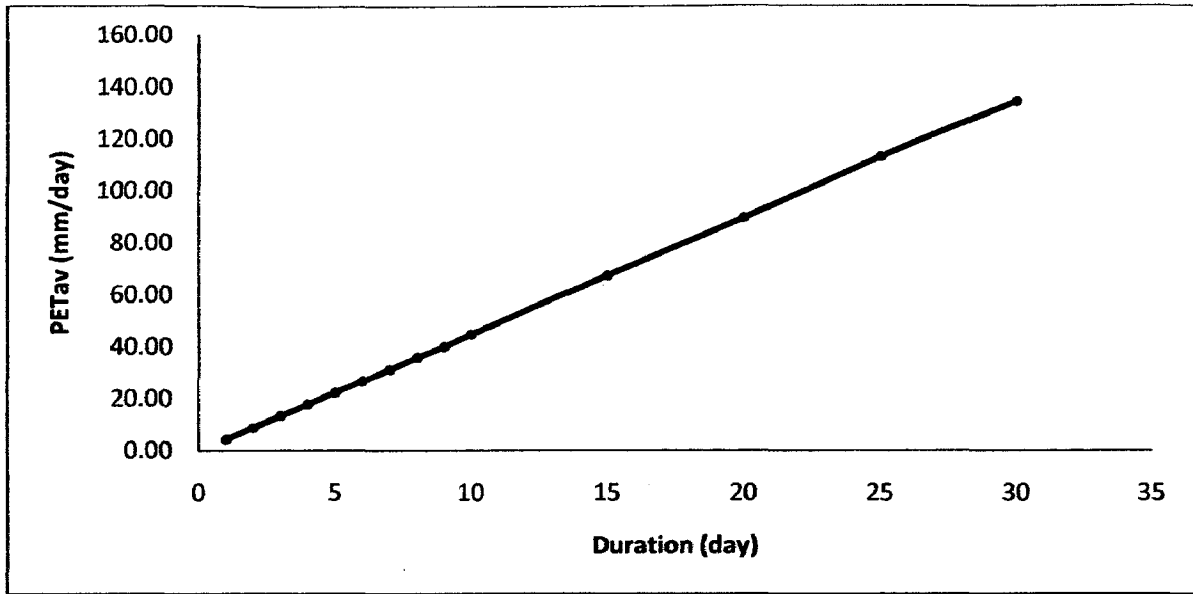


Figure 5.3c PET_{av} variation with rainfall duration (greater than or equal to 1 day) for Rapti catchment.

5.5 Relation between S and PET

Figs. 5.4a-c show the relations between S and PET_{av} for Maithon, Ramganga, and Rapti catchments, respectively. These can be expressed mathematically as below:

$$PET_{av} = 1.0 \times 10^{-5} S_I^{2.575} ; R^2 = 0.963 \quad \text{for Maithon watershed} \quad (5.1)$$

$$PET_{av} = 5.0 \times 10^{-5} S_I^{2.242} ; R^2 = 0.959 \quad \text{for Ramganga watershed} \quad (5.2)$$

$$PET_{av} = 5.0 \times 10^{-6} S_I^{2.328} ; R^2 = 0.989 \quad \text{for Rapti watershed} \quad (5.3)$$

These relations with high coefficient of determination indicate the strong dependence of PET_{av} on S (or CN), which may be quite useful and reliable tool for determination of PET_{av} from CN. For clarification, an example is briefly illustrated, if the duration of rainfall event is 3-d, then the CN for this duration is obtained from Fig. 5.2a for Maithon watershed is 54, and hence, S is equal to 216.37 mm and, in turn, PET_{av} from Eq. 5.1 is 10.30 mm for 3-d duration.

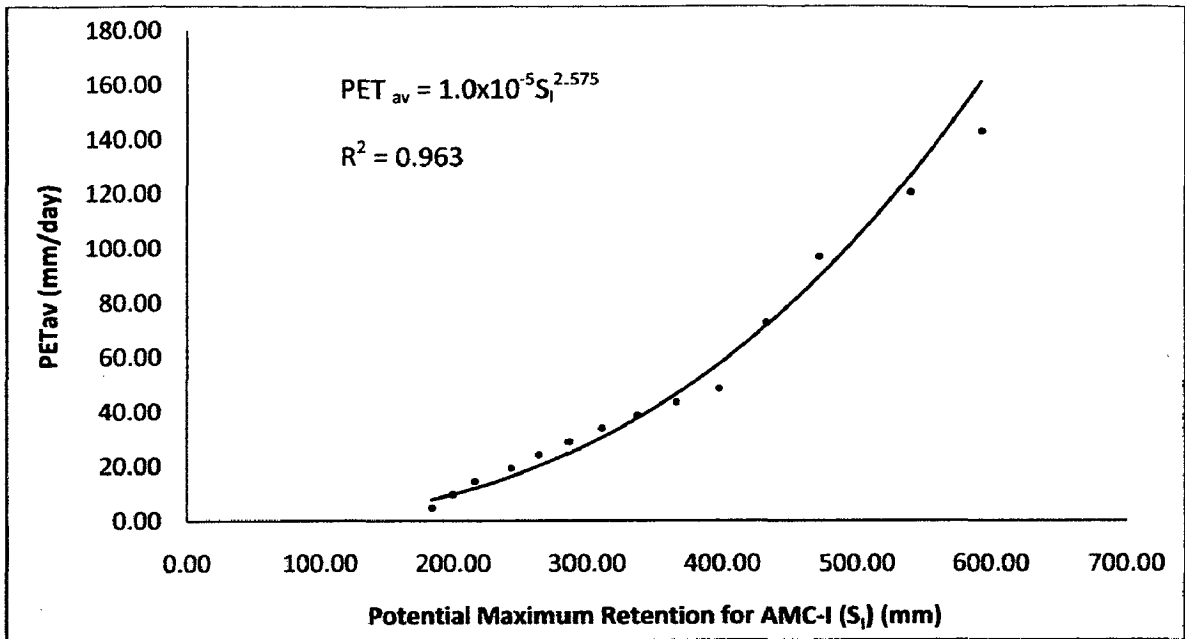


Figure 5.4a Potential maximum retention for AMC I (S_i) and PET relationship for Maithon catchment.

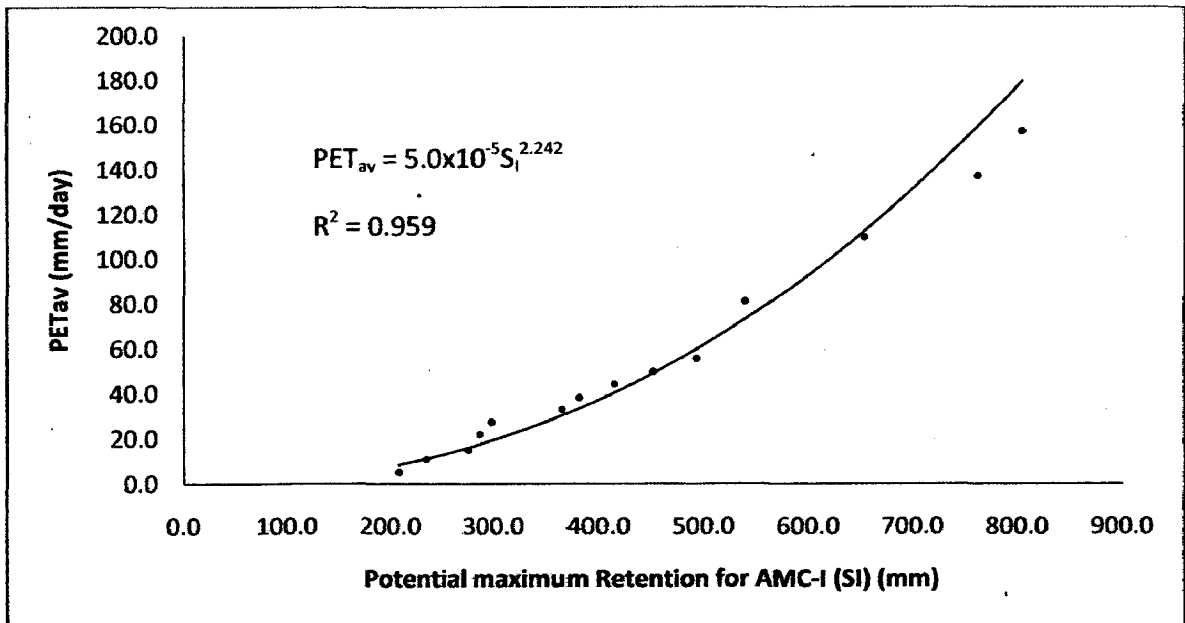


Figure 5.4b PET and potential maximum retention for AMC I (S_i) relationship for Ramganga catchment.

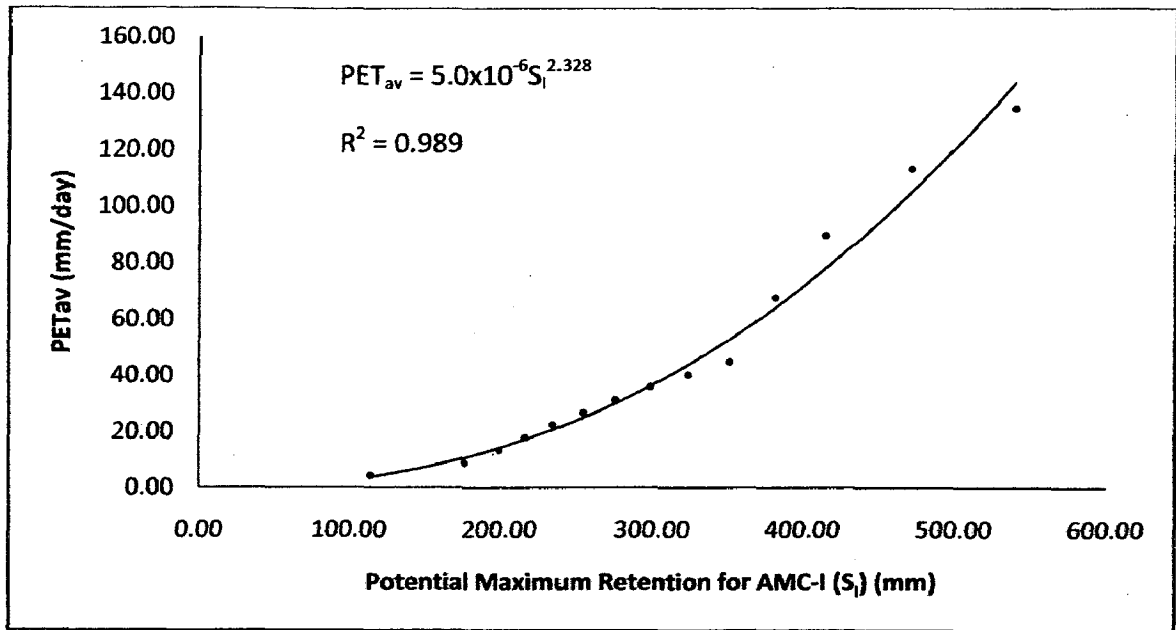


Figure 5.4c PET and potential maximum retention for AMC I (S_1) relationship for Rapti catchment.

5.6 Advantages and limitations of the proposed study

The encouraging results of this study suggest the methodology may be a substitute for the complex PET estimation methods, especially in developing countries where establishment of new meteorological stations are not ever possible due to their high installation and operational costs. In addition, the proposed concept eliminates the need of costly measurements of ground water inflow and outflow, required in the water balance method. However, the proposed concept helps derive a long-term mean of potential evapotranspiration, and therefore, is not time/duration/season specific. In addition, since parameter λ is a regional parameter that depends on geological and climatic factors and hence most sensitive parameter in PET estimation, results can be made more promising with the use of adequate value of λ other than the standard value of 0.2.

The following conclusions can be derived from the study based on the analysis of data of three watersheds, viz., Maithon (Jharkhand, India), Ramganga (UK, India), and Rapti (Nepal) watersheds:

- i. The runoff curve numbers derived from long-term daily rainfall runoff data of a watershed better represent the integrated effect of all precipitation (or in turn meteorologic or climatic) and watershed's physical characteristics than those derived using NEH-4 Tables based on only four watershed characteristics or than those derived only from a few historical rainfall-runoff events, ignoring a number of (although low) rainfall-runoff events.
- ii. The derived runoff curve numbers exhibited a strong dependence on the storm duration, consistent with the expectation that the larger rain duration provides greater opportunity time for water loss to occur in the watershed.
- iii. The computed PET_{av} exhibited a strong dependence on the storm duration. It is also consistent with the notion that as the duration increases, PET increases, and vice versa.
- iv. Like any other physical variable, there exists an upper limit for the initial abstractions to occur in a watershed. In this study, for Maithon, maximum $I_a = 36.8$ mm; for Ramganga, maximum $I_a = 41.6$ mm; and for Rapti, maximum $I_a = 25.0$ mm (AMC-I; 1d).
- v. PET and CN were inversely (or directly with potential maximum retention S) correlated (with $R^2 = 0.959$ to 0.989) indicating the larger the PET, the lesser the CN or the lesser the runoff, and vice versa. High R^2 values support the general applicability of the proposed concept. Such a relationship describes S in terms of the maximum possible evaporable depth.

APPENDIX-I

ANTHROPOGENIC CAUSES OF CLIMATE CHANGE

Anthropogenic climate change refers mainly to the production of greenhouse gases emitted by human activity. By examining the polar ice cores, scientists are convinced that human activity has increased the proportion of greenhouse gases in the atmosphere, which has skyrocketed over the past few hundred years. Before going to the illustration it is shouted to realise the mechanism of climate and the natural variability in the climate system.

I.1 The mechanism of climate

The major factors that determine the patterns of climate on earth can be explained in terms of:

- the strength of the incident radiation from the sun, which determines the overall planetary temperature of the earth;
- the spherical shape of the earth and the orientation of its axis;
- the greenhouse effect of water vapour and other radiatively active trace gases;
- the various physical, chemical and biological processes that take place within the atmosphere- geo-sphere-biosphere climate system, in particular:
 - the global energy balance,
 - the global water cycle,
 - the global carbon cycle and other biogeochemical cycles;
- the rotation of the earth, which substantially modifies the large-scale thermally-driven circulation patterns of the atmosphere and ocean; and
- the distribution of continents and oceans.

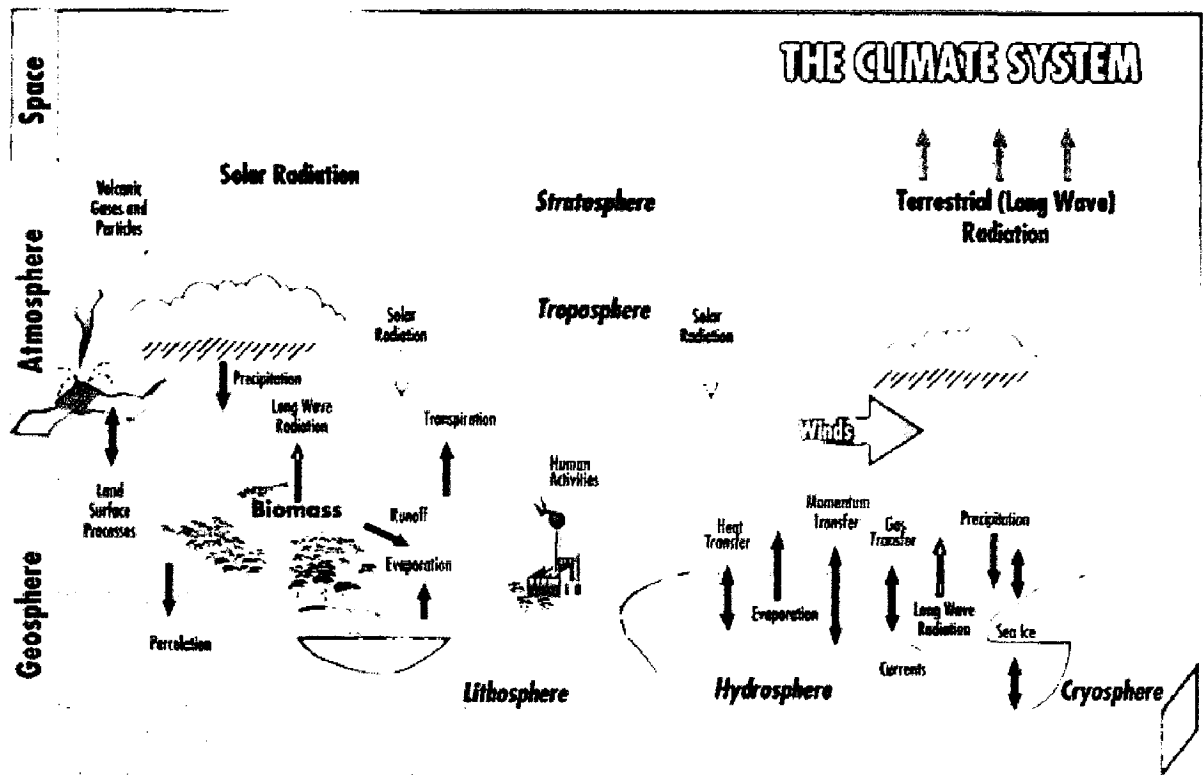


Figure I.1 The components of the global climate system.
(Source: www.google.com)

I.2 Natural variability in the climate system

In addition to the annual (seasonal) cycle of climate, global and regional climates are in a perpetual state of change on time-scales from months to millions of years. As a result, society and nature are in a continuous process of adaptation to change. A range of factors can lead to changes in climate on these time-scales, some internal to the climate system and some external, some naturally occurring. In addition to physical mechanisms of climate variability, there are also random, chaotic fluctuations within the climate system.

The leading factors are:

- The annual cycle
- Orbital cycles
- Fluctuations in solar output
- Fluctuations in earth's rotation rate
- Volcanic eruptions

- Changes in land and ocean floor topography
- El Niño – Southern Oscillation
- Pacific decadal oscillation
- North Atlantic oscillation
- Ocean and polar ice variations

The details of such natural factors have been described elsewhere in the literature.

I.3 Human influences on the climate system

The fact of the matter is that the natural impacts on the climate (changes in solar output, explosive volcanic activity etc.) have not been nearly significant enough to account for all this change. Rather, it has been the impact of humans driving climate change. As a result, we will face more severe droughts, floods, and storms and changes to our environment in the future. With industrialization and development, lifestyles/cultures that favor individualism and consumerism, and an increasing populace demanding their share—*all within the past few hundred years*—how could changes not take place?

I.3.1 Changing patterns of land use

Broad-scale changes in land-use patterns, such as deforestation, can significantly alter the roughness and reflectivity of the surface for solar radiation, and *hence the absorbed radiation, evaporation and evapotranspiration*. In the process, changes in regional climate can occur. Broad-scale changes in land use also impact on the global climate by enhancing the natural greenhouse effect, for example by reducing the land's capacity to absorb carbon dioxide (e.g. through deforestation) and by increasing the carbon emission from the land (e.g. through increased biomass decay), both of which lead to greater concentrations of greenhouse gases.

I.3.2 Changes in urban climate

The Urban Heat Island (UHI) refers to the observation that towns and cities tend to be warmer than their rural surroundings due to physical differences between the urban and natural landscapes. The concrete and asphalt of the urban environment tend to reduce a city's reflectivity compared with the natural environment. This increases the amount of solar radiation absorbed at the surface. Cities also tend to have fewer trees than the rural surroundings and hence the cooling effects of shade and *evapotranspiration are reduced*.

The cooling effects of winds can also be reduced by city buildings. The UHI is enhanced by human activities within the urban environment. Pollution has a warming effect on a city, in addition to the heat released by industrial processes, household heating and car use. As cities grow, the UHI effect becomes stronger, creating an artificial warming trend in the temperature record. The UHI is most noticeable during clear, still nights when rural areas are most effectively able to radiate the heat gained during the day back to space, while the urban environment retains a greater proportion of heat. Depending on the weather conditions, overnight temperatures in the centre of a large city can be up to 10°C warmer than the rural surroundings. The urban landscape has other impacts on the local climate, such as reduced average wind speed due to the blocking effect of buildings and greater frequency of flash flooding owing to the higher proportion of ground sealed with concrete and asphalt and a corresponding reduction in natural drainage.

I.3.3 Nuclear winter

One of the largest potential influences on future climate is the threat, now generally believed to have receded, of a nuclear winter resulting from the enormous increase in smoke and dust in the atmosphere that would follow a nuclear holocaust. Calculations of the potential characteristics of the nuclear winter have been performed for a range of nuclear war scenarios. A nuclear war would probably have the most sudden and disastrous impact on climate of which humanity is at present technologically capable. A somewhat similar and equally catastrophic effect could be expected to follow from earth's collision with a major asteroid or comet.

I.3.4 Anthropogenic sources of greenhouse gases

More than a hundred years the first scientific explanation of the earth's natural greenhouse effect given by a Swedish scientist Svante Arrhenius (1895), that the additional warming might be expected from increased carbon dioxide in the atmosphere. Over the past two decades, the evidence for a continuing build-up of carbon dioxide and other greenhouse gases as a result of human activities has become conclusive. These changes have come about as a combined effect of increase in emissions, such as fossil fuel burning, and decrease in sinks, such as reduced forest cover.

Table I.1 Greenhouse gases influenced by human activities.

Greenhouse gases	Principal sources	Sinks	Lifetime in atmosphere	Proportional contribution to greenhouse warming
Carbon-dioxide (CO ₂)	Fossil-fuel-burning, deforestation, biomass burning, gas flaring, cement production.	Photosynthesis, ocean surface	5 to 200 years	60%
Methane(CH ₄)	Natural wetlands, rice paddies, ruminant animals, natural gas drilling, venting and transmission, biomass burning, coal mining.	Reaction with tropospheric hydroxyl (OH), removal by soils.	12 years	20%
Halocarbons (includes CFCs, HFCs, HCFCs)	Industrial production and consumer goods (e.g., aerosol propellants, refrigerants, foam-blowing agents, solvents, fire retardants)	Varies (e.g., CFCs, HCFCs: removal by stratospheric photolysis, HCFC, HFC: reaction with tropospheric hydroxyl (OH))	2 to 50,000 years (e.g., CFC-11: 45 years, HFC-23: 260 years, CF ₄ : >50,000 years)	14%
Nitrous-oxide (N ₂ O)	Biological sources in oceans and soils, combustion, biomass burning, fertilizer	Removal by soils, stratospheric photolysis	114 years	6%

(Source: www.google.com)

I.3.5 Enhanced greenhouse effect

Any changes in the relative mix and atmospheric concentration of greenhouse gases, whether natural or human-induced, will lead to changes in the radiative balance of the atmosphere, and hence the level of greenhouse warming. Calculations with global climate models have drawn clear links between increased concentrations of greenhouse gases and large-scale surface warming and other changes of climate. It seems likely that, through the 21st century, enhanced radiative forcing by increases in these gases will have a significant influence on global climate, including a detectable warming '*signal*' above and beyond the '*noise*' of natural variability. The scientific basis for expectation of an enhanced greenhouse effect is conceptually simple. Increased concentrations of the radiatively active gases (such as carbon dioxide) increase the opacity of the lower atmosphere to radiation from the surface. Therefore, the lower atmosphere absorbs and re-emits more radiation. Some of this is directed downwards, increasing the heating of the surface. This heating continues until a new equilibrium temperature profile is established between the upward surface radiation and downward solar and long wave radiation.

I.3.6 Aerosols and other pollutants

Tropospheric aerosols (i.e. microscopic airborne particles) influence the radiative balance of the atmosphere and thus the climate. These aerosols result both from natural sources, such as forest fires, sea spray, desert winds and volcanic eruptions, and from human causes, such as the burning of fossil fuels, deforestation and biomass burning. They can impact on the radiative flux directly, through absorption and scattering of solar radiation, or indirectly, by acting as nuclei on which cloud droplets form. This in turn influences the formation, lifetime and radiative properties of clouds. Concentrations of tropospheric aerosols vary greatly in space and time and can have either a heating or cooling effect depending on their size, concentration, and vertical distribution. The cooling effect of aerosols from sulphur emissions may have offset a significant part of the greenhouse warming in the northern hemisphere during the past several decades. Because of their relatively limited residence time in the troposphere, the effect of aerosol pollutants from industrial processes and forest burning is largely at the regional level. With the pollutant

load on the atmosphere generally continuing to increase, the impacts of aerosols on climate will continue to be significant.

The processes just described are the major determinants of the present day patterns of climate over the globe. The previous sections also highlight the inherently international nature of climate. As climate knows no political boundaries, understanding it requires a cooperative international effort. This is particularly the case for understanding climate at a global scale where systematic and comprehensive global observations are required.

HARGREAVES METHOD

The Hargreaves Method (Hargreaves and Samani, 1982; 1985) is suggested as a means for estimating grass resistance PET (PET_o) in situations where data are limited and only maximum and minimum air temperature data are available. The Hargreaves equation is expressed as

$$PET_o = 0.0023(T_{max} - T_{min})^{0.5}(T_{mean} + 17.8) R_a \quad (I.1)$$

where T_{max} is the daily maximum temperature ($^{\circ}C$), T_{min} is the daily minimum temperature ($^{\circ}C$), T_{mean} is the daily mean temperature ($^{\circ}C$) and R_a is the extraterrestrial radiation (cm/day).

Extraterrestrial radiation for daily periods (R_a) ($MJ\ m^{-2}d^{-1}$)

$$R_a = \frac{24(60)}{\pi} G_{sc} d_r [\omega_s \sin(\varphi) \sin(\delta) + \cos(\varphi) \cos(\delta) \sin(\omega_s)] \quad (I.2)$$

where G_{sc} is the solar constant ($= 0.0820\ MJ\ m^{-2}\ min^{-1}$); d_r is the inverse relative distance earth-sun; ω_s is the sunset hour angle (rad); φ is the latitude (rad); and δ is the solar declination (rad). The inverse relative distance earth-sun, d_r , and the solar declination, δ , are given by

$$d_r = 1 + 0.033 \cos\left(\frac{2\pi}{365} J\right) \quad (I.3)$$

$$\delta = 0.409 \sin\left(\frac{2\pi}{365} J - 1.39\right) \quad (I.4)$$

where J is the number of the day in the year between 1 (1 January) and 365 or 366 (31 December.) The sunset hour angle, ω_s , is given by:

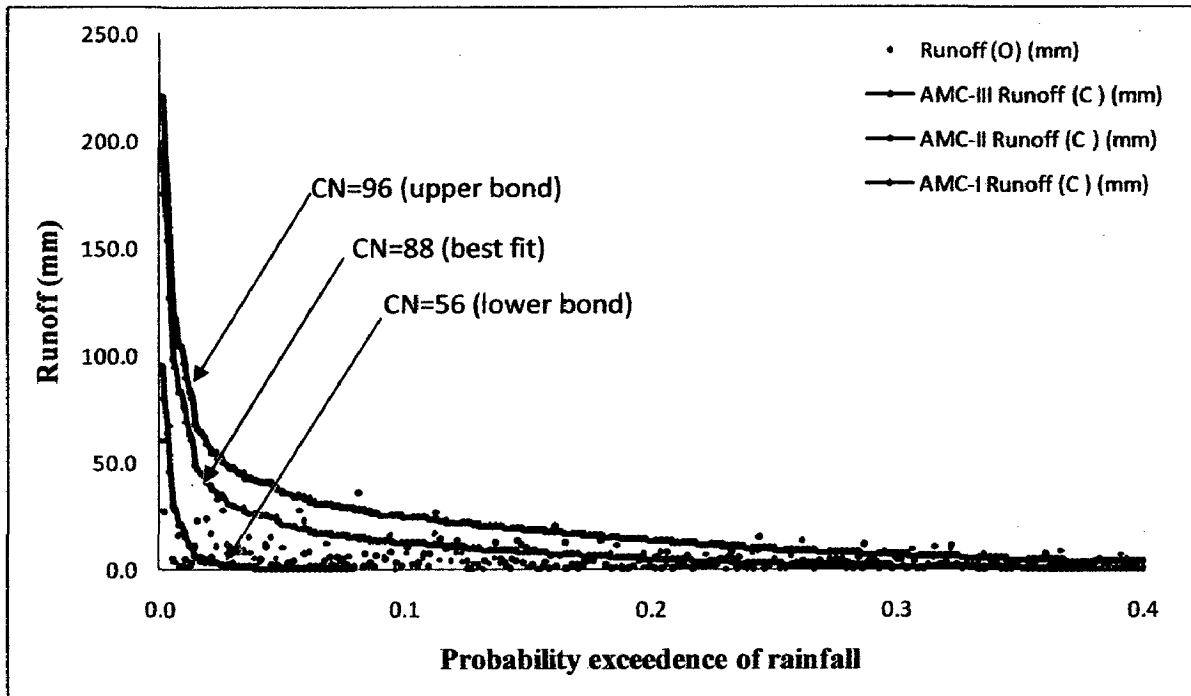
$$\omega_s = \arccos[-\tan(\varphi)\tan(\delta)] \quad (1.5)$$

The R_a -values (Table I.1) dependent on latitude and available elsewhere (K. C. Patra,2008) were taken for use in the present study.

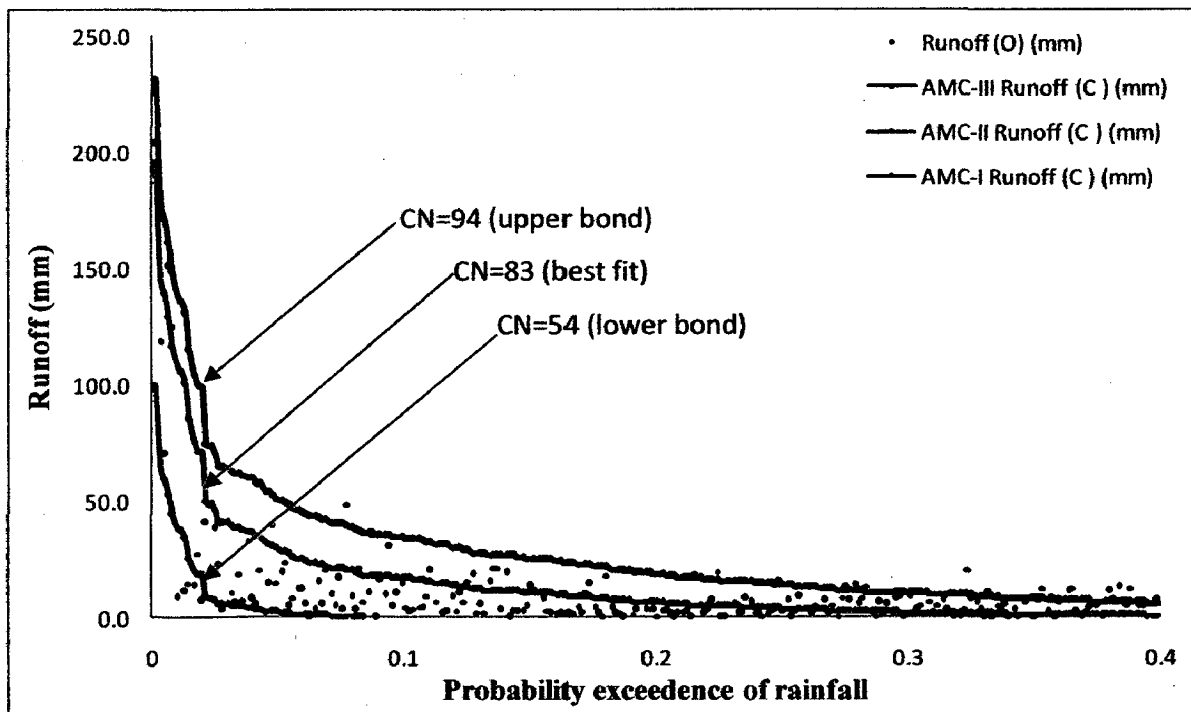
Table II.1 Extraterrestrial Radiation in mm of evaporable water per day.

North Latitude in Degrees										
Month	0°	10°	20°	30°	40°	50°	60°	70°	80°	90°
Jan.	14.5	12.8	10.8	8.5	6.0	3.6	1.3	--	--	--
Feb.	15	13.9	12.3	10.5	8.3	5.9	3.5	1.1	--	--
Mar.	15.2	14.8	13.9	12.7	11.0	9.1	6.8	4.3	1.8	--
Apr.	14.7	15.2	15.2	14.8	13.9	12.7	11.1	9.1	7.8	7.9
May	13.9	15	15.7	16.0	15.9	15.4	14.6	13.6	14.6	14.9
Jun.	13.4	14.8	15.8	16.5	16.7	16.7	16.5	17.0	17.8	18.1
Jul.	13.5	14.8	15.7	16.2	16.3	16.1	15.7	15.8	16.5	16.8
Aug.	14.2	15.0	15.3	15.3	14.8	13.9	12.7	11.4	10.6	11.2
Sep.	14.9	14.9	14.4	13.5	12.2	10.5	8.5	6.8	4.0	2.6
Oct.	15.0	14.1	12.9	11.3	9.3	7.1	4.7	2.4	0.2	--
Nov.	14.6	13.1	11.2	9.1	6.7	4.3	1.9	0.1	--	--
Dec.	14.3	12.4	10.3	7.9	5.5	3.0	0.9	--	--	--

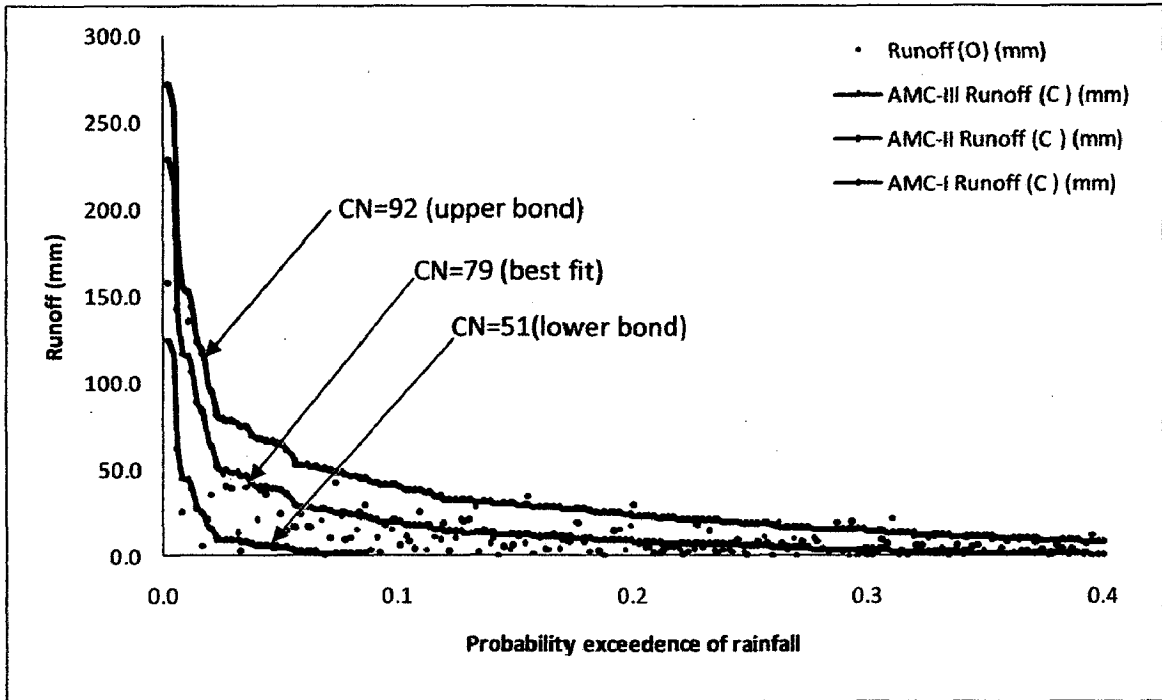
ORDERED DAILY RAINFALL-RUNOFF EVENTS FOR DIFFERENT CATCHMENTS



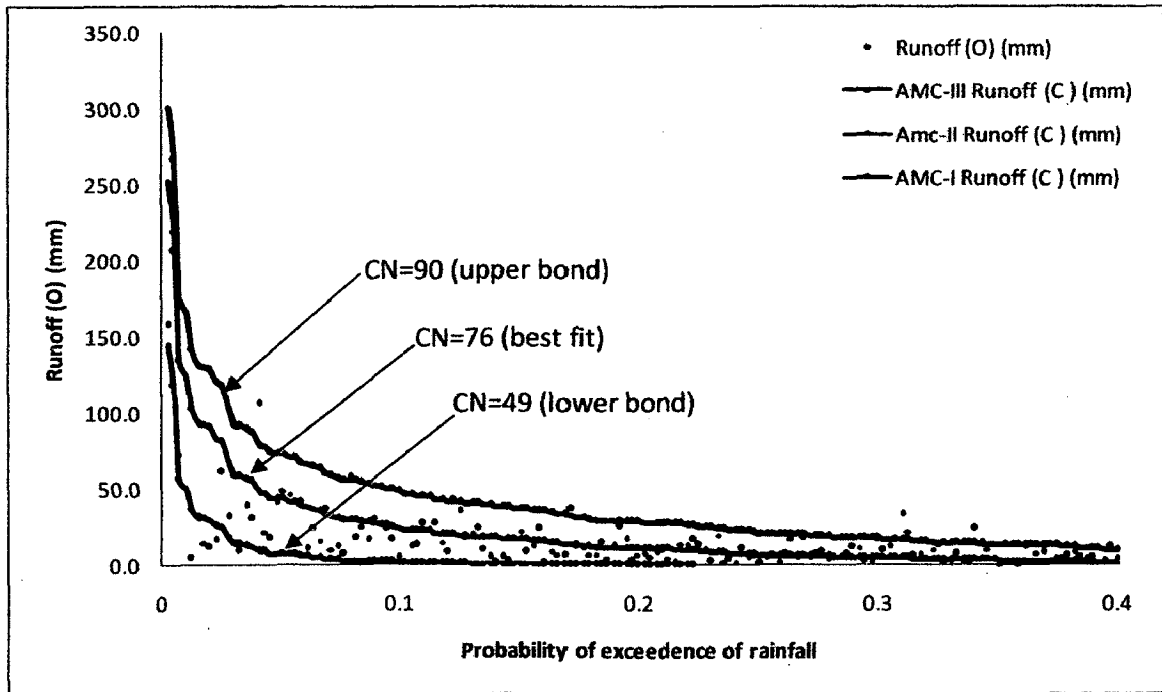
(a) 2-Daily duration analysis



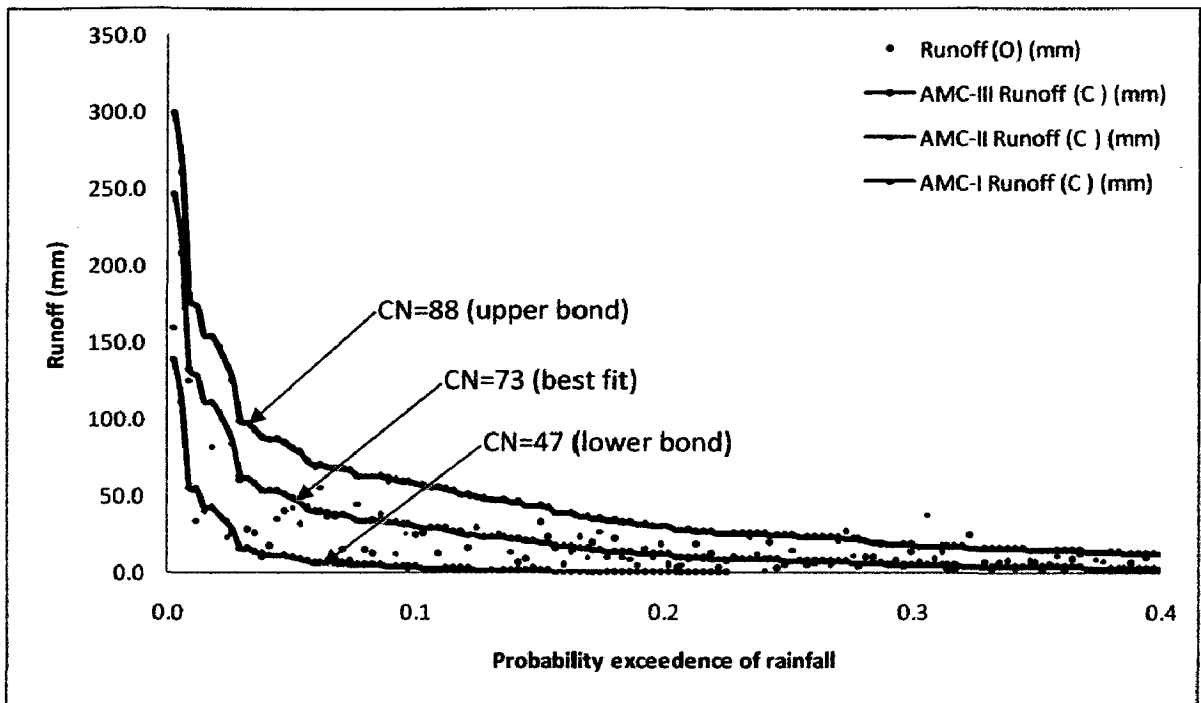
(b) 3-Daily duration analysis



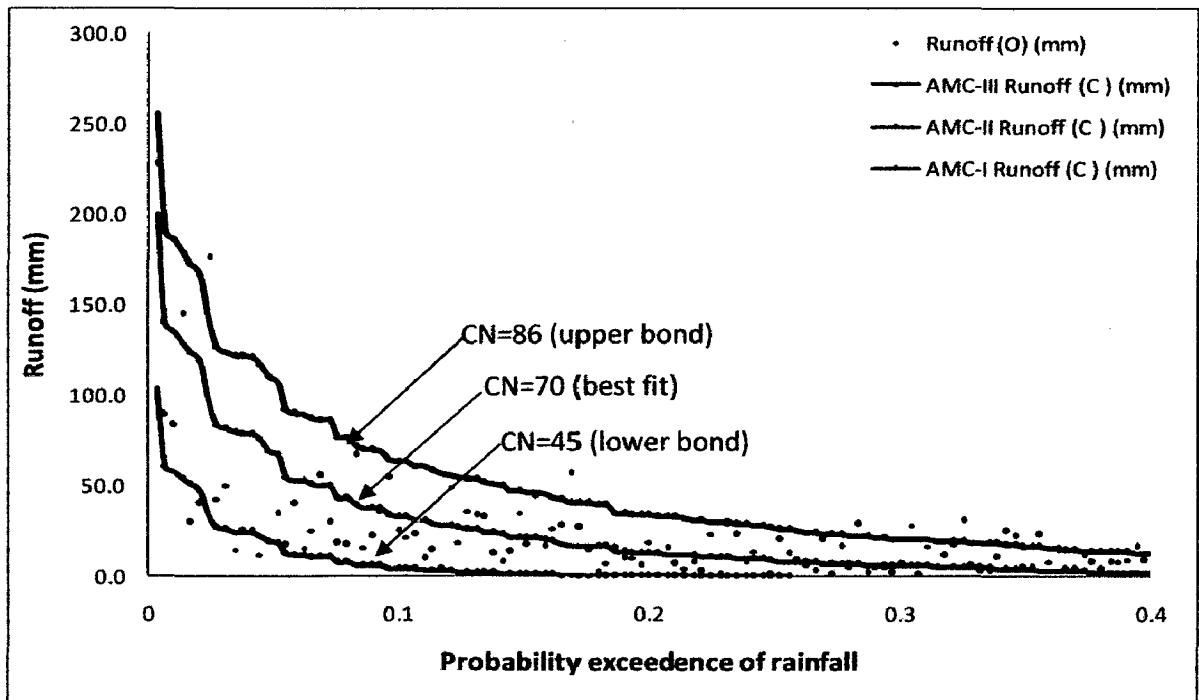
(c) 4-Daily duration analysis



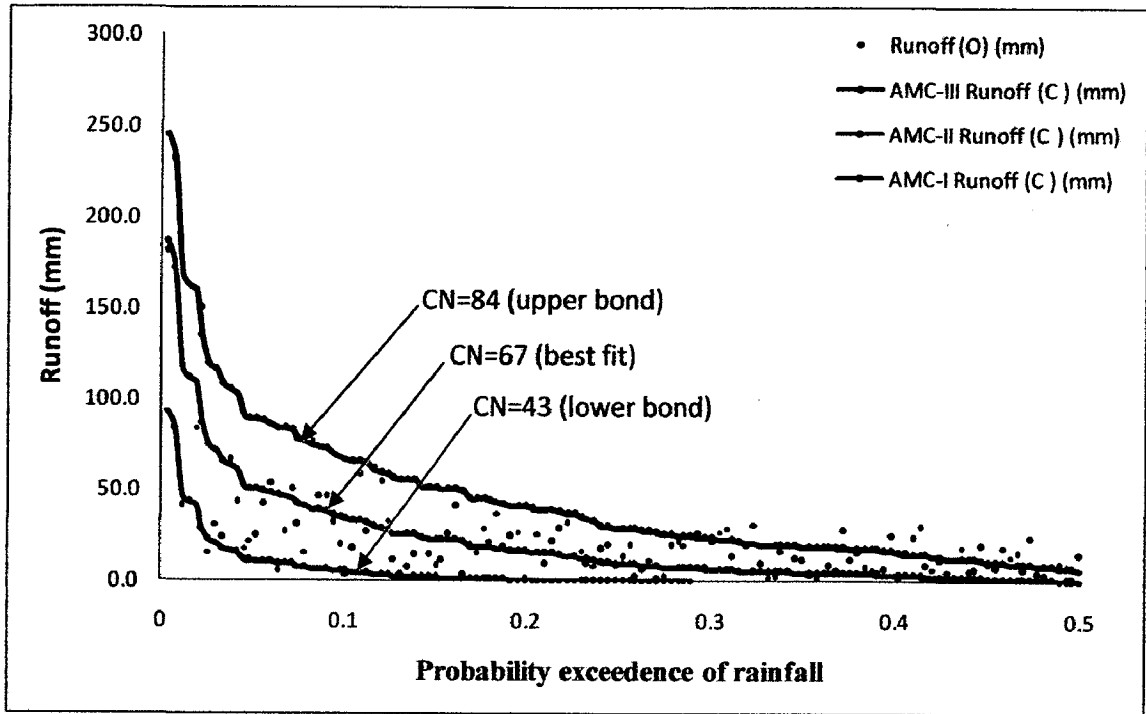
(d) 5-Daily duration analysis



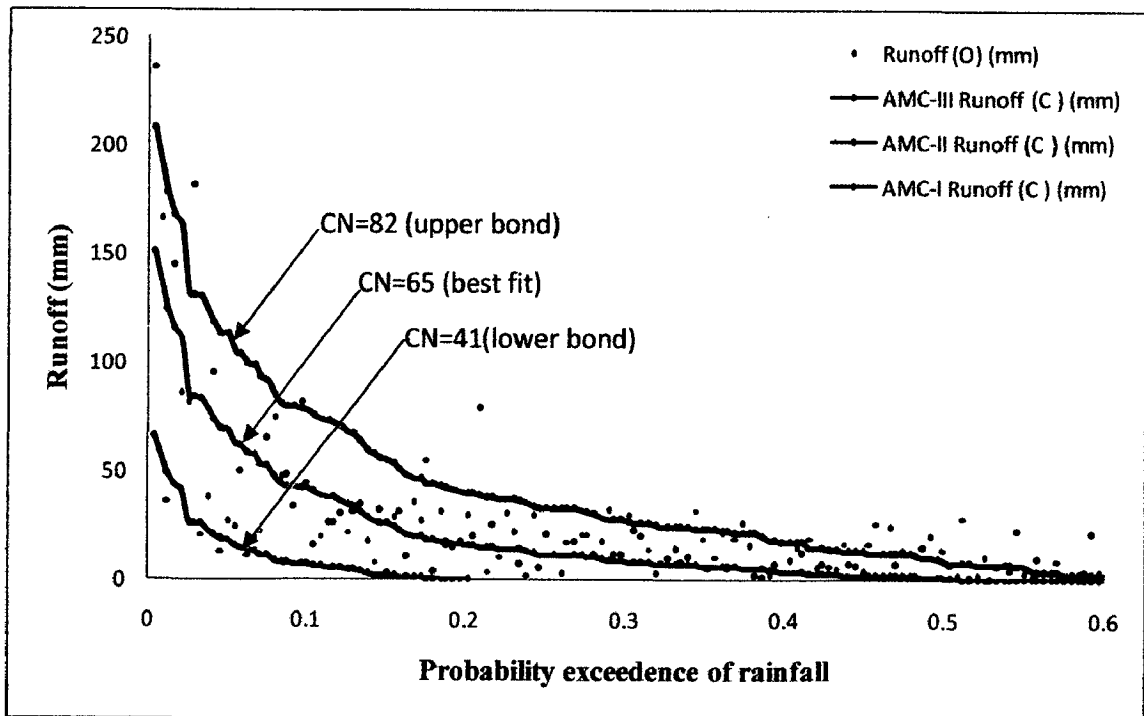
(e) 6-Daily duration analysis



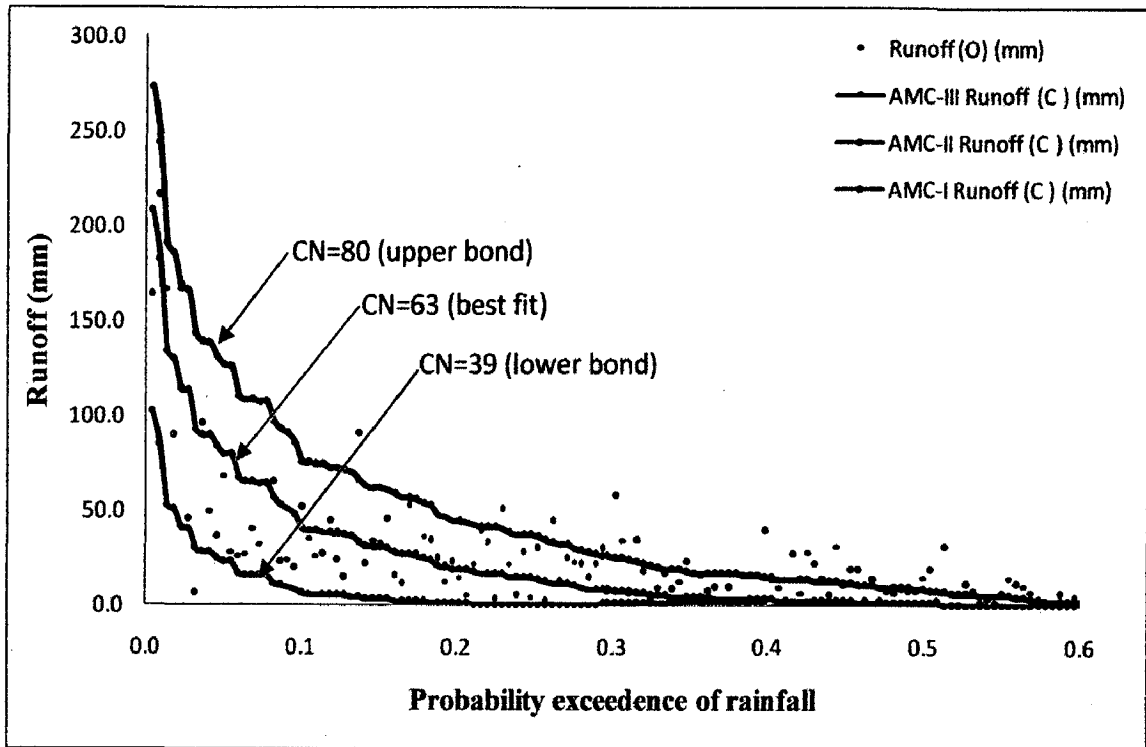
(f) 7-Daily duration analysis



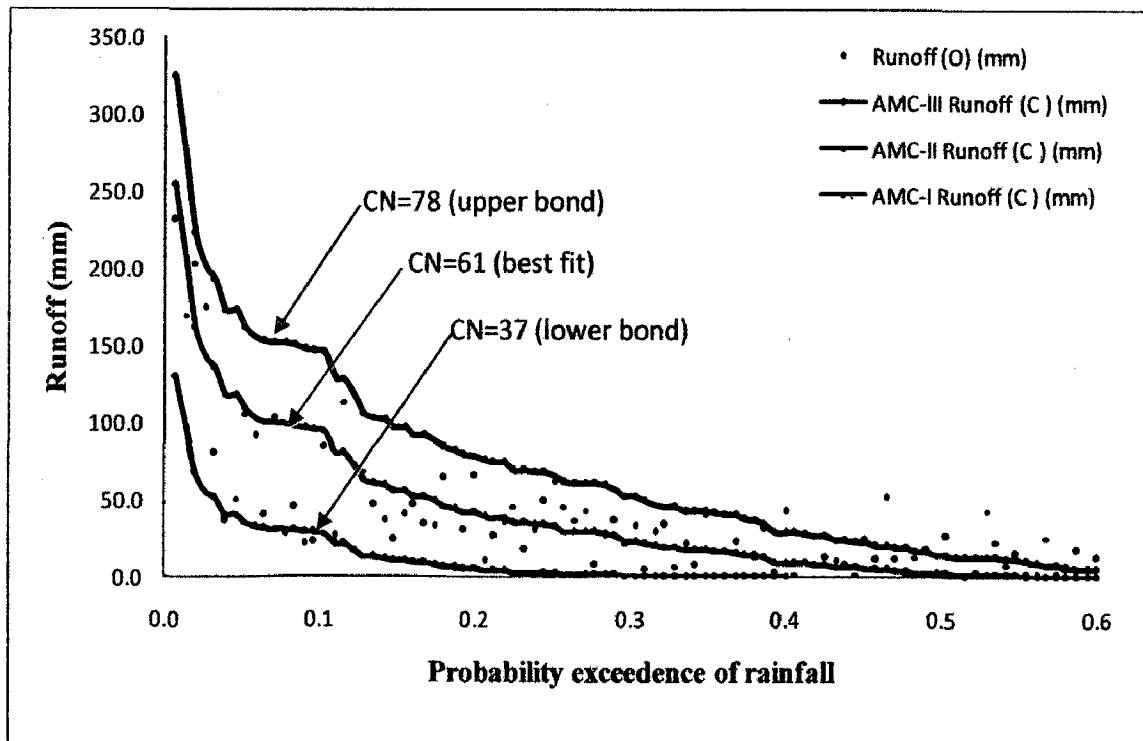
(g) 8-Daily duration analysis



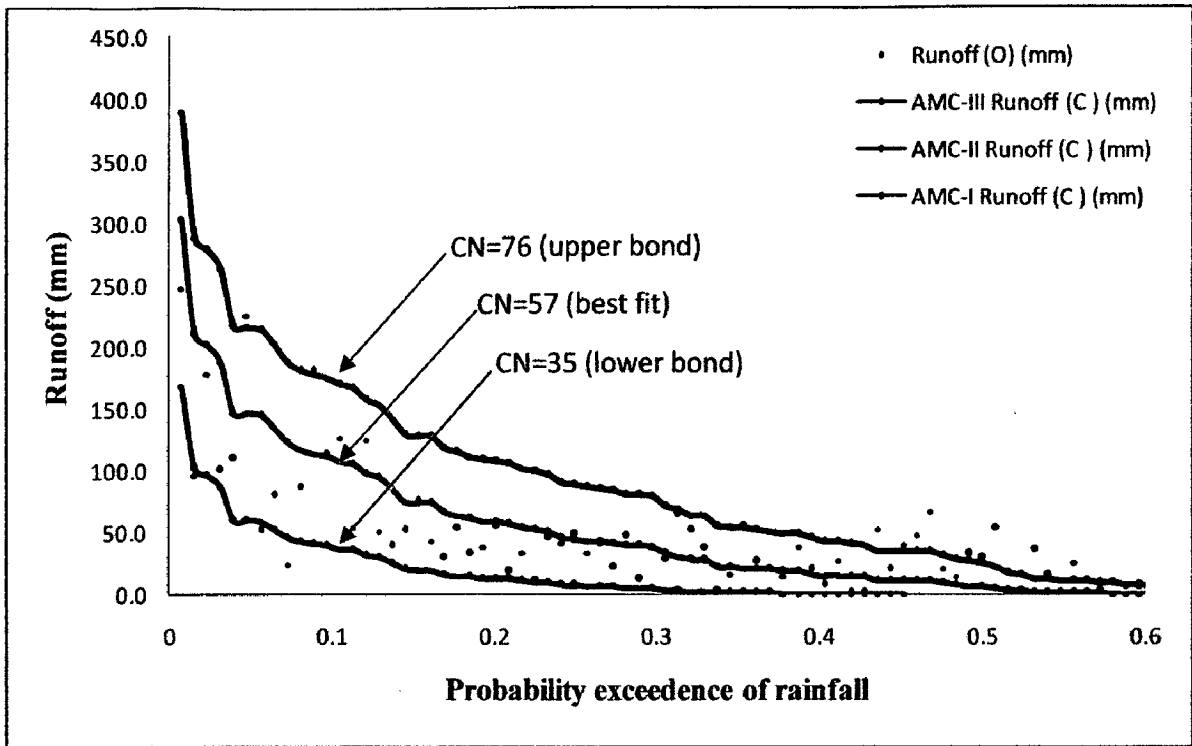
(h) 9-Daily duration analysis



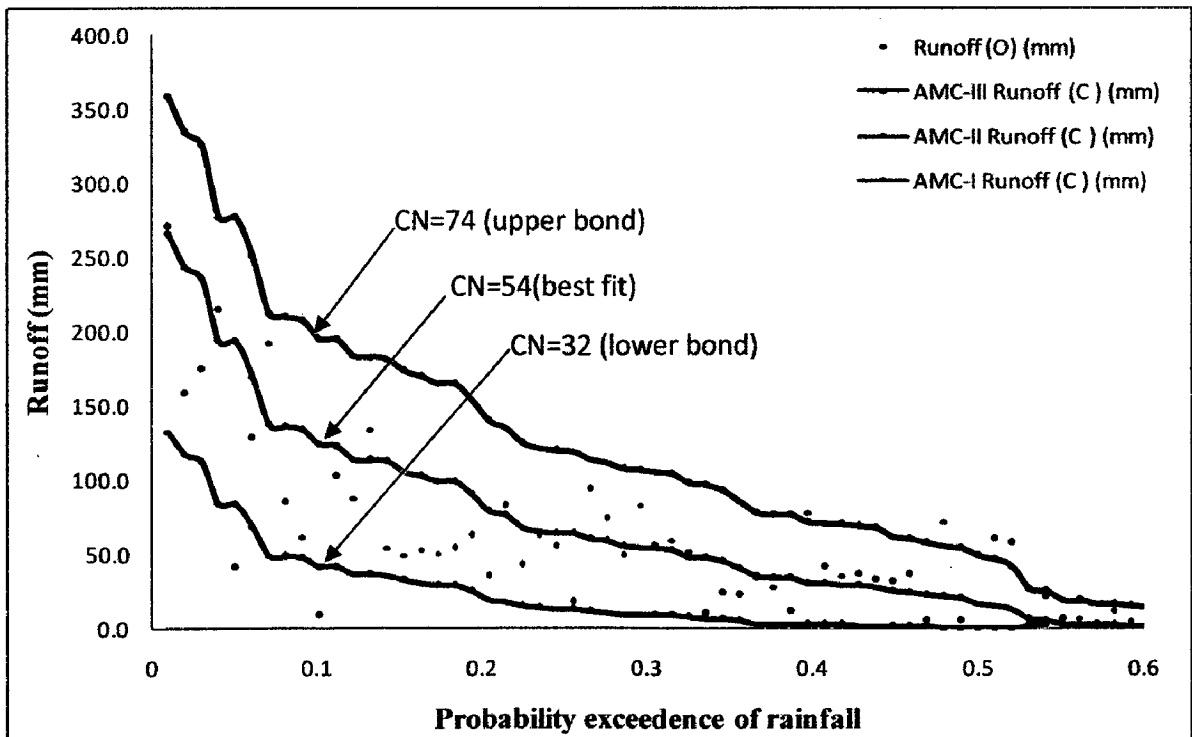
(i) 10-Daily duration analysis



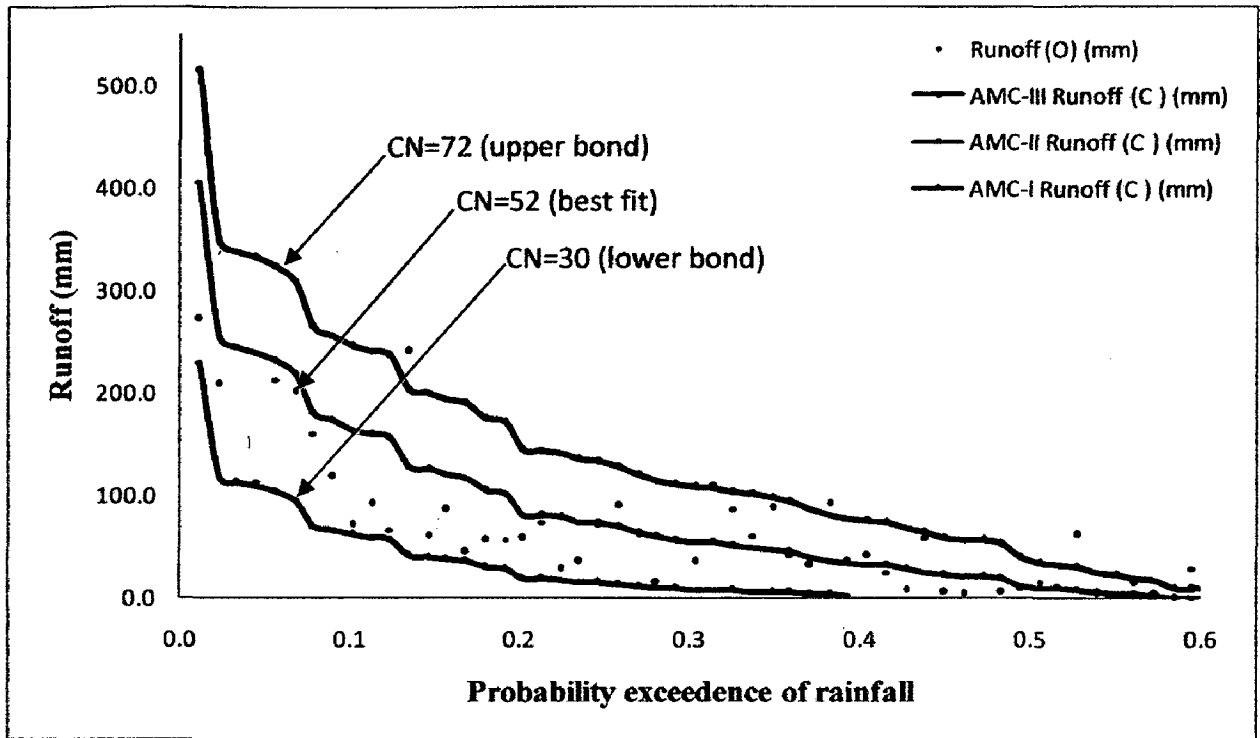
(j) 15-Daily duration analysis



(k) 20-Daily duration analysis

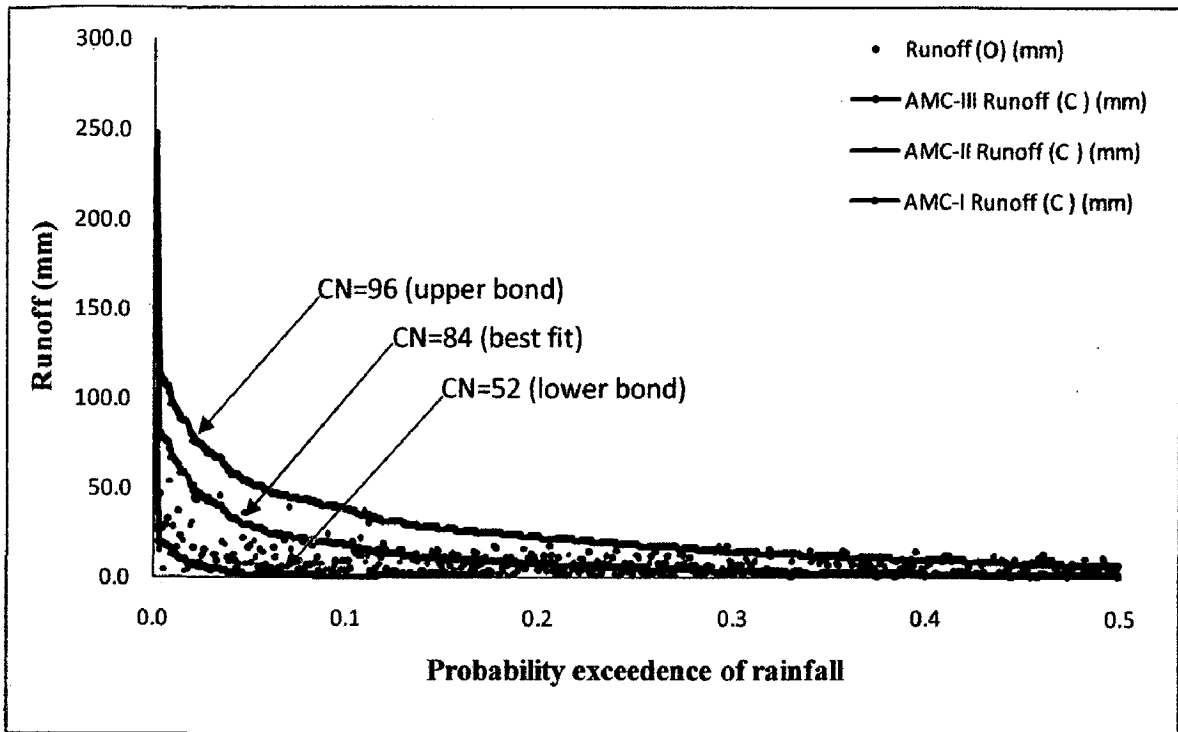


(l) 25-Daily duration analysis

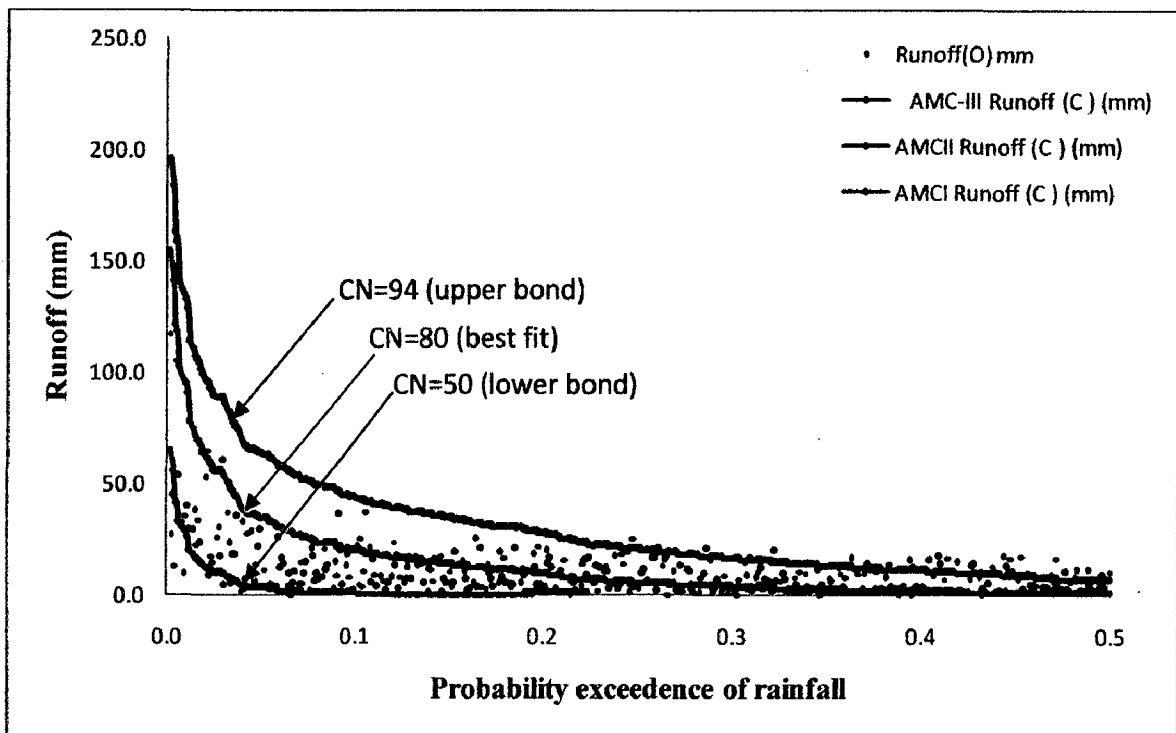


(m) 30-Daily duration analysis

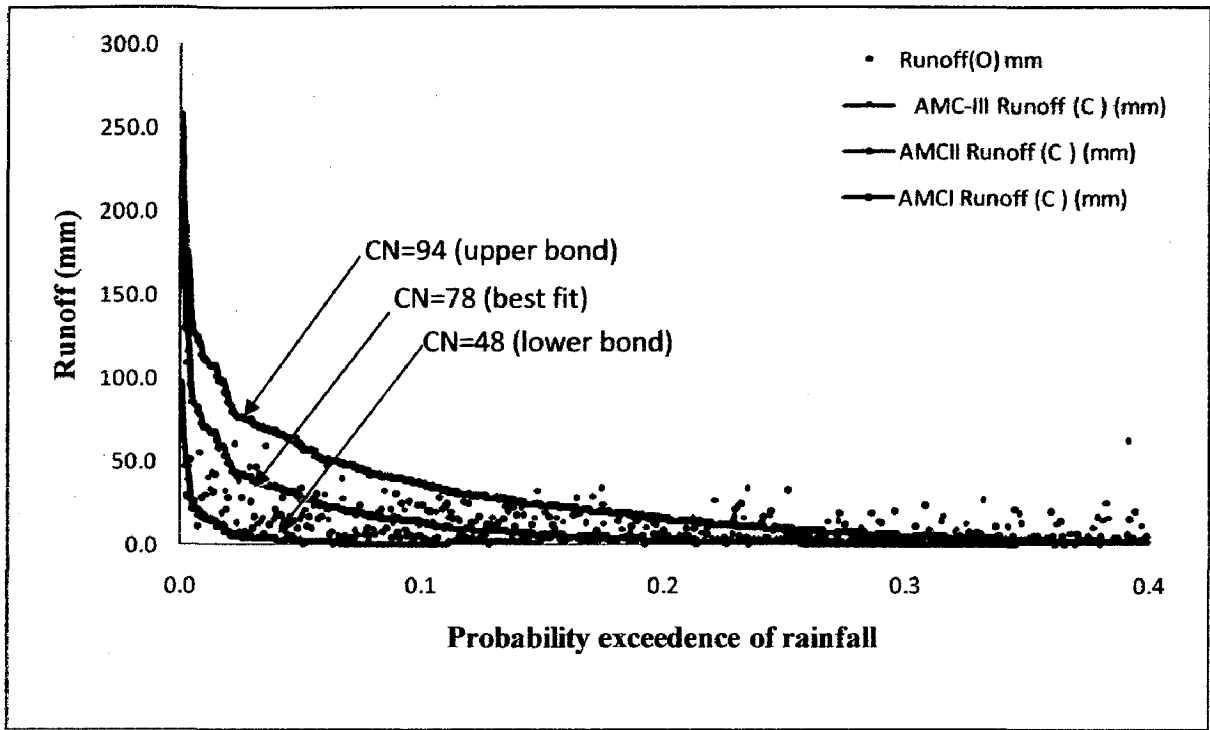
Figure III.1 Ordered different daily runoff data of Maithon catchment for determination of CN for three AMCs. Upper and lower bound curve numbers refer to AMC-II and AMC-I respectively and best-fit to AMC-II.



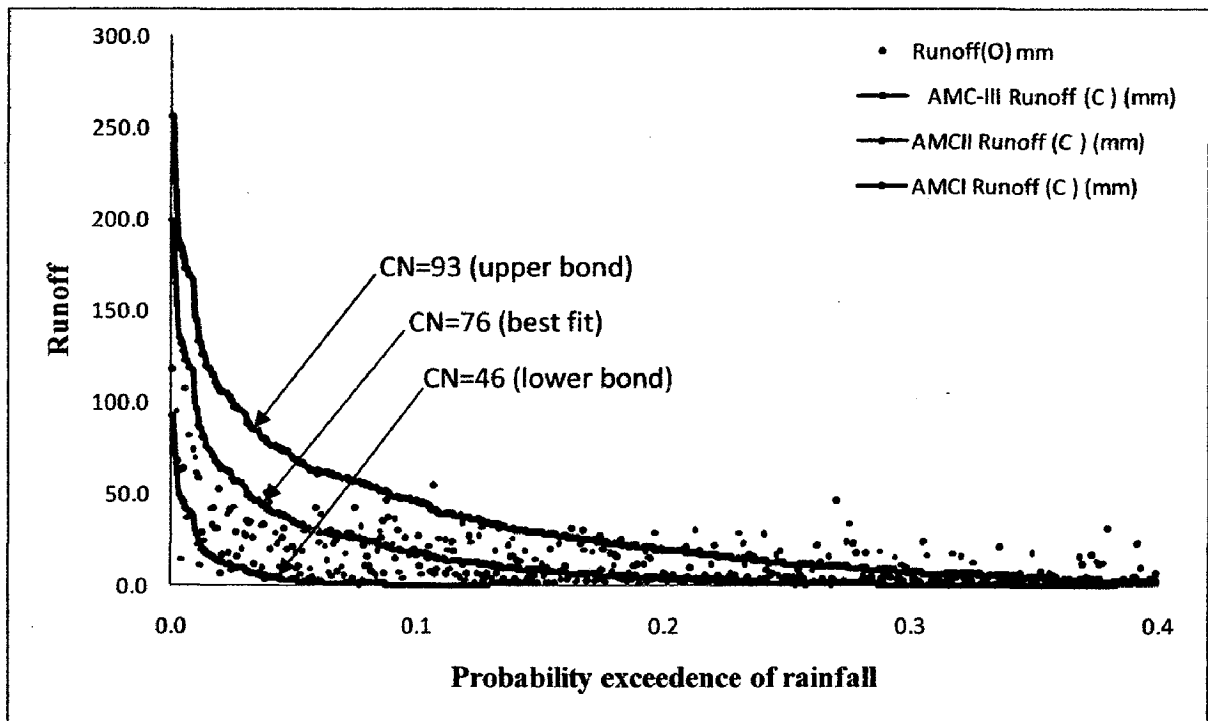
(a) 2-Daily duration analysis



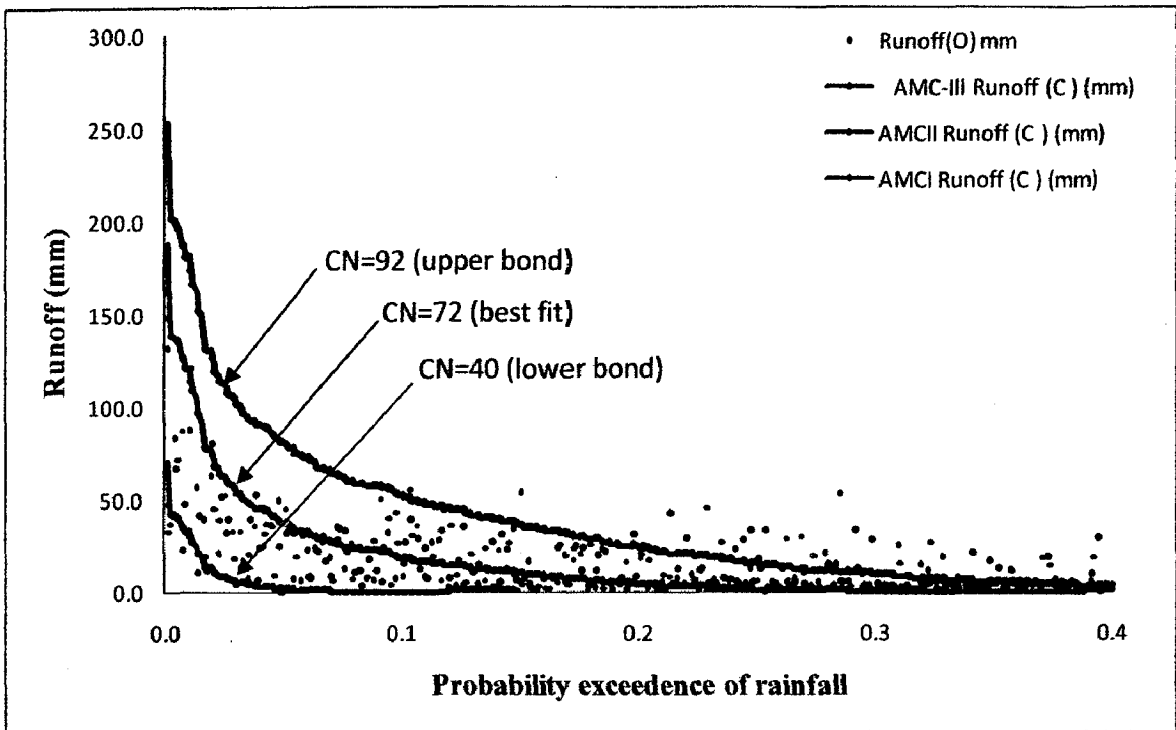
(b) 3-Daily duration analysis



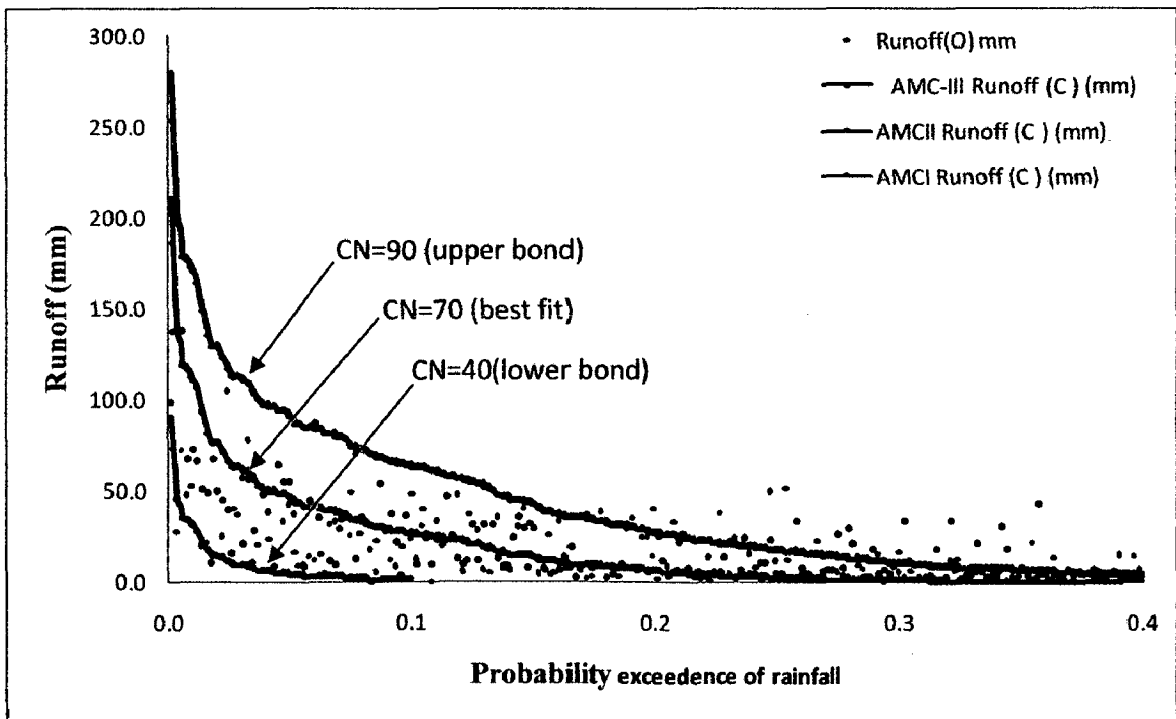
(c) 4-Daily duration analysis



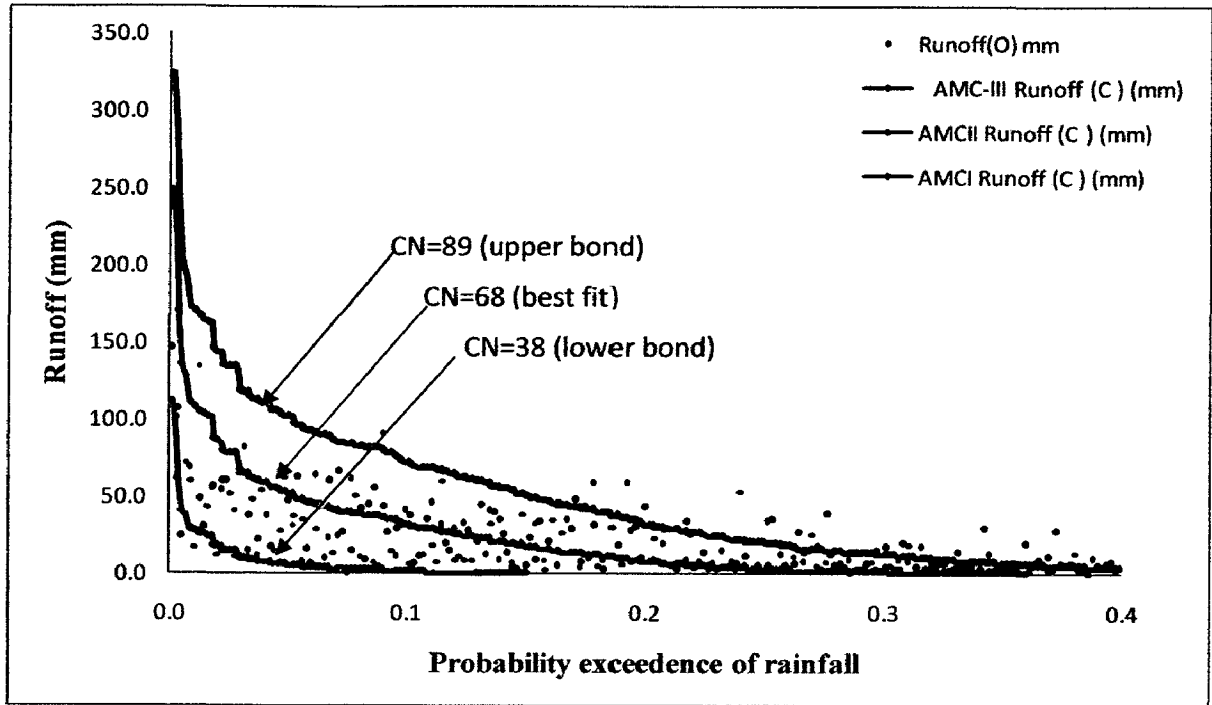
(d) 5-Daily duration analysis



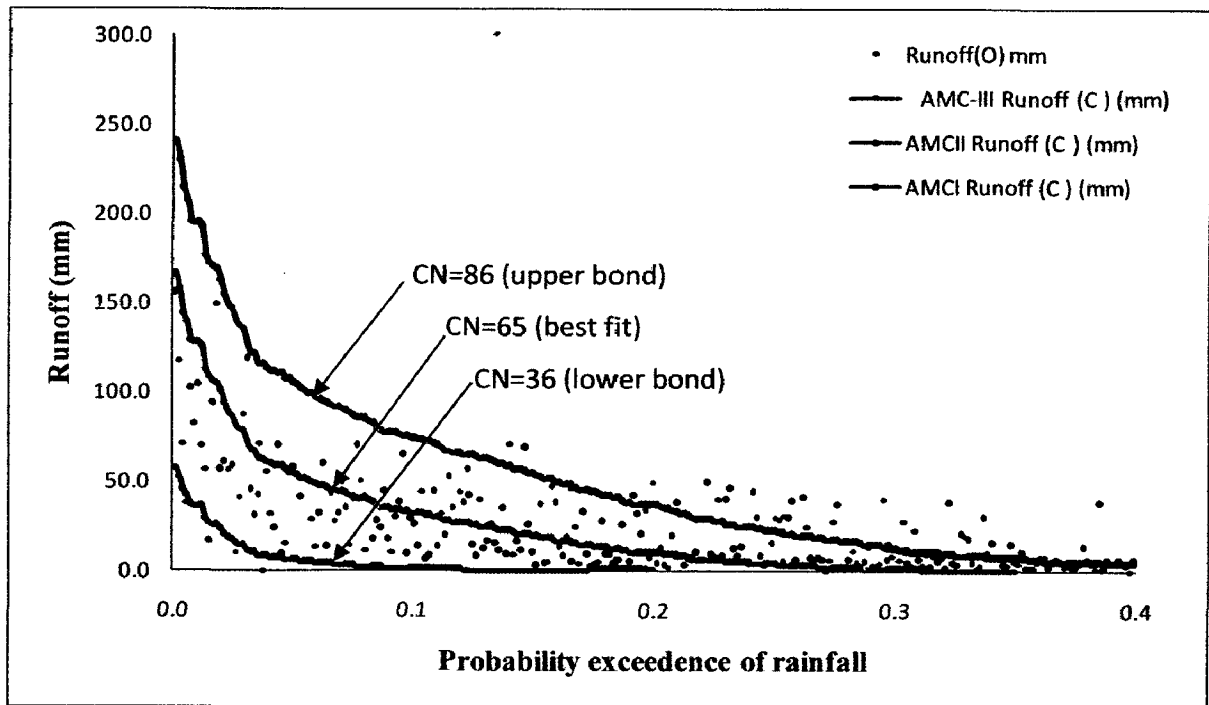
(e) 6-Daily duration analysis



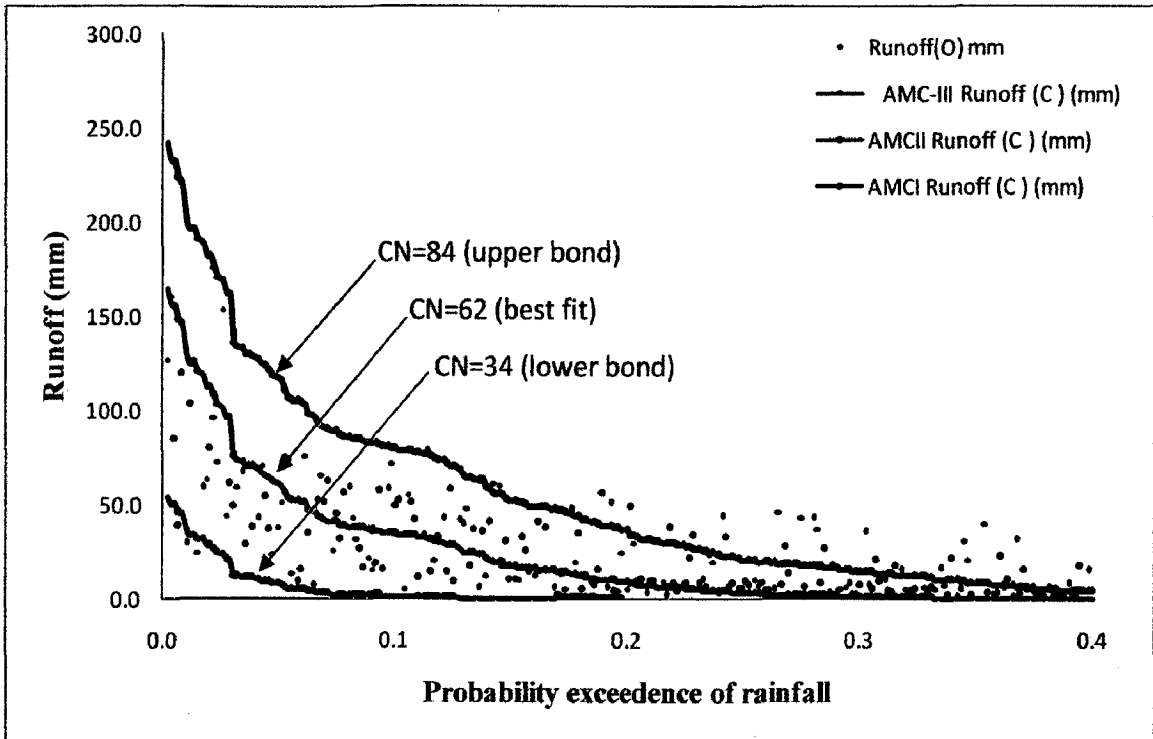
(f) 7-Daily duration analysis



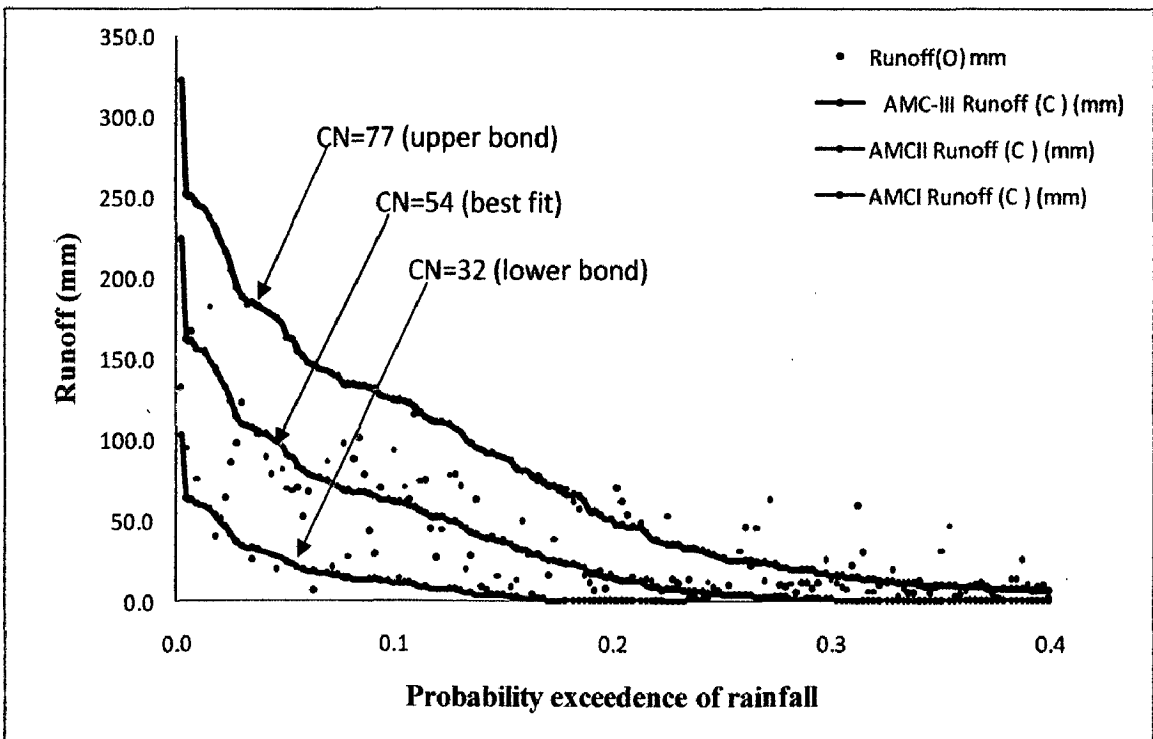
(g) 8-Daily duration analysis



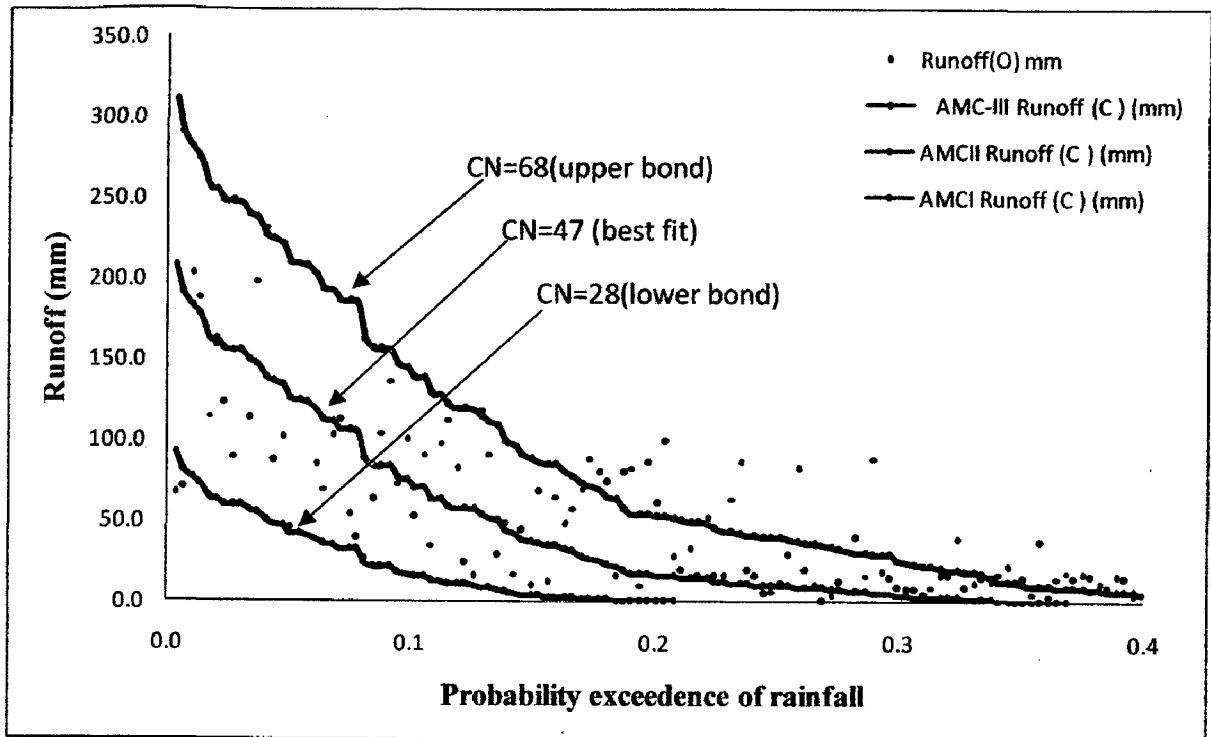
(h) 9-Daily duration analysis



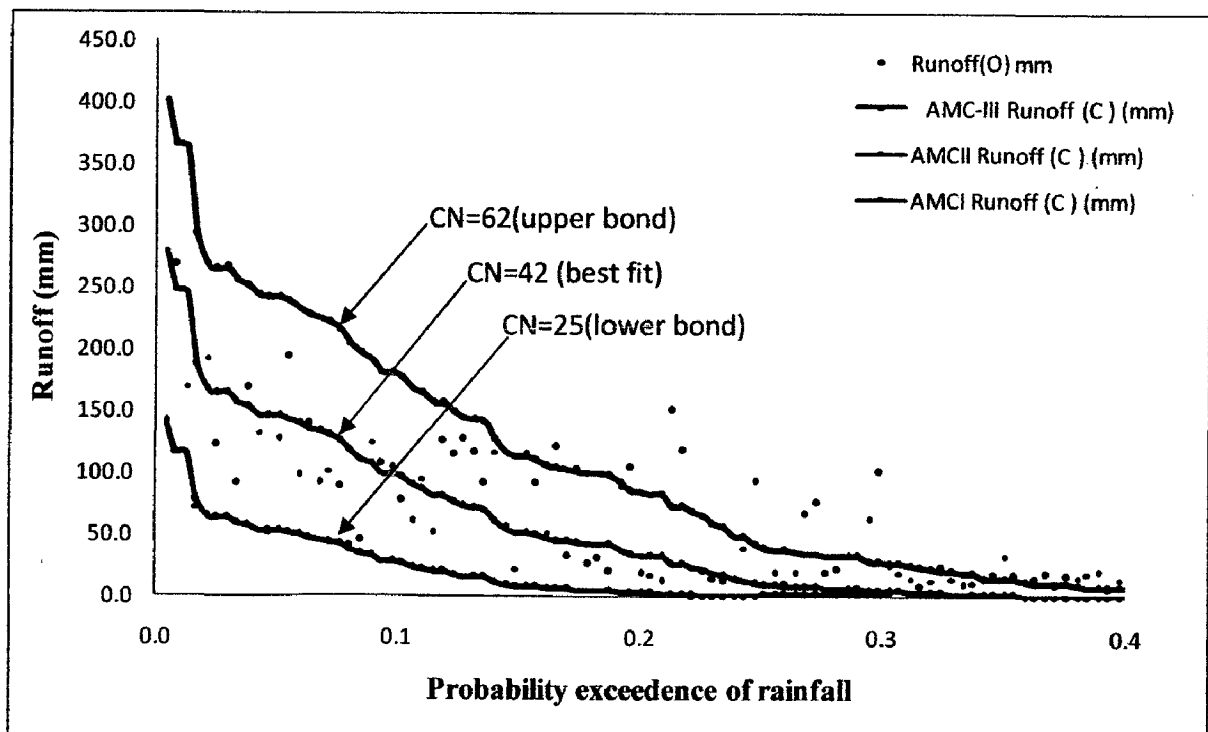
(i) 10-Daily duration analysis



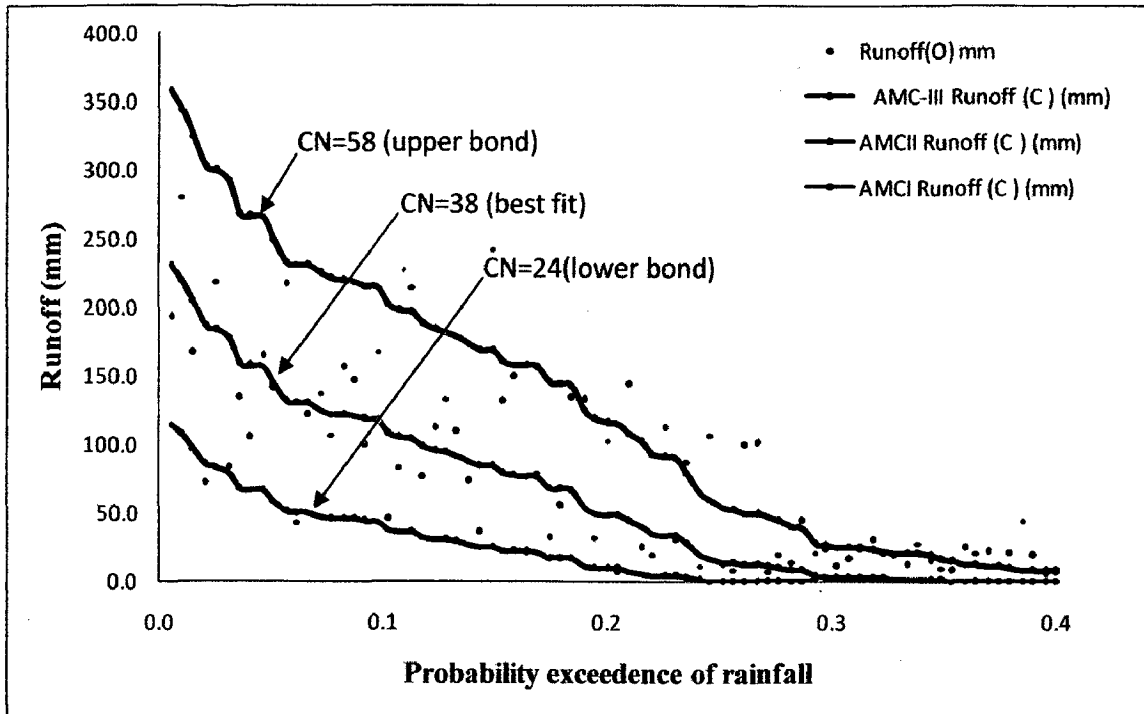
(j) 15-Daily duration analysis



(k) 20-Daily duration analysis

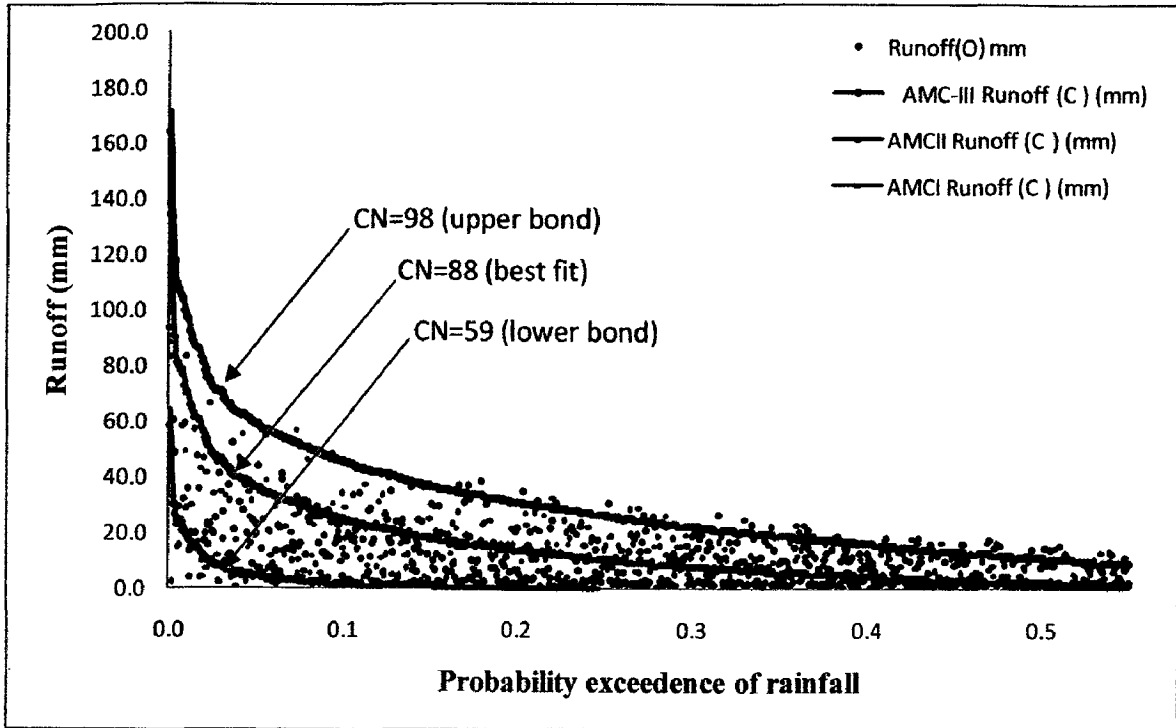


(l) 25-Daily duration analysis

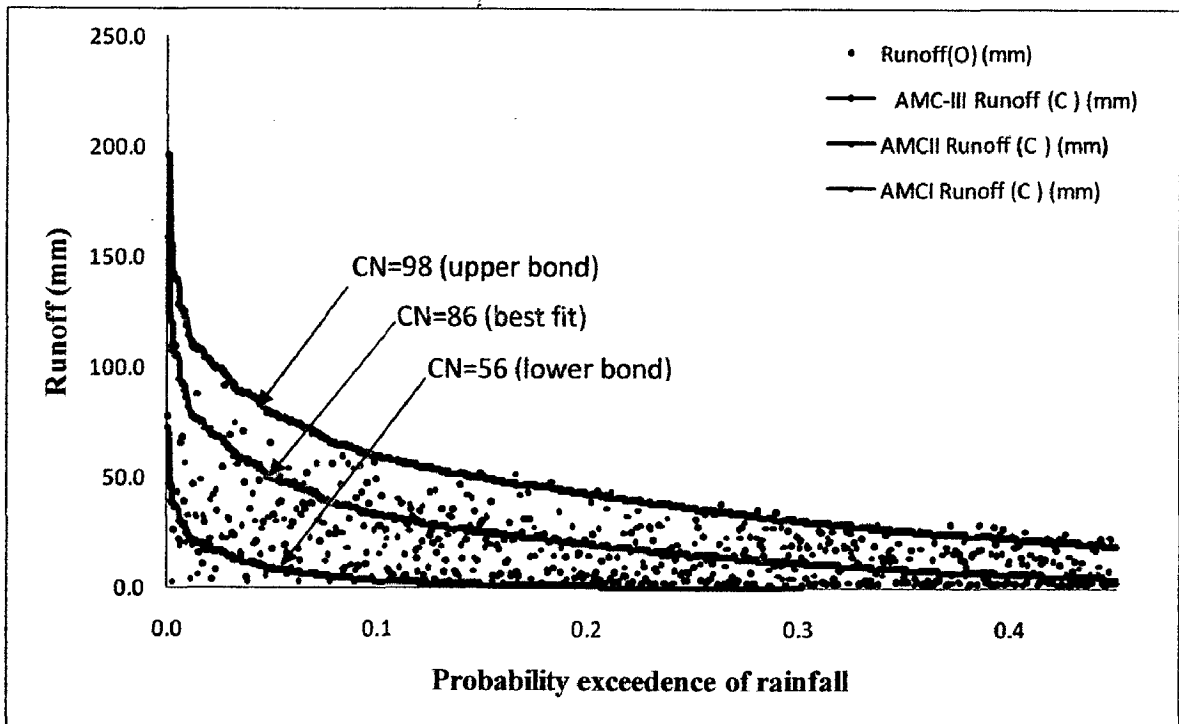


(m) 30-Daily duration analysis

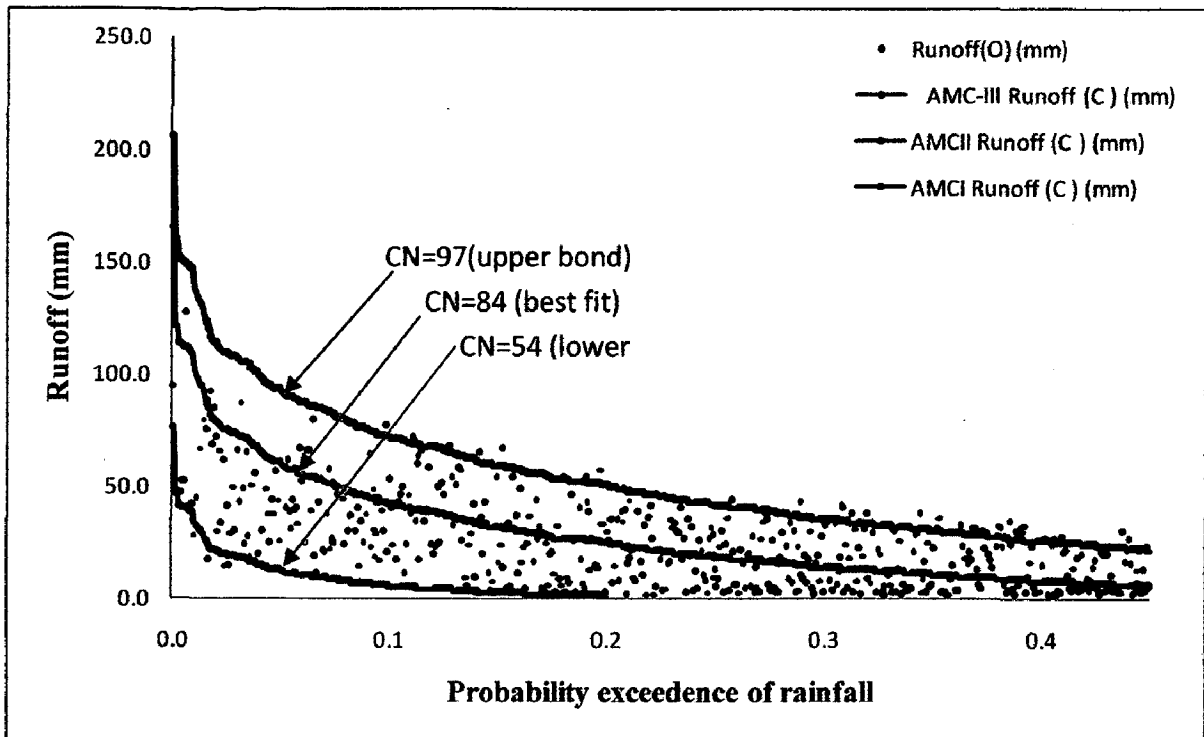
Figure III.2 Ordered different daily runoff data of Ramganga catchment for determination of CN for three AMCs. Upper and lower bound curve numbers refer to AMC-II and AMC-I respectively and best-fit to AMC-II.



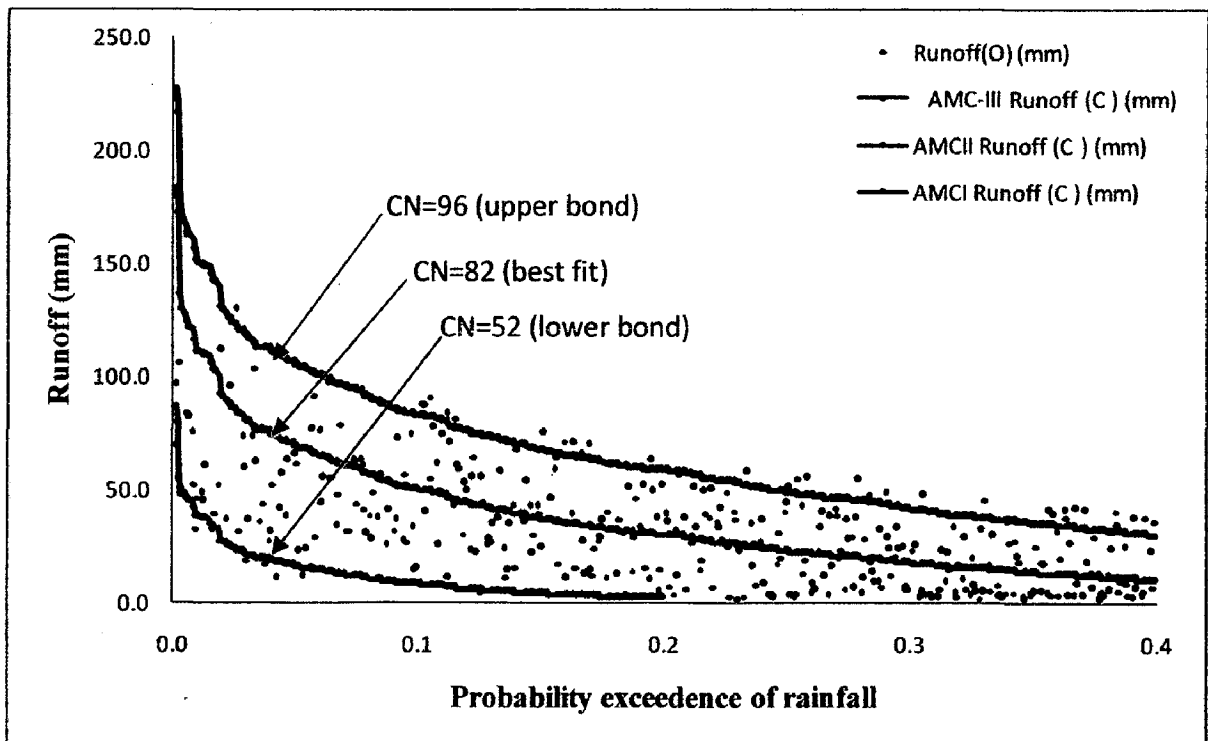
(a) 2-Daily duration analysis



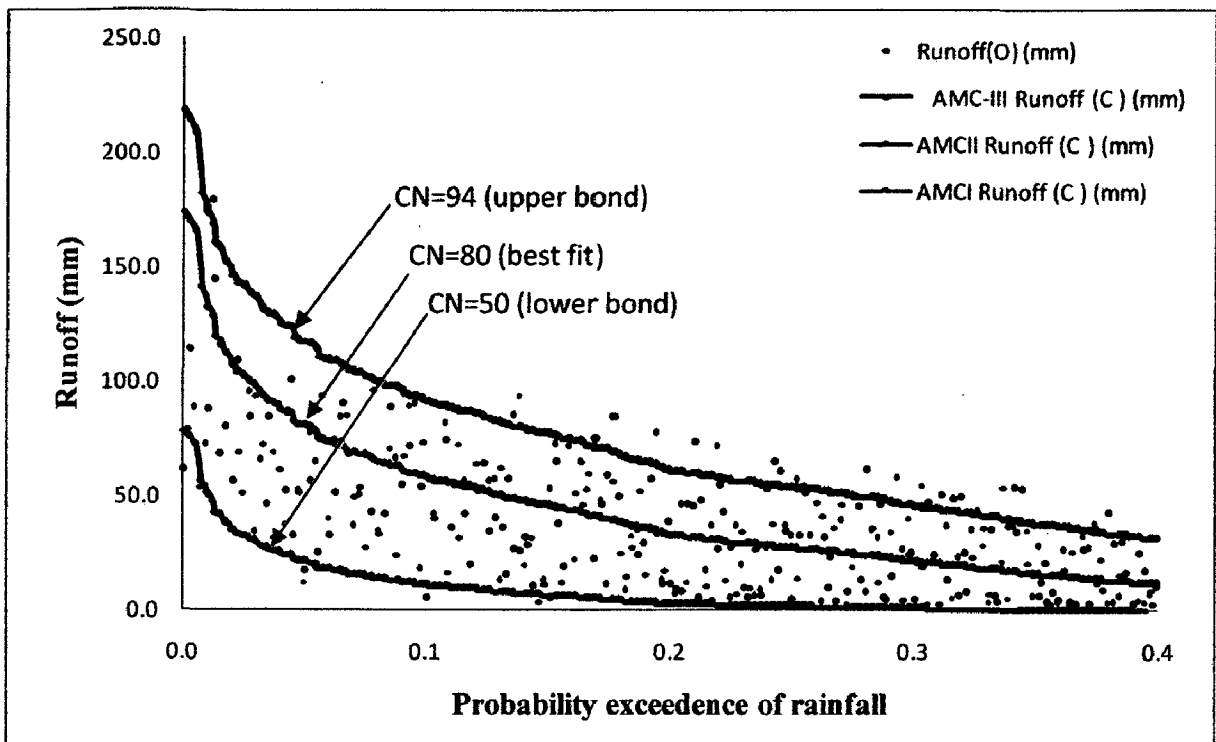
(b) 3-Daily duration analysis



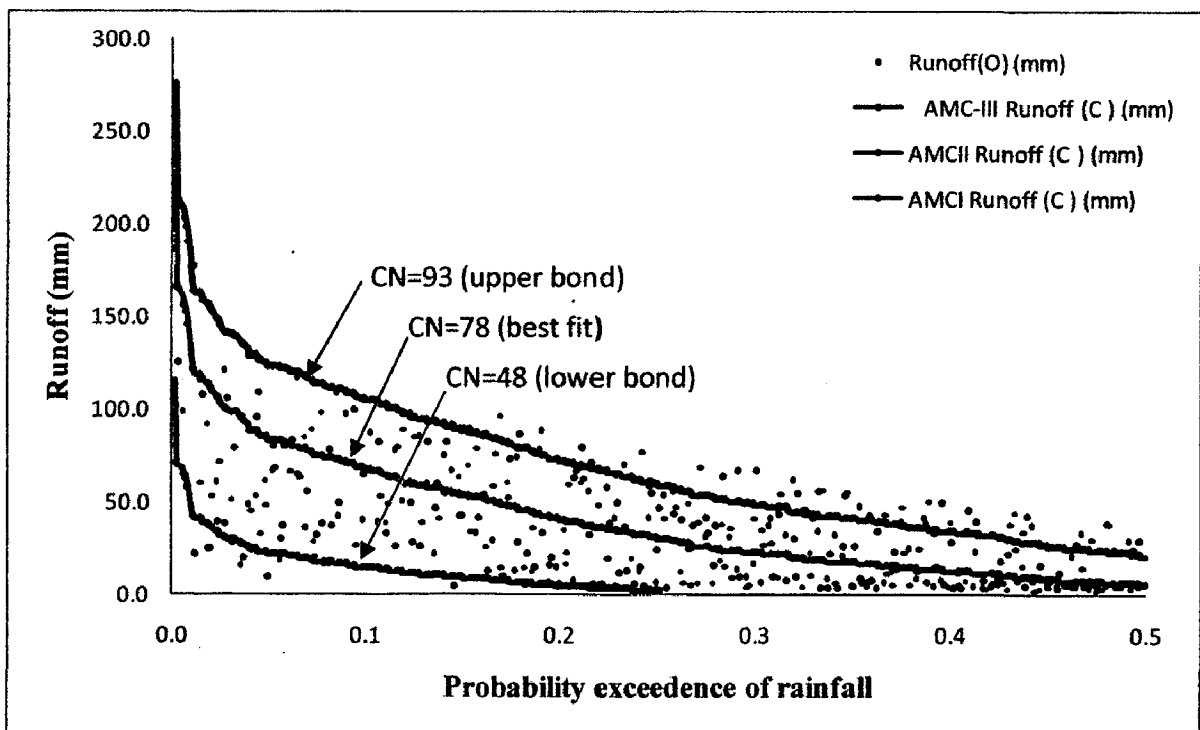
(c) 4-Daily duration analysis



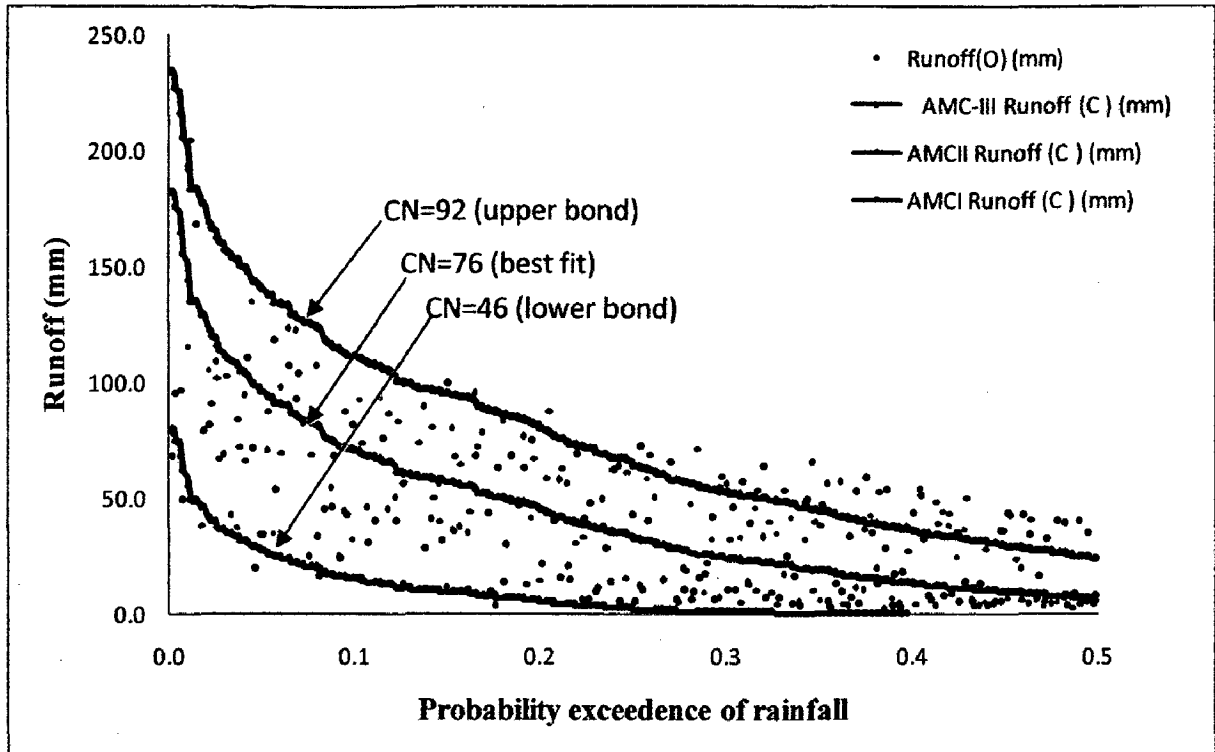
(d) 5-Daily duration analysis



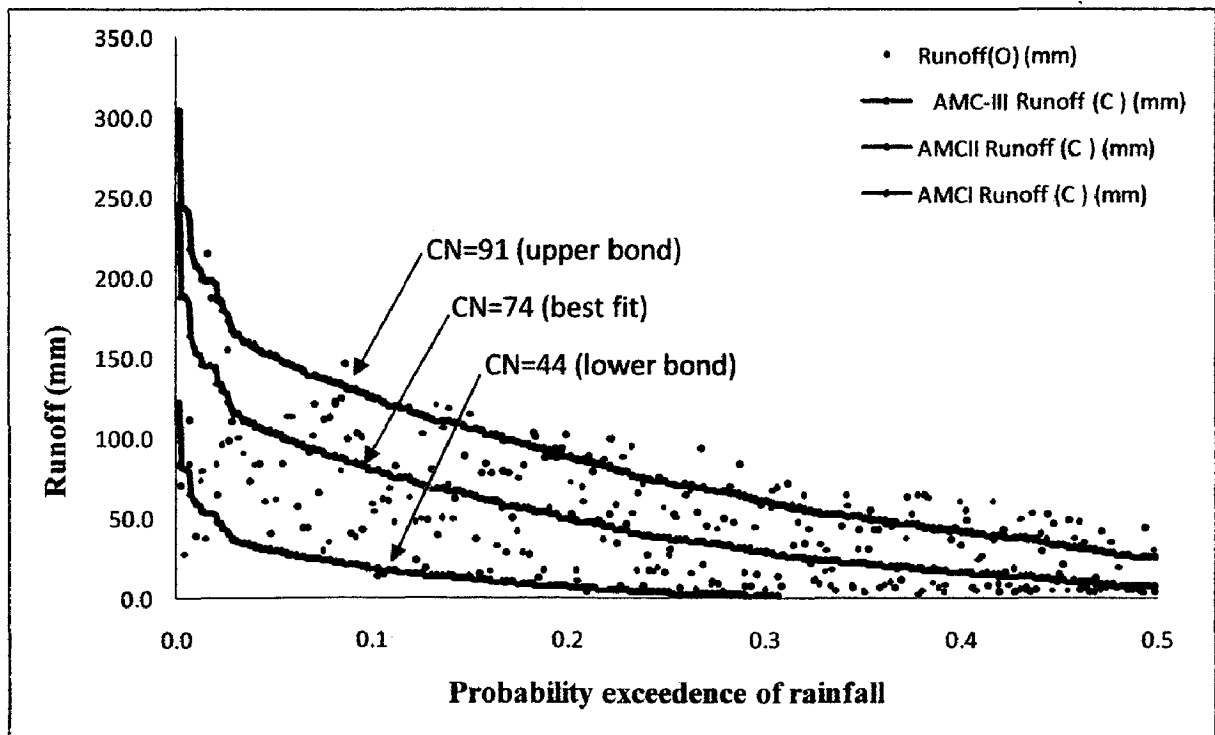
(e) 6-Daily duration analysis



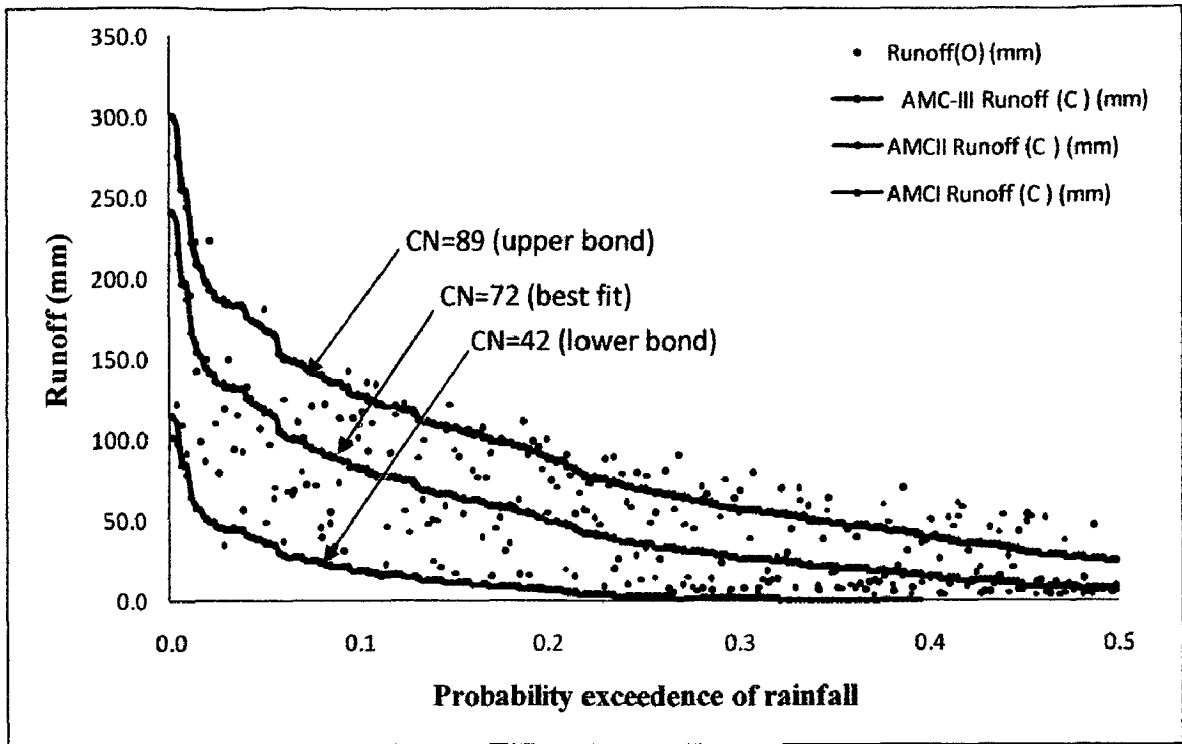
(f) 7-Daily duration analysis



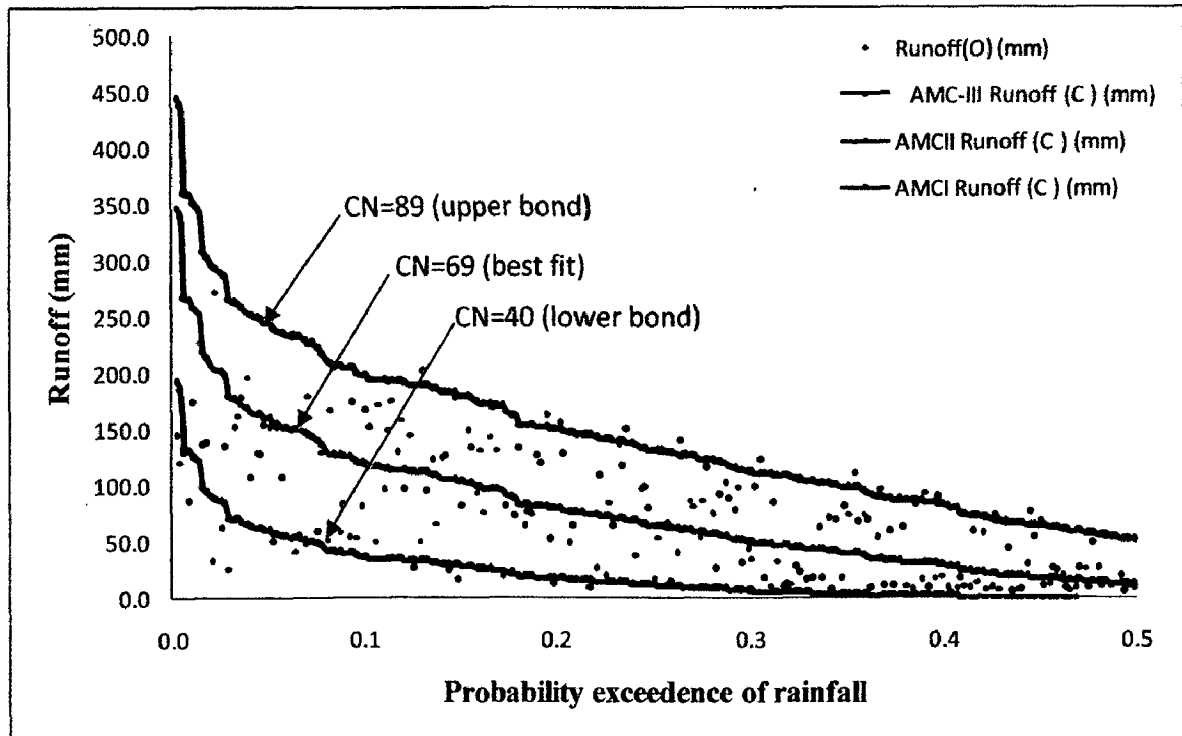
(g) 8-Daily duration analysis



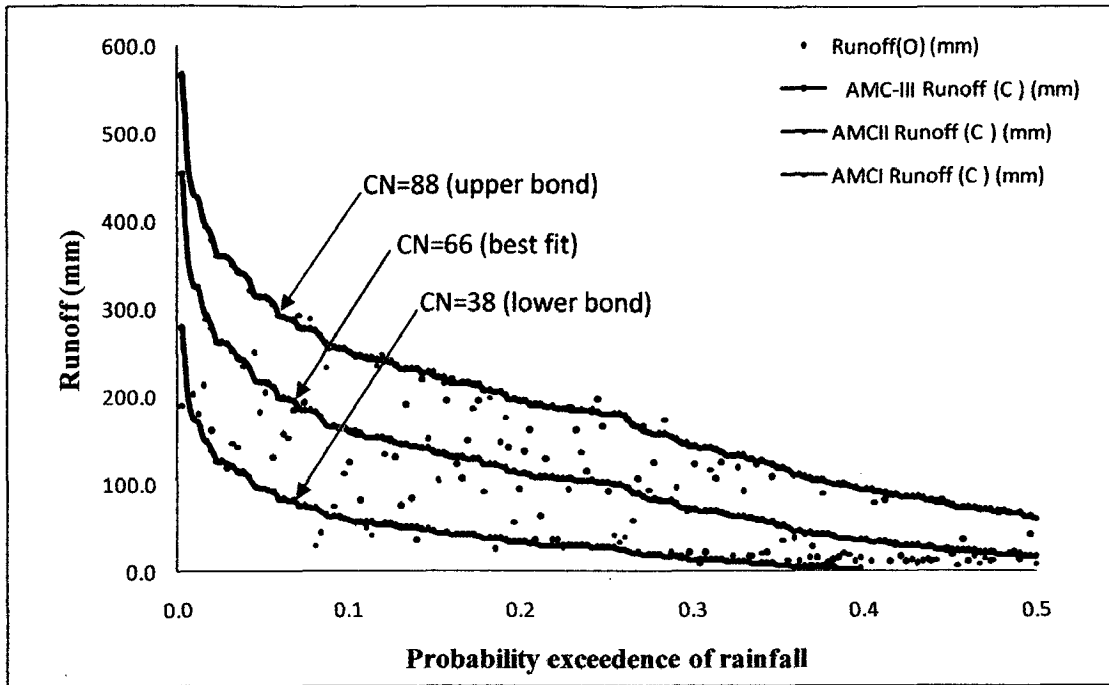
(h) 9-Daily duration analysis



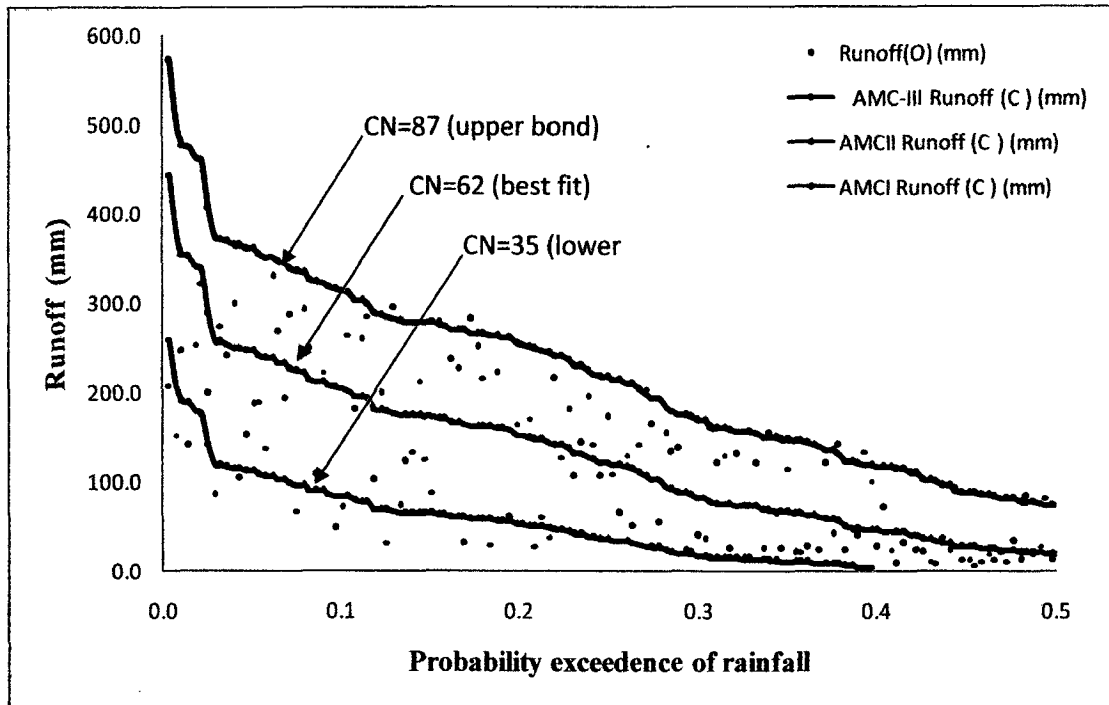
(i) 10-Daily duration analysis



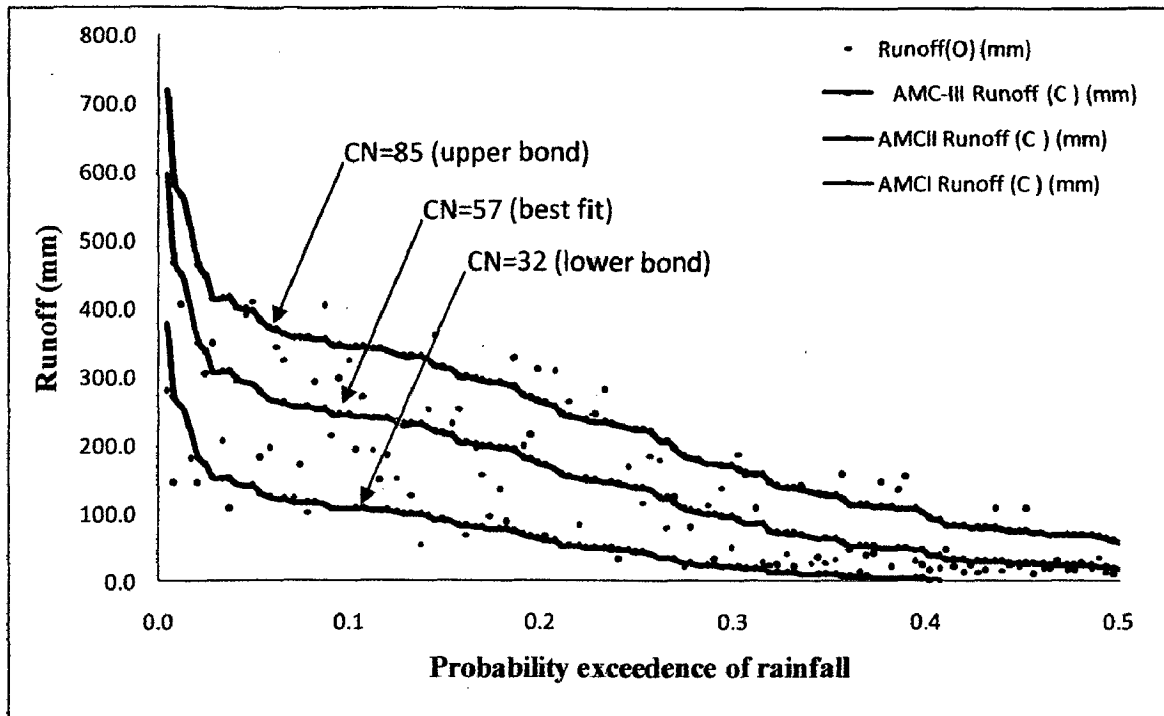
(j) 15-Daily duration analysis



(k) 20-Daily duration analysis



(l) 25-Daily duration analysis



(m) 30-Daily duration analysis

Figure III.3 Ordered different daily runoff data of Rapti catchment for determination of CN for three AMCs. Upper and lower bound curve numbers refer to AMC-II and AMC-I respectively and best-fit to AMC-II.

References:

- ⌘ A Tribute to the Memory of *Svante Arrhenius* (1859–1927); Presented at the 2008 Annual Meeting of the Royal Swedish Academy of Engineering Sciences by Gustaf Arrhenius, Karin Aldwell and Svante Wold.
- ⌘ Adler, R.F., 2003: The version 2 Global Precipitation Climatology Project (GPCP) monthly precipitation analysis (1979–present). *J. Hydrometeorol.*, 4, 1147–1167.
- ⌘ Allen R, Pereira LS, Raes D, Smith M. 1998. *Crop evapotranspiration: guidelines for computing crop water requirements*. Irrigation and Drainage Paper, 56. FAO, Rome, Italy
- ⌘ Allen RG, Jensen ME, Wright JL, Burman, RD. 1989. Operational estimates of reference evapotranspiration. *Agron. J.* 81: 650–662.
- ⌘ Andersson L, Harding R.J. 1991. Soil-moisture deficit simulation with models of varying complexity for forest and grassland sites in Sweden and the UK. *Water Resources Management.* 5: 25-46.
- ⌘ Arnell, N.W., Livermore M.J.L., Kovats S. , Levy P.E., Nicholls R., Parry M.L. and Gaffin S.R., 2004: Climate and socio-economic scenarios for global-scale climate change impacts assessments: characterizing the SRES storylines. *Global Environ. Chang.*, 14, 3–20.
- ⌘ Auerswald K, Haider J. 1996. Runoff curve numbers for small grain under German cropping conditions. *Journal of Environmental Management*, Academic Press Ltd. 47, 223-228.
- ⌘ Beck, C., Grieser J. and Rudolph B., 2005: A New Monthly Precipitation Climatology for the Global Land Areas for the Period 1951 to 2000. DWD, *Klimastatusbericht 2004*, 181–190.
- ⌘ Betts, R.A., Boucher O., Collins M., Cox P.M., Falloon P.D., Gedney N., Hemming D.L., Huntingford C., Jones C.D., Sexton D. and Webb M., 2007: Projected increase in continental runoff due to plant responses to increasing carbon dioxide. *Nature*, 448, 1037-1041.
- ⌘ Betts, R.A., P.M. Cox, S.E. Lee and F.I. Woodward, 1997: Contrasting physiological and structural vegetation feedbacks in climate change simulations. *Nature*, 387, 796–799.

- ☒ Beven KJ, 2001. *Rainfall–runoff modelling: the primer*. Wiley, New York. 360 pp.
- ☒ Blaney HF, Criddle WD. 1950. Determining water requirements in irrigated areas from climatological and irrigation data. *Technical Paper no. 96, US Department of Agriculture, Soil Conservation Service, Washington, DC*.
- ☒ Bosznay, M. 1989. Generalization of SCS Curve Number Method. *J. Irrigation and Drainage Engineering, ASCE*, 115(1),139-144.
- ☒ Brutsaert W. 1982. *Evaporation into the Atmosphere: Theory, History, and applications*. Reidel, Higham, MA, 229 pp.
- ☒ Brutsaert W. 1986. Catchment-scale evaporation and the atmospheric boundary layer. *Water Resour. Res.*, 22(9): 39s-45s.
- ☒ Brutsaert, W. and Parlange M.B., 1998: Hydrologic cycle explains the evaporation paradox. *Nature*, 396, 30.
- ☒ Burnash RJC. 1995. In: Singh, V.P. (Ed.), *The NWS river forecast system catchment modeling Computer Models of Watershed Hydrology*. Water Resources Publications, Highlands ranch, Co., pp. 311–366.
- ☒ Calder IR. 1983. An objective assessment of soil-moisture deficit models. *Journal of Hydrology* 60, 329–355.
- ☒ Cazier, D. J. and Hawkins, R.H. 1984. Regional application of the curve number method. *Water Today and Tomorrow, Proc., ASCE, Irrigation and Drainage Division Special Conf., ASCE, New York*.
- ☒ Chang M, Ting JC, Wong KL. 1983. Soil moisture regimes as affected by silvicultural treatments in humid East Texas, in *Hydrology of Humid Tropical Regions with Particular References to the Hydrological Effects of Agricultural and Forestry Practices*, IAHS Publ. No. 137, pp. 175-186.
- ☒ Chang M. 2005. *Forest Hydrology: An Introduction to Water and Forests*. Boca Raton: Taylor and Francis group.
- ☒ Chattopadhyay N., and Hulme M., 1997: Evaporation and potential evapotranspiration in India under conditions of recent and future climate change. *Agric. For. Meteorol.*, 87, 55–73.
- ☒ Chen, M., Xie P., and Janowiak J.E., 2002: Global land precipitation: a 50-yr monthly analysis based on gauge observations. *J. Hydrometeorol.*, 3, 249–266.

- ✎ Christensen, J.H. and Christensen O.B., 2003: Severe summertime flooding in Europe. *Nature*, 421, 805.
- ✎ Cleugh HA, Leuning R, Mu QZ, Running SW. 2007. Regional evaporation estimates from flux tower and MODIS satellite data. *Remote Sensing of Environment*, 106(3): 285-304.
- ✎ Dai, A. and Trenberth K.E., 2002: Estimates of freshwater discharge from continents: Latitudinal and seasonal variations. *J.Hydrometeorol.*, 3, 660–687.
- ✎ Dooge, J.C.I. (1992), *Hydrologic Models and climate change*, Journal of Geophysical Research, 97(D3): 2677-2686.
- ✎ Feng, S. and Hu Q., 2004: Changes in agro-meteorological indicators in the contiguous United States: 1951-2000. *Theor. Appl. Climatol.*, 78, 247-264.
- ✎ Fowler A. 2002. Assessment of the validity of using mean potential evaporation in computations of the long-term soil water balance. *Journal of Hydrology*, 256 (3–4): 248–263.
- ✎ Fujimaki H, Shimano T, Inoue M, Nakane K. 2006. Effect of salt crust on evaporation from a bare saline soil. *Vadose Zone Journal, Soil Science Society of America*, 5:1246-1256.
- ✎ Gedney, N., Cox P.M., Betts R.A., Boucher O., Huntingford C. and Stott P.A., 2006: Detection of a direct carbon dioxide effect in continental river runoff records. *Nature*, 439(7078), 835–838.
- ✎ Genovese, G., Lazar C., and Micale F., 2005: Effects of observed climate fluctuation on wheat flowering as simulated by the European crop growth monitoring system (CGMS). *Proc. Workshop on Adaptation of Crops and Cropping Systems to Climate Change, 7-8 November 2005, Dalum Landbrugsskole, Odense, Denmark* Nordic Association of Agricultural Scientists, 12 pp.
- ✎ Gerten, D., Schaphoff S., Haberlandt U., Lucht W. and Sitch W. S., 2004: Terrestrial vegetation and water balance: hydrological evaluation of a dynamic global vegetation model. *J. Hydrol.*, 286(1–4), 249–270.
- ✎ Gidrometeoizdat. 1967. *The Water resources and Water Balance of the Territory of the Soviet Union*. Leningrad:, 199 p.

- ✎ Golubev, V.S. and Co-authors, 2001: Evaporation changes over the contiguous United States and the former USSR: a reassessment. *Geophys. Res. Lett.*, 28, 2665–2668.
- ✎ Griffiths, G.M., Salinger M.J. and Leleu I., 2003: Trends in extreme daily rainfall across the South Pacific and relationship to the South Pacific Convergence Zone. *J. Climatol.*, 23, 847–869.
- ✎ Groisman, P.Y., Knight R.W., Karl T.R., Easterling D.R., Sun B. and Lawrimore J.H., 2004: Contemporary changes of the hydrological cycle over the contiguous United States: trends derived from *in situ* observations. *J. Hydrometeorol.*, 5, 64–85.
- ✎ Hamlet, A.F., 2003: The role of transboundary agreements in the Columbia River Basin: an integrated assessment in the context of historic development, climate, and evolving water policy. *Climate, Water, and Transboundary Challenges in the Americas*, H. Diaz and B. Morehouse, Eds., Kluwer Press, Dordrecht, 263-289.
- ✎ Hargreaves GH, Samani ZA. 1982. Estimating potential evapotranspiration. Technical note. *Journal of Irrigation and Drainage Engineering* 108 (3): 225–230.
- ✎ Hawkins, R.H., Jiang, R., Woodward, D.E., Hjelmfelt, A.T. Jr. and VanMullem, J.E. 2002. Runoff curve number method: examination of the initial abstraction ratio. *Second Federal Interagency Hydrologic modelling Conference, Las Vegas, NV, 1-12.*
- ✎ Hawkins, R.H. 1993. Asymptotic determination of Runoff curve numbers from data. *J. Irrigation and Drainage Division, ASCE*, 119(2), 334-345.
- ✎ Haylock, M.R. and Goodess C.M., 2004: Interannual variability of extreme European winter rainfall and links with mean large-scale circulation. *Int. J. Climatol.*, 24, 759–776.
- ✎ Herath, S. and Ratnayake U., 2004: Monitoring rainfall trends to predict adverse impacts: a case study from Sri Lanka (1964–1993). *Global Environ. Change*, 14, 71–79.
- ✎ Hillel D. 1971. *Soil and Water: Physical Principles and Processes*. Academic Press, New York.
- ✎ Hillel D. 1980. *Fundamentals of Soil Physics*. Academic Press, New York.
- ✎ Hillel D. 1982. *Introduction to soil physics*. Academic Press, New York.

- ✎ Hjelmfelt, A.T., Kramer, L.A. and Burwell R. 1982. Curve numbers as random variables. *In Singh, V. (ed.) Rainfall-Runoff Relationships. Water Resources Publications, Highlands Ranch, CO, 365-370.*
- ✎ Hobbins, M.T., J.A. Ramirez, and T.C. Brown, 2004: Trends in pan evaporation and actual evapotranspiration across the conterminous U.S.: Paradoxical or complementary? *Geophys. Res. Lett.*, 31, L13503, doi:10.1029/2004GL019846.
- ✎ Hodgkins, G.A., R.W. Dudley and T.G. Huntington, 2003: Changes in the timing of high river flows in New England over the 20th century. *J. Hydrol.*, 278(1–4), 244–252
- ✎ Hodgkins, G.A., R.W. Dudley and T.G. Huntington, 2005: Summer low flows in New England during the 20th century. *J. Am. Water Resour. Assoc.*, 41(2), 403–412.
- ✎ Houghton, John 1997. *Global Warming: the Complete Briefing.* Cambridge University Press, 251 pp.
- ✎ Intergovernmental Panel on Climate Change (IPCC), 2008. *Climate change and water*, IPCC Technical Paper –VI.
- ✎ Jensen ME, Burman RD, Allen RG. 1990. Evapotranspiration and water requirements, *ASCE Manual 70*, New York, USA 1990. 332 pp.
- ✎ Jones J.A.A.: *Global Hydrology: Process, resources and environmental management*(2002), Longman Limited.
- ✎ Kergoat, L., Lafont S., Douville H., Berthelot B., Dedieu G., Planton S. and Royer J.F., 2002: Impact of doubled CO₂ on global-scale leaf area index and evapotranspiration: conflicting stomatal conductance and LAI responses. *J. Geophys. Res.*, 107(D24), 4808.
- ✎ Kharkina, M.A., 2004: Natural resources in towns. *Energia*, 2, 44–50.
- ✎ Klein Tank, A.M.G. and Können G.P., 2003: Trends in indices of daily temperature and precipitation extremes in Europe, 1946–1999. *J. Clim.*, 16, 3665–3680.
- ✎ Kunkel, K.E., 2003: Temporal variations of extreme precipitation events in the United States: 1895–2000. *Geophys. Res. Lett.*, 30, 1900, doi:10.1029/2003GL018052.

- ✎ Kustas WP. 1990. Estimates of evapotranspiration with a one- and two-layer model of heat transfer over partial canopy cover. *J. Appl. Meteorol.*, 29: 704-715.
- ✎ Labat, D., 2004: Evidence for global runoff increase related to climate warming. *Adv. Water Resources*, 27, 631–642.
- ✎ Legates, D.R., H.F. Lins and G.J. McCabe, 2005: Comments on “Evidence for global runoff increase related to climate warming” by Labat et al. *Adv. Water Resour.*, 28, 1310-1315.
- ✎ Leipprand, A. and Gerten D., 2006: Global effects of doubled atmospheric CO₂ content on evapotranspiration, soil moisture and runoff under potential natural vegetation. *Hydrol. Sci. J.*, 51, 171–185.
- ✎ Lindstrom, G. and S. Bergstrom, 2004: Runoff trends in Sweden 1807–2002. *Hydrol. Sci. J.*, 49(1), 69–83.
- ✎ Liu, B.H. and Co-authors, 2004: A spatial analysis of pan evaporation trends in China, 1955–2000. *J. Geophys. Res.*, 109, D15102, doi:10.1029/2004JD004511.
- ✎ Liu, Y.B. and Y.N. Chen, 2006: Impact of population growth and landuse change on water resources and ecosystems of the arid Tarim River Basin in western China. *Int. J. Sust. Dev. World*, 13, 295-305.
- ✎ Magrin, G.O., Travasso M.I. and Rodríguez G.R., 2005: Changes in climate and crops production during the 20th century in Argentina. *Climatic Change*, 72, 229–249.
- ✎ Majumdar, P.P. and Ghosh, S. 2008. “Climate Change Impact on Hydrology and Water Resources”, *ISH Journal of Hydraulic Engineering*, Vol.14, No-03.
- ✎ Makkeasorn A, Chang NB, Beaman M, Wyatt C, Slater C. 2006. Soil moisture estimation in a semiarid watershed using RADARSAT-1 satellite imagery and genetic programming. *Water Resources Research*, 44, doi: 10.1029/2005WR004033.
- ✎ McCabe G.J. and Ayers, M.A. 1989. *Hydrologic Effects of Climate Change in the Delaware River Basin*, WaterResource Bulletin, Dec. Vol. 25, No. 7 pp. 1231-1242.
- ✎ McCuen, R.H. 1982. *A Guide to Hydrologic Analysis using SCS Methods*. Prentice-Hall Inc., Englewood Cliffs, New Jersey 07632.

- ✎ McCuen, R.H. 1989. Hydrologic Analysis and Design. *Prentice Hall, Englewood Cliffs, New Jersey 07632.*
- ✎ McCuen, R.H. 2002. Approach to confidence interval estimation for curve numbers. *J. Hydrologic Engineering, 7(1), 43-48.*
- ✎ Menzel, A., Jakobi G., Ahas R., Scheifinger H. and Estrella N., 2003. Variations of the climatological growing season (1951-2000) in Germany compared with other countries. *Int. J. Climatol., 23, 793-812.*
- ✎ Menzel, L. and Bürger G., 2002: Climate change scenarios and runoff response in the Mulde catchment (Southern Elbe, Germany). *J. Hydrol., 267(1-2), 53-64.*
- ✎ Michel, C., Andreassian, V., and Perrin, C. 2005. Soil conservation service curve number method. How to mend a wrong soil moisture accounting procedure? *J. Water resources Research, 41 (2), 1-6.*
- ✎ Miles, E.L., Snover A.K., Hamlet A., Callahan B. and Fluharty D., 2000: Pacific Northwest Regional Assessment: the impacts of climate variability and climate change on the water resources of the Columbia River Basin. *J. Amer. Water Resour. Assoc., 36, 399-420.*
- ✎ Milly, P.C.D., Dunne K.A. and Vecchia A.V., 2005. Global pattern of trends in streamflow and water availability in a changing climate. *Nature, 438(7066), 347-350.*
- ✎ Mimikou, M., Blatas E., Varanaou E. and Pantazis K., 2000: Regional impacts of climate change on water resources quantity and quality indicators. *J. Hydrol., 234, 95-109.*
- ✎ Mintz Y, Walker GK. 1993. Global fields of soil moisture and land surface evapotranspiration derived from observed precipitation and surface air temperature. *Journal of Applied Meteorology, 32:1305-1334.*
- ✎ Mirnikou, M.A. and Kouvopoulos Y.S. 1991, *Regional climate change impacts: I. Impacts on water resources*, Hydrologic Science Journal, 36(3): 247-258.
- ✎ Mishra S K, Singh VP. 2002. SCS-CN method: Part-I: Derivation of SCS-CN based models. *Acta Geophysica Polonica 50 (3): 457-477.*
- ✎ Mishra S K, Singh VP. 2003b. SCS-CN method Part-II: Analytical treatment, *Acta Geophysica Polonica 51(1): 107-123.*

- ✎ Mishra S K, Singh, VP. 2003a. *Soil conservation Service Curve Number (SCS-CN) Methodology*, Kluwer Academic Publishers, P. O. Box 17, 3300 AA Dordrecht, The Netherlands.
- ✎ Mitchell, T.D. and Jones P.D., 2005: An improved method of constructing a database of monthly climate observations and associated high-resolution grids. *Int. J. Climatol.*, 25, 693–712.
- ✎ Mockus, V. 1949, “Estimation of total (peak rates of) Surface Runoff for Individual Storms.” Exhibit A of Appendix B, Interim Survey Rep. Grand (Neosho) River Watershed, USDA, Washinton, D.C.
- ✎ Moonen, A.C., Ercoli L., Mariotti M. and Masoni A., 2002: Climate change in Italy indicated by agrometeorological indices over 122 years. *Agr. Forest Meteorol.*, 111, 13-27.
- ✎ Morton FI. 1994. Evaporation research—a critical review and its lessons for the environmental sciences. *Critical Reviews in Environmental Science and Technology* 24 (3): 237–280.
- ✎ Mote, P.W., Parson E.A., Hamlet A.F., Keeton W.S., Lettenmaier D., Mantua N., Miles E.L., Peterson D.W., Peterson D.L., Slaughter R. and Snover A.K., 2003: Preparing for climatic change: the water, salmon, and forests of the Pacific Northwest. *Climatic Change*, 61, 45-88.
- ✎ Nagler PL, Clerverly J, Glenn E, Lampkin D, Huete A, Wan Z. 2005. Predicting riparian evapotranspiration from MODIS vegetation indices and meteorological data. *Remote Sensing of Environment* 94: 17-30.
- ✎ Patra K.C. 2008. *Hydrology and Water Resources Engineering*, Second edition. Narosa Publishing House.
- ✎ Payne, J.T., Wood A.W., Hamlet A.F., Palmer R.N. and Lettenmaier D.P., 2004: Mitigating the effects of climate change on the water resources of the Columbia River basin. *Climatic Change*, 62(1–3), 233–256.
- ✎ Penman HL. 1948. Natural evaporation from open water, bare soil and grass. *Proceedings of Royal Society London* 193: 120–145.
- ✎ Peterson, B.J., Holmes R.M., McClelland J.W., Vorosmarty C.J., Lammers R.B., Shiklomanov A.I., and Rahmstorf S., 2002: Increasing river discharge to the Arctic Ocean. *Science*, 298, 2172–2173.

- ✎ Peterson, T.C. and Vose R.S., 1997: An overview of the Global Historical Climatology Network temperature database. *Bull. Am. Meteorol. Soc.*, 78, 2837–2848.
- ✎ Peterson, T.C., Golubev V.S. and Groisman P.Y., 1995: Evaporation losing its strength. *Nature*, 377, 687–688.
- ✎ Philip BB, Huber WC. 2002. *Hydrology and floodplain analysis (3rd edition)*. Prentice Hall, Upper Saddle River, NJ 07458.
- ✎ Priestley CHB, Taylor RJ. 1972. On the assessment of surface heat flux and and evaporation using large scale parameters. *Mon. Wealth. Rev* 100:81-92.
- ✎ Prof. Sawalia Bihari Verma, Dr. Anand Bhusan Saran, Dr. Sunil Kumar Verma: *Environment and Climate Change* (First edition, 2009), Pentagon Press.
- ✎ Qian, Y., 2006b: More frequent cloud-free sky and less surface solar radiation in China from 1955 to 2000. *Geophys. Res. Lett.*, 33, L01812, doi:10.1029/2005GL024586.
- ✎ Qudin L, Hervieu F, Michel C, Perrin C, Andreassian V, Anctil F, Loumagne C. 2005. Which potential evapotranspiration input for a lumped rainfall-runoff model? Part 2-Towards a simple and efficient potential evapotranspiration model for rainfall-runoff modeling. *Journal of Hydrology* 303: 290-306.
- ✎ Robeson, S.M., 2002: Increasing growing-season length in Illinois during the 20th century. *Climatic Change*, 52, 219-238.
- ✎ Roderick, M.L. and G.D. Farquhar, 2004: Changes in Australian pan evaporation from 1970 to 2002. *Int. J. Climatol.*, 24, 1077-1090.
- ✎ Roderick, M.L. and G.D. Farquhar, 2005: Changes in New Zealand pan evaporation since the 1970s. *Int. J. Climatol.*, 25, 2031-2039.
- ✎ Rosenberg, N.J., Brown R.A., Izaurralde C. and Thomson A.M., 2003. Integrated assessment of Hadley Centre HadCM2 climate change projections on agricultural productivity and irrigation water supply in the conterminous United States. I. Climate change scenarios and impacts on irrigation water supply simulated with the HUMUS model. *Agri. Forest Meteorol.*, 117(1–2), 73–96.

- ☞ SCD. 1972. *Handbook of Hydrology*. Soil Conservation Department, Ministry of Agriculture, New Delhi.
- ☞ Schaake, J.C., 1989 *From Climate to Flow In: Waggoner, P.E. Climate Change and U.S. Water Resources*. Wiley Series in Climate and the Biosphere.
- ☞ SCS. 1956. *Hydrology*. *National Engineering Handbook*, Supplement A, Section 4, Chapter 10, Soil Conservation Service, USDA, Washington, D.C.
- ☞ SCS. 1971. *Hydrology*. *National Engineering Handbook*. USDA, Washington, D.C.
- ☞ SCS. 1972 *Hydrology*. *National Engineering Handbook*. USDA, Washington, D.C.
- ☞ SCS. 1985. *Hydrology*. *National Engineering Handbook*. USDA, Washington, D.C.
- ☞ Semenov, S.M., Yasukevich V.V. and Gel'ver E.S., 2006: *Identification of Climatogenic Changes*. Publishing Centre, Meteorology and Hydrology, Moscow, 325 pp.
- ☞ Shaw EM. 1988. *Hydrology in Practice*. Chapman and Hall, London.
- ☞ Shuttleworth WJ. 1993. Evaporation, in: Maidment DR. (Ed.), *Handbook of Hydrology*. McGraw-Hill, New York.
- ☞ Shuttleworth WJ. 1993. Evaporation, in: Maidment DR. (Ed.), *Handbook of Hydrology*. McGraw-Hill, New York.
- ☞ Singh, V. P. 1992. *Elementary Hydrology*. Printice Hall, Englewood Cliffs, New Jersey 07632.
- ☞ Smith MR, Allen RG, Monteith JL, Pereira LS, Segeren A. 1991. Rep. on the Expert Consultation on *Procedures for Revision of FAO Guidelines for Predicting Crop Water Requirements*. FAO, Land and Water Devel. Div., Food and Agricultural Organization of the United Nations, Rome.
- ☞ Springer, McGurk E. P., Hawkins, R.H. and Goltharp, G.B. 1980. Curve numbers from watershed data. Proc., ASCE irrigation and Drainage System on Watershed Management, ASCE, New York, Vol. II, 938-950.
- ☞ Strzepek, K. and Smith J. Implications Editors, Cambridge University Press, Cambridge, U.K. *Climatic Change*, 13(1): 69-97.

- ☒ Tebakari, T., Yoshitani J., and Suvanpimol C., 2005: Time-space trend analysis in pan evaporation over kingdom of Thailand. *J. Hydrol. Eng.*, 10, 205-215.
- ☒ Thom AS, Oliver HR. 1977: On Penman's equation for estimating regional evapotranspiration." Quarterly *J. Royal Meteorological Soc.*, Bracknell, U.K., 103, 345–357.
- ☒ Thornthwaite CW. 1948. 'An approach toward a rational classification of climate. *Geographical Review* 38: 55-95.
- ☒ Xu CY, Singh VP. 2002. Cross comparison of empirical equations for calculating potential evapotranspiration with data from Switzerland. *Water Resources Management* 16 (3): 197–219.
- ☒ Yu B. 1998. Theoretical justification of SCS-CN method for runoff estimation. *Journal of the Irrigation and Drainage Division*, ASCE, 124(6): 306–310.